Roles of Fibroblast Growth Factors During Induction and Morphogenesis of the Inner Ear of the Mouse (*mus musculus*, Linnaeus, 1758) and Chicken (*Gallus gallus*, Linnaeus, 1758)

Dissertation

zur Erlangung des Doktorgrades

des Fachbereiches Biologie

der Universität Hamburg

Vorgelegt von

Laura Zelarayán

aus Tucumán, Argentienien

Hamburg, July 2005

The work for this doctoral thesis was carried out at the Center for Molecular Neurobiology Hamburg (ZMNH) from February 2002 to July 2005 under the supervision of Dr. Thomas Schimmang.

To my family

Table of Contents

SUMMARY

The vertebrate inner ear consists of two parts: the *vestibular system* responsible to sense balance and the *auditory system* that processes sound. Thus, alterations in the formation of this organ lead to problems in both audition and balance. The inner ear develops adjacent to the developing hindbrain from the placodal ectoderm, which invaginates to form the otic vesicle to subsequently undergo morphogenesis to reach the mature inner ear. Members of the Fibroblast Growth Factor (FGF) gene family have been shown to be widely implicated in otic formation in different species, but the molecular pathways acting to execute this developmental program are not completely understood. Several members of the FGF family, including FGF2, FGF3, FGF8, FGF10 and FGF15/19 are implicated during different stages of inner ear formation.

The aim of this study was to adressed the role of members of the FGF family such as FGF3, FGF2, FGF8 and FGF10 during otic development of mice and chicken. For this purpose, histological analysis, white paint injection into the inner ears, immunohistochemistry assays, RNA *in situ* hybridization, apoptosis studies and *in ovo* electroporation were carried out during this work.

Based on the conserved expression of *Fgf3* in vertebrates in the hindbrain close to the developing otocyst, it has been proposed as an otic inducer. The function of this factor for inner ear induction has not been fully explored in mice. Therefore, *Fgf3* null mutants in which all coding exons for *Fgf3* had been deleted were analyzed in the present study. The vast majority of these mutants showed normal inner ear development. In contrast, *Fgf3* null mutants in which the *Fgf3*-coding region was replaced by a neo^r cassette were often found to display a severe otic phenotype consisting in malformed semicircular canals, and defective cochlea and vestibule. The latter result suggests that the inner ear phenotype in $Fgf3^{neo/neo}$ mutants is possibly partially due to the presence of the neo^r gene rather than to the absence of the *Fgf3*-coding region.

Since *Fgf10* expression coincides partially with *Fgf3* expression in the hindbrain and developing otocyst, double homozygous and homoheterozygous mutants for *Fgf3* and *Fgf10* were analysed. The severe lack of otic tissue observed in $Fgf3^{-/-}Fgf10^{-/-}$ mice demonstrated that both FGF10 and FGF3 play essential roles in a redundant manner to reinforce and to

maintain otic induction, as well as to pattern the otocyst**.** Moreover, the analysis of *Fgf3*$^{-/-}$ *Fgf10*$^{+/-}$ mutants showed the importance of both FGFs for the correct formation of the otocyst.

Fgf8 has been shown to be expressed in mesoderm and endoderm close to the future otic vesicle and within the developing otocyst. Since *Fgf8* null mutant mice die prior to otic development due to severe gastrulation defects, animals with a specific inactivation of *Fgf8* in the otic placode and vesicle were analyzed in the present research project. The analysis of the mutants did not show major defects in the developing otocyst but only a slight reduction of inner ear innervation. However, *Fgf3+8* double mutants showed several defects in otic morphogenesis from E11 onwards. Expression of *Fgf8* in wild-type mice was detected at E12.5 in the vestibular system which coincided partially with the expression of *Fgf3*. Therefore, this study proposes that FGF3 and FGF8 work redundantly to direct proper otic morphogenesis.

Additionally, loss- and gain-of-function approaches were carried out in chicken embryos in order to define the role of FGFs in otic induction and morphogenesis in this species. *In ovo* electroporation was performed to transiently overexpress *Fgf3*, *Fgf8* and *Fgf10* during early stages of otic induction. The overexpression of *Fgf3* and *Fgf10* in the neural tube resulted in ectopic otic structures. Their otic nature was confirmed by RNA *in situ* hybridization with otic markers and histological analysis. The otic vesicles obtained by *Fgf8* electroporation were smaller suggesting that FGF8 has a negative influence on otic vesicle formation. Furthermore, functional knockdown of FGF3 by electroporation of morpholino oligonucleotides directed against *Fgf3* and *Fgf3*siRNA lead to a failure to form the otic vesicle from the otic placode thus indicating the participation of FGF3 during crucial step of otic morphogenesis in chicken.

This study demonstrates the importance of FGF signalling during inner ear development and the mechanisms through which they can compensate for each other to finally ensure the success of inner ear organogenesis in birds and mammals.

I-INTRODUCTION

The mammalian ear is the organ of hearing and balance and consists of three parts: the outer ear, the middle ear, and the inner ear. The outer ear and middle ear are the apparatus for the collection and transmission of sound. The inner ear or labyrinth in vertebrates consists of two parts: the *vestibular system* that is responsible for balance and detection of the acceleration, and the *auditory system* which is responsible for the sense of hearing. Induction and morphogenesis events of the inner ear development have been extensively studied in mice, chicken and zebrafish. Fibroblast growth factors have been widely implicated in inner ear formation (Mansour*, et al.*, 1993, Ladher*, et al.*, 2000, Pirvola*, et al.*, 2000, Vendrell*, et al.*, 2000, Pauley*, et al.*, 2003) but the precise molecular mechanism of otic induction remains still unclear. The present work attempts to elucidate the role of several FGFs during mouse and chicken inner ear formation. In order to understand the mechanism of otic development and to compare between species, a brief introduction of anatomy and evolution of the inner ear will be given. Secondly, the molecular mechanisms of otic formation and the FGFs involved in these mechanisms will be shortly introduced and last an overview of the genetic modified mice and chicken embryos used in this study will be given.

1.1-The Vertebrate Inner Ear

1.1.*1*-Inner Ear through Evolution

The inner ear underwent some changes along evolution in response to its adaptation to the environment. The structures changed dramatically starting from the jawless hagfish ear, the first vertebrate ear, which has only some rudimentary sensory epithelia (Löwenstein*, et al.*, 1970, Lewis, 1985, Fritzsch, 2001b). Those structures have changed to the formation of two distinct semicircular canals found in derived jawless vertebrates, the lampreys. Jawed vertebrates subsequently evolved several distinct sensory epithelia and a third horizontal canal allowed a direct coding of angular movement in all three cardinal planes (Fritzsch, 1998).

To detect head orientation and movement all of the vestibular organs of the ear in different vertebrates are positioned within the skull. The ear is able to perceive sound either through specialized organs positioned near the sound conducting perilymph pathways (De Burlet, 1934, Werner, 1960, Fritzsch, 1992) or in aquatic vertebrates, through direct impact of sound on the otolithic organs (Schellart*, et al.*, 1992).

All amniotes (reptiles, birds, and mammals) have a common ancestry, share a common structure, and develop from the same genetic substrate; thus the functional units of the hearing process are homologous (Manley, 2000). In all amniotes a newly evolved tuning mechanism, known as micromechanical tuning, extended the sensitive response to higher frequencies. It was accompanied by papillar elongation. Thus the coiled cochlea was probably a mechanism for accommodating a long papilla. However the true "cochleas" only occur in placental and pouched mammals, relatively recent in evolution (Manley, 1998).

1.1.*2*-Anatomy and Function of the Vertebrate Inner Ear

As mentioned before, the inner ear consists of a labyrinth shaped structure. The osseous labyrinth (a bony cavity) is filled with perilymph and contains the membranous labyrinth (Fig. 1.1A). The membranous labyrinth contains the endolymph (the otic fluid, which provides the media for vibrations involved in hearing and maintenance of equilibrium). The labyrinths consist of three structural and functional divisions: the **vestibule**, the **semicircular canals** and the **cochlea** (Fig. 1.1B).

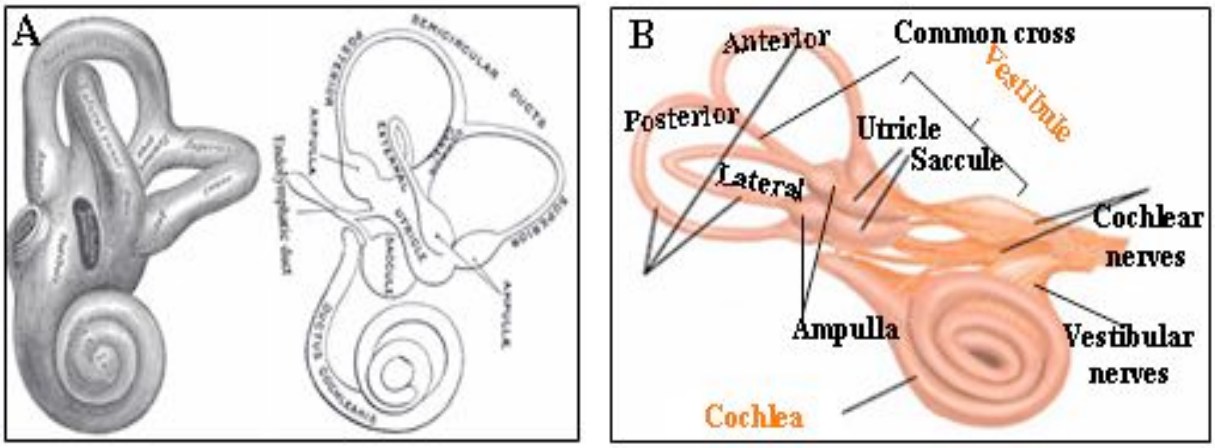

Figure 1.1*:* (**A**) *Left:* Osseous or bony labyrinth. The different parts of the inner ear are indicated in the pictures. *Right*: Membranous labyrinth located inside the osseous labyrinth, which contains all the functional structures of the inner ear (Gray, 2000). (**B**) Inner ear and its components in vertebrates are shown in this picture. The three structural and functional divisions of the membranous labyrinth semicircular canals, vestibule and cochlea and its components are indicated in the figure (The figure B was taken from www.driesen.com, Dr. J. Driesen, 2004)

The **vestibule** is the central part of the osseous labyrinth. Within the osseous vestibule the membranous labyrinth consists of two membranous sacs, the utricle and saccule. The utricle forms a sort of pouch communicating with the semicircular canals and the endolymphatic

duct (Fig. 1.1A). The sense organ of the utricle is called utricular macula and consists of a thickened epithelium (Fig. 1.2), which receives the utricular filaments of the afferent nerve fibers. The saccule is another chamber in the vestibule that also forms a pouch and opens into the endolymphatic duct and cochlea (Fig. 1.1B). The sensory region of the saccule is a thickened epithelium called saccular macula. The epithelium of utricular and saccular macula consists of supporting and hair cells (HCs) (Fig. 1.2). The HCs are the sensory receptor cells, which detect movements of the endolymph to perceive gravity and linear acceleration. HCs contain stereocilia (Fig 1.2B) that project from the apical surface of the cells into a gelatinous coating called the otolith organ, a membrane composed of calcareous particles (otoconia), and a mucopolysaccharide gel (Fig 2B and C). The stereocilia movements produce depolarization and lead to an increased rate of firing in the vestibular afferent nerves. The supporting cells (Fig. 2B and C) are thought to be important for maintaining and regeneration of the HC (Lanford*, et al.*, 1996, Presson*, et al.*, 1996, Fekete*, et al.*, 1998, Haddon*, et al.*, 1999, Baird*, et al.*, 2000). The vestibular HCs are innervated by sensory neurons that project towards the vestibular nucleus in the brainstem.

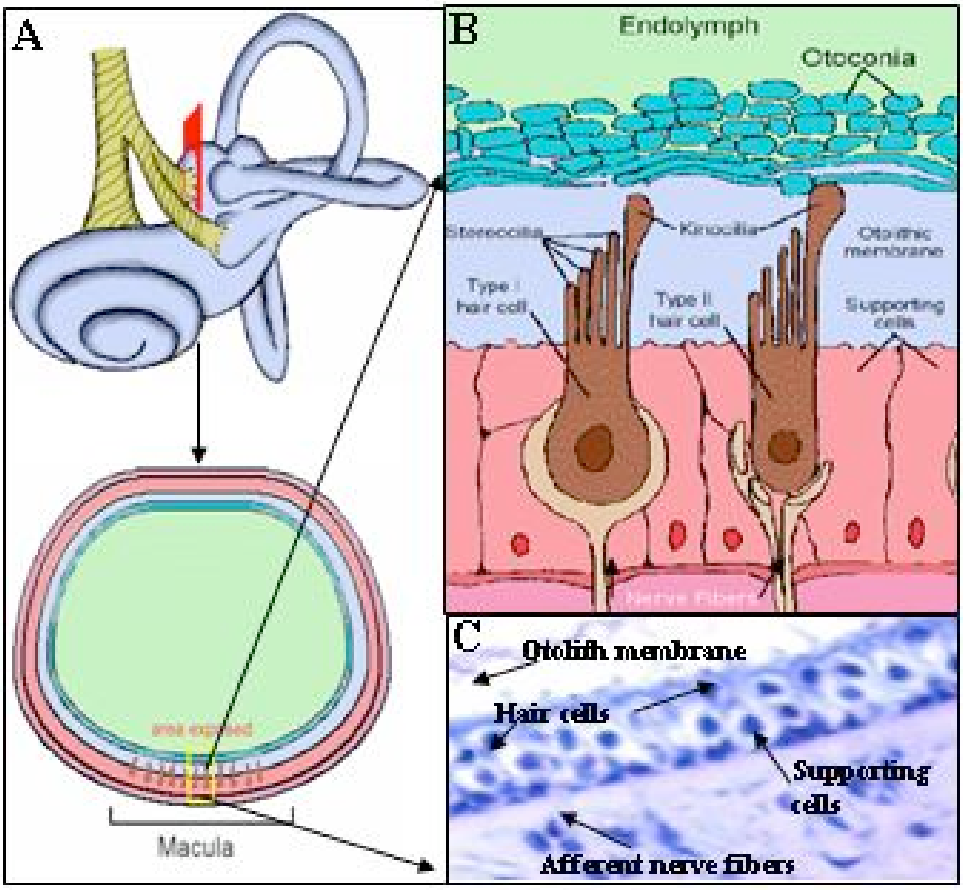

Figure 1.2: (**A**) Scheme of the inner ear and a section at the level of the utricular macula (**B**) Scheme corresponding to the boxed area in (A) showing the components of the macula. (**C**) Mouse adult

section of the inner ear at the level of the macula stained with Toluidine Blue shows the cells that are present in the macula.

(The pictures A and B were taken from the website http://medic.med.uth.tmc.edu/Lecture/Main/ear.htm#inner)

The **bony semicircular canals** (SC) contain the membranous semicircular canals. They are three: superior, posterior and lateral, located in perpendicular planes. They open into the vestibule and one of the apertures is common to two of the canals forming the so-called common cross (Fig. 1.1A and 1.1B). Like the utricle, saccule and cochlea, the semicircular canals are filled with endolymph. The sensory organ of the semicircular canals is called ampullar crista (*crista ampullaris*) and is positionated in a dilatation at one end, called ampulla (Fig. 1.3). Like the macula of the utricle and saccule, the epithelium consists of supporting and HCs. The ampullar crista consists of a sensory epithelium covered by a gelatinous mass called the cupula that contains the projections of the hair cells (Fig. 1.3). The sensory HCs are surrounded by supporting cells. The information from the macula and crista is conveyed to the vestibular nuclei in the brainstem, which also receive information from other sensory sources.

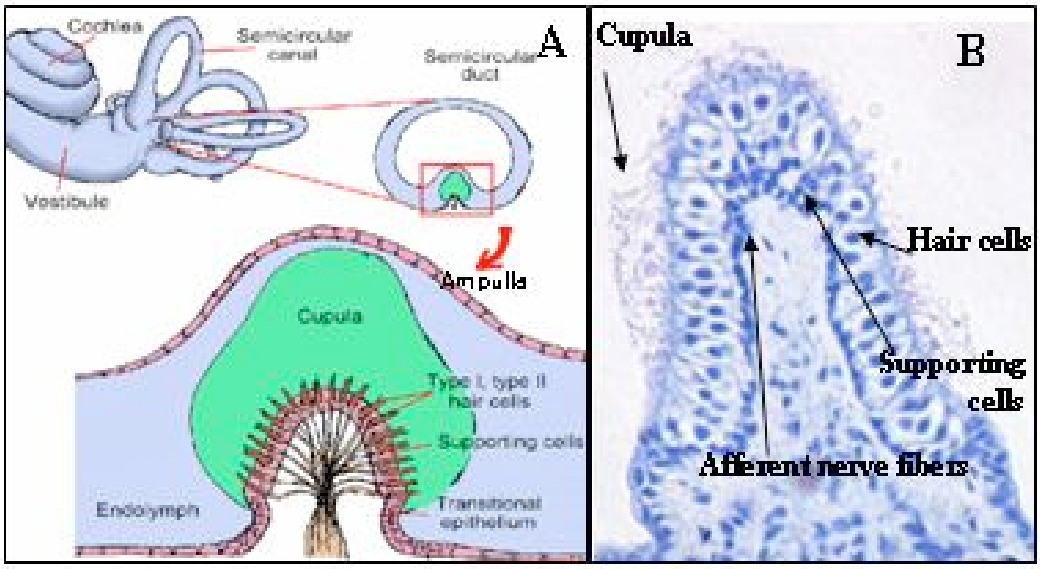

Figure 1.3: (**A**) Portion of the semicircular duct, which is sectioned to expose the sensory epithelium (ampullar crista). (**B**) Adult inner ear mouse section at the level of the ampulla stained with Toluidine Blue shows the cells that are present in the crista.

(Picture A was taken from the website "Ear" http://medic.med.uth.tmc.edu/Lecture/Main/ear.htm#inner)

The bony **cochlea** is conical and forms the anterior part of the labyrinth. The cochlea consists of three components: a conical shaped central axis, the modiolus; a canal that forms a spiral around the axis (two and three-quarters of a turn); and of a delicate lamina, the osseous spiral

lamina, that partially subdivides the modiolus into two parts (Figure 1.4A). The membranous cochlea or cochlear duct consists of a spirally arranged tube enclosed in the bony canal of the cochlea (Fig 1.4A) and is divided into three cavities, the vestibular duct (*scala vestibuli)* and the tympanic duct (*scala tympani)* filled with perilymph and the cochlear duct *(scala media)* filled with endolymph (Figure1.4A).

The roof of the cochlea duct is delineated by the vestibular membrane (Reissner´s membrane) (Fig. 1.4B and C), its outer wall by the periostium, lining the bony canal and its floor by the basilar membrane, and the outer part of the osseous spiral lamina. The periostium forming the outer wall of the cochlear duct contains numerous capillaries and forms the *stria vascularis* in its upper portion (Fig. 1.4B), that maintains the precise concentration of potassium ions.

The organ of Corti (Figure 1.4C) is composed of an epithelium placed on the basilar membrane. The more central part of these structures are two rows of cells, the inner hair cells (IHCs), arranged in a single row and outer hair cells (OHCs) arranged in three rows (Fig. 1.4C). The free ends of the outer hair cells occupy a series of apertures in a net-like membrane (reticular membrane). IHC and OHC form together with the pillar cells (inner and outer) a close triangular tunnel that is called the tunnel of Corti. The pillar cells are interlaced microfibrils and microtubules in contact with the IHC and OHC, respectively, providing structural stability and ensuring the transmission of the movement of the HCs. Between the HCs there are rows of supporting cells (Fig. 1.4C). Another membrane, the tectorial membrane covers the entire organ. The HCs are the sensory receptors of the auditory organ of Corti, which at their deep ends are in contact with the terminal filaments of the cochlear nerve. The organ of Corti is responsible for the sense of hearing by converting sound pressure impulses into electrical impulses, which are passed on to the brain via the auditory nerve. This conversion is made by the HCs in response to the movement of the endolymph that is in contact with them. The acoustic nerve divides into a cochlear and a vestibular branch. The spiral ganglion of the cochlea occupies the spiral canal of the modiolus (Fig. 1.4A). The somas of the nerve fibers are located within two ganglia, reflecting again the dual function of the organ (Gray, 2000, Prass*, et al.*, 2004).

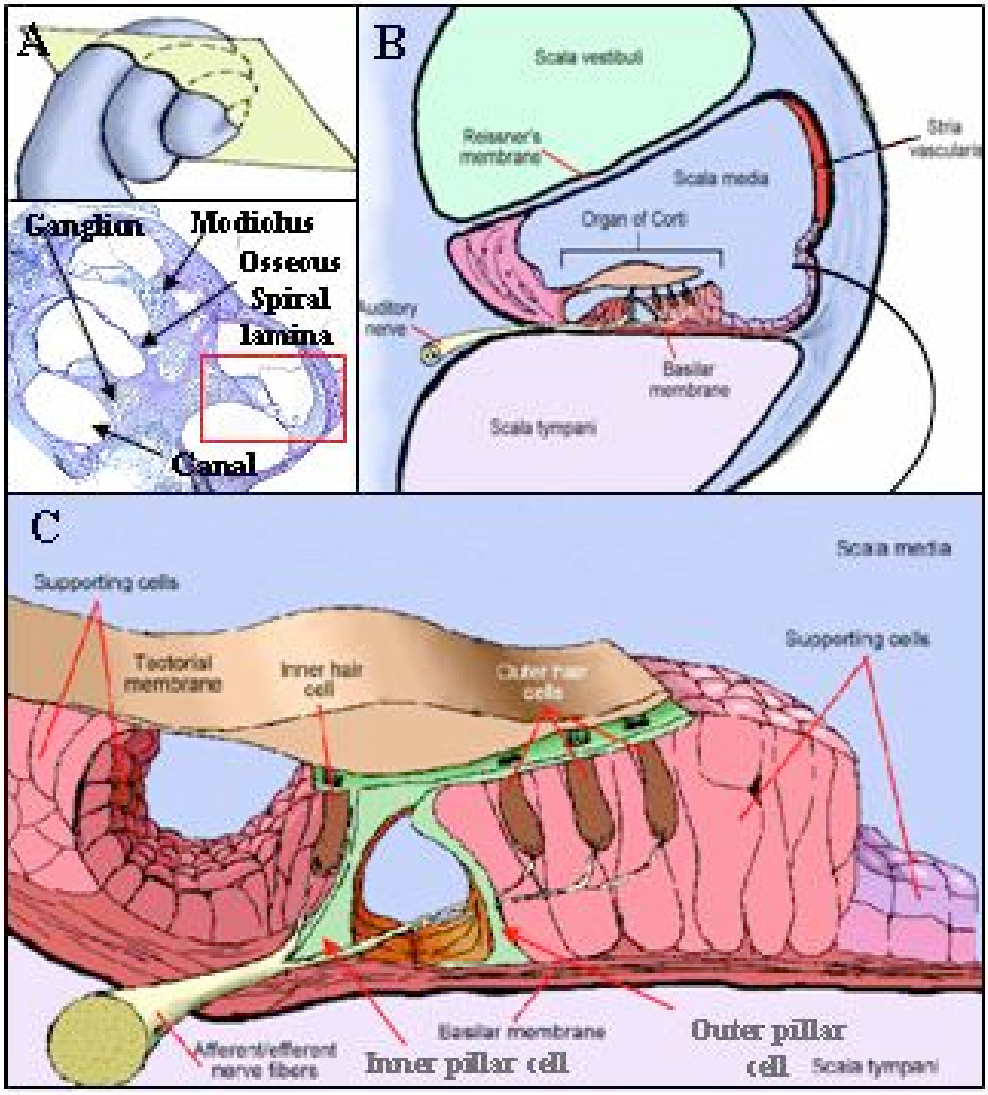

Figure 1.4: (**A**) Section of the cochlea across the modiolus stained with Toluidine Blue. The square in red marks the Tunnel of Corti. (**B**) The scheme shows the three subdivisions of the cochlea. (**C**) High magnification of the scheme in (B) shows the organ of Corti and its different epithelial structures.

(The schemes were taken from the website"Ear" http://medic.med.uth.tmc.edu/Lecture/Main/ear.htm#inner).

1.1.*3*-Anatomy of the Developing Inner Ear in Mice

The inner ear arises from the otic vesicle undergoing a morphogenetic process to model the final mature structure (Fig. 1.5). In mice at day 9.5 of gestation (E 9.5) the otocyst is already closed and starts a differentiation process. At E10.75 the endolymphatic duct appears as a tube-like structure projecting dorsally from the medial part of the otocyst. The cochlear anlage forms as a ventral bulge from the otocyst. At E11.5 the cochlea continues to expand ventrally and the vertical canal plate (anlage of the superior and posterior canals) begins to form dorsolaterally. At E12 the posterior and anterior canals start to be delineated due to the

reabsorptsion of the vertical canal plate. The horizontal canal plate (primordium of the lateral canal) appears in the lateral part of the otocyst. The utricle appears as an anterior protrusion. The cochlea starts to differentiate into a proximal and distal part. At E13 the endolymphatic duct becomes thinner and the dorsal portion forms the primordium of the endolymphatic sac. The semicircular canals and the common cross are already defined. The saccular anlage appears ventrally to the utricle. At this point, the distal part of the cochlea begins coiling and forms half of a turn. At E15 the utriculosaccular and cochleosaccular connections appear at this point and the cochlea completes one and a half turns. By E17 the membranous labyrinth reaches the mature shape and the coiling process of the cochlea completes one and a three-quarters turns (Morsli, et al., 1998).

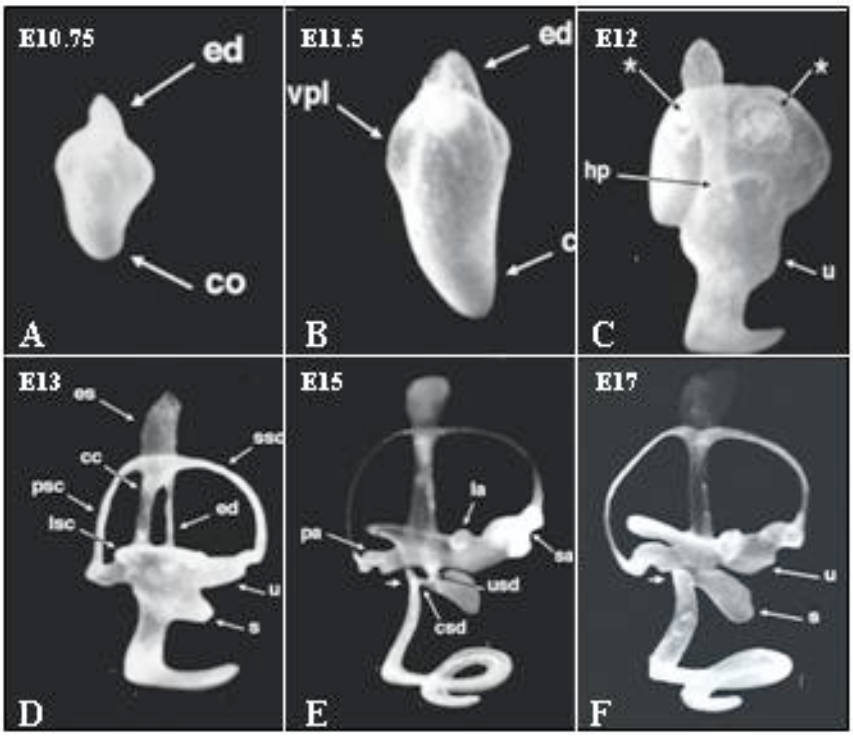

Figure 1.5: Paint-filling of developing mouse inner ear from 10.75 to 17 dpc. (**A, B**) Otic vesicle stage, the developing structures are indicated. (**C**) The otic vesicle undergoes morphogenesis. *Asterisks* point out areas of reabsortion in the central regions of the developing superior and posterior canals. (**D-F**) Different structures that later form part of the inner ear start to be visible. **cc:** Common crus; **co:** cochlea; **csd:** cochleosaccular duct; **ed:** endolymphatic duct; **es:** endolymphatic sac; **hp:** horizontal canal plate; **la:** lateral ampulla; **lsc:** lateral semicircular canal; **pa:** posterior ampulla; **psc:** posterior semicircular canal; **s:** saccule; **sa:** superior ampulla; **ssc:** superior semicircular canal; **u:** utricle; **usd:** utriculosaccular duct; **vpl:** vertical canal plate (Morsli, *et al.,* 1998).

1.1.*4*-Anatomy of the Developing Inner Ear in Birds

Chicken embryos as well as zebrafish have been used extensively to study induction and morphogenesis events of the inner ear although they differ anatomically from the murine inner ear. In birds, eight sensory organs are found, seven vestibular and one auditory organ. Sensory organs can be divided into two groups, anterior (superior and lateral cristae; utricular and saccular macula) and posterior (posterior crista, basilar papilla, lagena and the macula neglecta). The chick inner ear, similar to other vertebrates, (Figure 1.6) can be divided into dorsal vestibular and ventral auditory components. The **auditory** component of the chick, the lagena (cochlear duct), is a relatively straight tube which has an arc-shaped structure rather than the coiled structure found in higher vertebrates. The **vestibular** component consists of two connecting sacs, the utricle and the saccule, three semicircular canals and their corresponding ampulla, which contains the cristae and the opposite side ends with the common cross. Each semicircular canal is situated in a different plane (Wu*, et al.*, 1998).

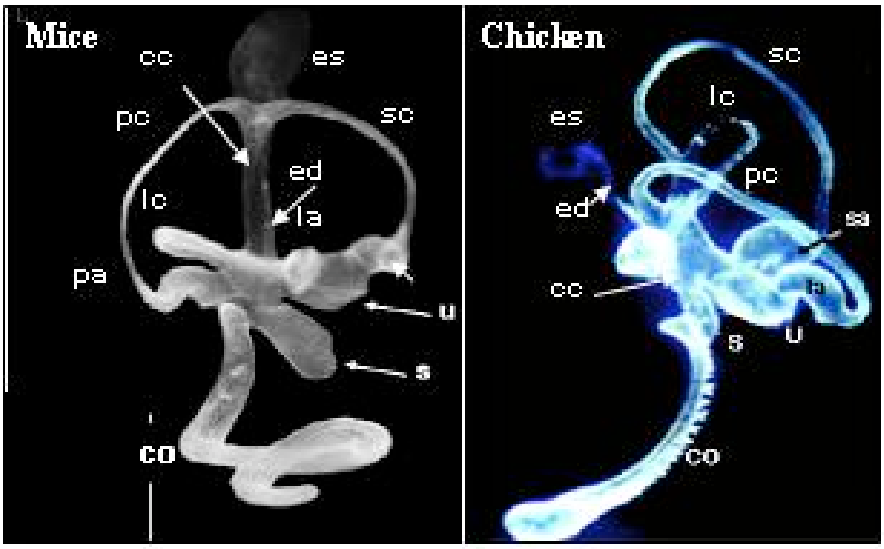

Figure 1.6: Comparative mouse and chicken paint-filling inner ear. *Left:* Mouse inner ear. *Right*: Chick inner ear. Note the coiled cochlea of the mouse inner ear in comparison to the more extended cochlea in chicken. **CC:** common cross; **CO:** cochlea; **ED:** endolymphatic duct, **ES:** endolymphatic sac, **LA:** lateral ampulla, **LC:** lateral canal, **PA:** posterior ampulla, **PC:** posterior canal, **S:** saccule; **SA:** superior ampulla, **SC:** superior or anterior canal, **U:** utricle (Morsli, *et al.*, 1998).

1.2-Early Events During Inner Ear Formation

1.2.*1*-The Inner Ear arises from a Neurogenic Placode

Sensory organs of the brain in vertebrates arise from embryonic structures known as *cranial sensory placodes* that appear on the head ectoderm as focal regions of thickened ectoderm, which give rise to both neuronal and non-neuronal structures. They comprise the olfactory, lens, otic, trigeminal and epibranchial placodes. Of these only olfactory and otic placodes give rise to neuronal and non-neuronal components (Streit, 2004, Zou, *et al.*, 2004). It has been suggested that the territory next to the neural plate, the neural plate border, represents a common placodal field (prepacodal domain) which forms a common anlage from which all placodes originate. Within this domain the cells are competent to give rise to any of the placodes (Knouff, 1935, Graham, *et al.*, 2000, Baker, 2001). The existence of such a field implies that initially all placode cells go through a generic placodal state that is set up by a common molecular mechanism and common expression of multiple genes such as *Dlx* (Distal-less), *Msx* (Muscle segment homoebox), *Six* (Sinus Oculis), *Eya* (eye-absent) and *BMP* (Bone morphogenetic protein) (Baker, 2001, Streit, 2002). Later the cells diversify to acquire characteristics specific for individual placodes (Streit, 2001) becoming progressively spatially restricted (Torres & Giraldez, 1998). Many studies have adresseded the otic placode induction but the exact molecular event remains still unclear.

1.2.*2*-Induction and Morphogenesis of the Vertebrate Inner Ear

Despite its complexity and multiple functions, the origin of the inner ear epithelium is simple. Except for the melanocyte cells of the stria vascularis, glial and Schwann cells in the otic ganglia, which are of neural crest origin, all cellular components of the otic epithelium derive from the embryonic otic vesicle which arises from the otic placode. The vertebrate inner ear forms on the ectoderm encompassing the posterior of rhombomeres (r) 4 down to r6 (Noramly, *et al.*, 2002). Rhombomeres are repetitive units that are found in the hindbrain and are fundamental for many aspects of neural organization (Kandel, *et al.*, 2000). The initial morphological event in ear development in all vertebrates is the formation of the embryonic otic placode, on the head ectoderm next to the developing hindbrain at the 8-10 somite stage (ss) (Anniko, *et al.*, 1984, Hilfer, *et al.*, 1989, Haddon, *et al.*, 1996). Strong evidence indicates that early intrinsic and extrinsic signals begin to pattern the otocyst almost immediately after its

formation at E9 in mice (Morsli, *et al.*, 1998), 24 h post fertilization in zebrafish (Liu, *et al.*, 2003), and HH 12 (Hamburger, 1951) in chick (Fekete, *et al.*, 2002). The steps of otic development are illustrated in Fig. 1.7. The initial otic placode invaginates to form the otic cup and subsequently the otocyst, an ellipsoid-shaped structure lined by a pseudo-stratified epithelium. This process occurs through the interaction between the otic vesicle and other embryonic tissues (Anniko, *et al.*, 1984, Noden, *et al.*, 1986, Couly, *et al.*, 1993, Torres & Giraldez, 1998). The cochlea and vestibular neurons are formed very early in development by delaminating from the otic cup. Initially they form a single structure, the cochleovestibular ganglion, which later splits into cochlear and vestibular ganglia. The otocyst enters proliferation prior to a differentiation phase, during which morphogenesis and patterned development of specific cell types takes place (Torres & Giraldez, 1998).

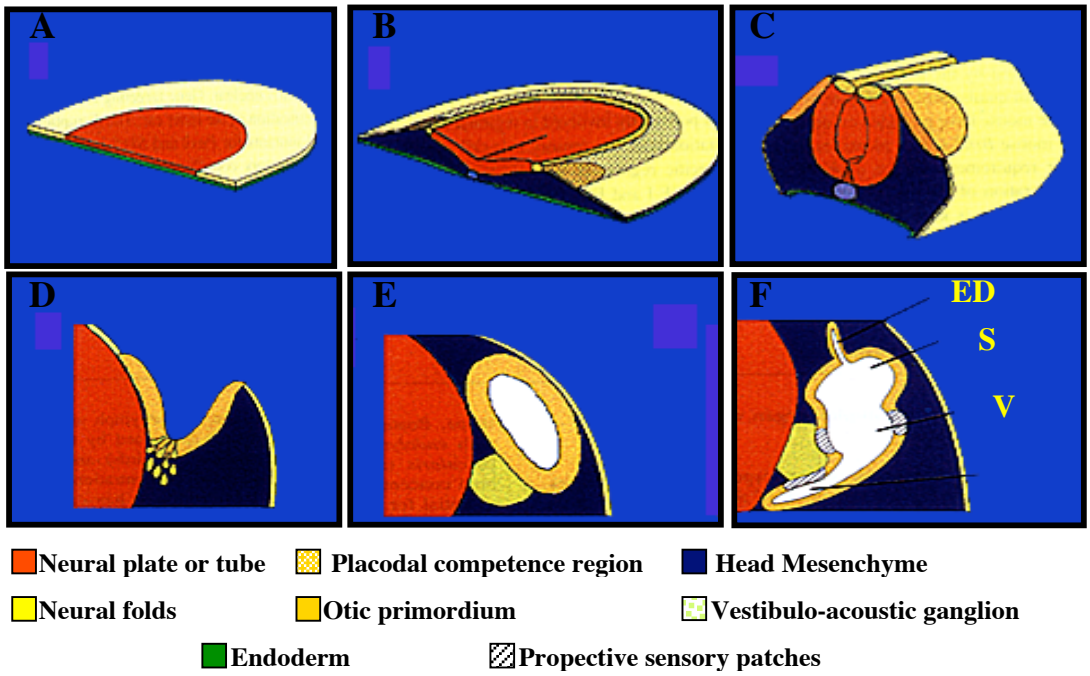

Figure 1.7: Scheme of inner ear development in vertebrates. (**A**, **B**) Representations of anterior halves of early embryos, sectioned at the prospective otic area to show the disposition of embryonic layers. In **B** the multiplacodal competent ectoderm is depicted (**C**) Representation of a transverse segment of the head region at the otic placode level. (**D-F**) Transversal sections at the otic level. Color code indicates the actual structures or their prospective areas before they appear. Stages: (**A**) Pregastrula, the prospective neural plate is indicated in red. (**B**) Head fold, the prospective otic placode is indicated in orange and the prospective multiplacodal ectoderm stripe is indicated around the neural fold. (**C**) Otic placode. (**D**) Otic cup, neuroblasts appear delaminating from the otic epithelium. (**E**) Otic vesicle. (**F**) Otocyst differentiation, the primordia of the different anatomical regions is indicated. **ED:** Endolymphatic duct, **S:** Saccule, **V:** Vestibuli, **C:** Cochlea (Torres & Giraldez, 1998).

1.3-Molecules and Tissues Implicated in Otocyst Formation

1.3.*1*-Role of the Rhombencephalon and Mesenchyme during the Earliest Events of Ear Development

There is evidence indicating that the process of gastrulation may, by bringing different tissues into contact with the presumptive otic ectoderm, play a major role in facilitating the inductive interactions that lead to inner ear formation (Noramly, et al., 2002). The close proximity of the developing otocyst to the hindbrain was shown to be essential during the early stage of otic development in the mouse, chick, amphibian and zebrafish (Li, *et al.*, 1978, Model, *et al.*, 1981). In a current model, the neural tissue seems to play a dual role in otic development. During early steps of otic induction it acts in concert with the mesodermal signals to initiate the otic development and at later stages it is essential for patterning and morphogenesis of the otocyst (Streit, 2001). Furthermore, it was suggested that neural genes may influence, directly or indirectly, the development of the inner ear by producing diffusible growth factors, since defects of ear morphogenesis were consistently associated with inherited neural tube defects (Deol, 1966). In chick, the ablation of the neural tube before HH 9 abrogates otic vesicle formation suggesting that the neural tube is necessary for otic vesicle formation (Giraldez, 1998). Natural mouse inner ear mutants and targeted gene inactivation experiments reveal that several transcription factors, which control diversification of hindbrain rhombomeres, also contribute to the formation of the inner ear (Rinkwitz, *et al.*, 2001). For instance, otic patterning defects are seen in mice and zebrafish mutants, which show a defective hindbrain. *Kreisler* is a regulatory gene expressed in r5/r6 involved in hindbrain segmentation (Marin, *et al.*, 2000). The *kreisler* and *valentino* (zebrafish homologue of kreisler) mutants show impaired differentiation of r5 and r6. In parallel, the patterning of the otic vesicle is aberrant and cochlear development is impaired, resulting in deafness and circling behavior due to the loss of vestibular function (Deol, 1964, Mendonsa, *et al.*, 1999). However, otic induction and early inner ear development are normal in these mutants. In turn FGF3, which is known to be expressed in r5 and r6 and to be important for otic development, was downregulated in *kreisler* mutants (McKay, *et al.*, 1994, McKay, *et al.*, 1996). Upon mutation of *Hoxa1* in mice, which is normally expressed in r 4-7, r4 is markedly reduced, whereas r5 is almost absent and the expression of FGF3 fails in the hindbrain (Pasqualetti, *et al.*, 2001). This mutant shows abnormal labyrinth development (Chisaka, *et al.*, 1992).

The mesenchyme may also be a source of factors that modulate the genetic influence of the hindbrain on the otocyst or acting independently (Van De Water, 1983). Yntema already

described an early mesodermal phase of otic induction followed by a later neural phase in axolotl. In parallel, the ectoderm displayed two cycles of competence to respond to mesoderm and neural activation (Yntema, 1950). In zebrafish, the prechordal cells are the first to involute during gastrulation and pass underneath the presumptive otic territory. Mutants with a deficiency in prechordal mesoderm show defective and delayed otocysts, indicating the importance of the mesoderm-ectoderm contact for otic induction (Mendonsa, *et al.,* 1999). In chick, the mesoderm invaginating through Hensen´s node, contributes to the head mesoderm below the presumptive otic placode and extirpation of the mesoendoderm of Hensen´s node leads to the complete lack of otic vesicle formation (Rosenquist, 1966). Recent molecular evidence from chick suggests that FGF19 from paraxial mesoderm cooperates with Wnt8c from the hindbrain to induce some otic placode markers and thickening of the placodal ectoderm (Ladher, *et al*., 2000).

The role of the mesoderm and neural tube in otic induction supports a two-step model of otic formation, in which initial induction occurs at late gastrula/early neurula stages via signals from mesendoderm, and later signals, probably emanating from the hindbrain, serve to reinforce the early induction and pattern the ear (Baker, 2001).

1.3.*2*-Early Genes Expression in the Developing Otocyst

In this study early otic gene expression were used to follow the otic program and to identify otic structures. Genes expressed during otic development encode transcription factors, diffusible molecules, receptors, and cell adhesion proteins belonging to families shown to play important roles in development. Initially, the winged helix transcription factor *BF1* (*Foxg1*, Kaestner *et al.,* 2000) is expressed at the placodal stage in all placode-derived cells (Hatini, *et al.*, 1999, Kaestner, *et al.*, 2000) (Table 1.1) and later in the otic vesicle (Hebert, *et al.*, 2000). Subsequently, the paired class homeobox transcription factor *Pax8* appears expressed in preotic cells during the second half of gastrulation as the earliest otic marker, in all vertebrates. The expression is maintained through early vesicle formation and subsequently lost. (Mansouri, *et al.*, 1998, Pfeffer, *et al.*, 1998, Heller, *et al.*, 1999, Solomon, *et al.*, 2003) (Table 1.1). Another transcription factor of this family, *Pax2,* is expressed by early somitogenesis in preotic cells and later confined to the ventromedial part of the otic vesicle, hair cells, and endolymphatic duct in mouse (Torres, *et al.*, 1996, Herbrand, *et al.*, 1998, Pfeffer, *et al*., 1998, Lawoko-Kerali, *et al.*, 2002). In chicken, *Pax2* is expressed in the otic placode, otocyst (dorsomedial

wall), and later in the endolymphatic duct and cochlea (Hutson, *et al.*, 1999) (Table 1.1). *Dlx5* is expressed also earlier in the preplacodal domain in chick and mouse and later it is confined to the dorsal otic vesicle (Acampora, *et al.*, 1999, Depew, *et al.*, 1999, Feledy, *et al.*, 1999, Pera, *et al.*, 1999, Luo, *et al.*, 2001). Limb homeobox transcription factor 1 (*Lmx1)* is expressed in chicken in the early otic field to be restricted later dorsolaterally during otic vesicle formation (Giraldez, 1998) (Table 1.1). The Eph receptors, a tyrosine kinase receptor (*sek1/cek8*) is also expressed at the placodal stage and in the otocyst in mouse (Nieto, *et al.*, 1992, Rinkwitz-Brandt, *et al.*, 1996) whereas in chicken it is expressed in the otic placode, dorsal otocyst and cochlear ganglion (Pickles, *et al.*, 1997) (Table 1.1).

Table 1.1: Expression of otic genes relevant for this study

Otic Genes	Expression Pattern	References
Transcription factor BF1 (mouse) (Brain factor 1 or Foxg1);	-Head surface ectoderm from the 6 ss. -E9.5: restricted to the placodes and placode-derived cells. - Otic vesicle	(Hatini, *et al.*, 1999, Hebert, *et al*., 2000, Kaestner, *et al.*, 2000)
Transcription factor Pax2 (mouse/chick)	-Otic placode and vesicle. -ED and cochlear duct -Sensory epithelium (HC) (mouse)	(Torres, *et al.,* 1996, Herbrand, et al., 1998, Pfeffer, *et al*., 1998, Hutson, *et al.,* 1999, Lawoko-Kerali, *et al.*, 2002).
Transcription factor Lmx1 (chick)	-Prospective otic region at the 4-5 ss -Otic vesicle.	(Giraldez, 1998)
Tyrosine kinase receptor sek1/cek8 (mouse/chick)	-Otic placode and vesicle (mice and chicken) -Later in the vestibular epithelium and cochlea (mouse) -Cochlear nerve (chicken)	(Nieto, *et al*., 1992, Rinkwitz-Brandt, *et a*l., 1996, Pickles, *et al.*, 1997, Torres & Giraldez, 1998).

1.4-The Role of Fibroblast Growth Factors (FGFs)

The fibroblast growth factor (FGF) family constitutes one of the most important groups of paracrine factors that act during development. They are diffusible molecules that are widely involved in cellular migration, proliferation, and differentiation (Spivak-Kroizman*, et al.*, 1994, Ornitz*, et al.*, 2001, Pickles*, et al.*, 2002).

The FGF family consists of at least 22 structurally related polypeptide growth factors, which share 13-71% amino acid identity. Among vertebrate species these molecules are highly conserved in both gene sequences and structure. FGFs signal via four known receptors (FGFRs 1-4), which contain three extracellular immunoglobulin-like (Ig) loops, the third of which contains the FGF binding site. In FGFRs 1-3 the FGF binding site is subject of splice variation. Some FGFs show a greater affinity to certain splice variants (Pickles, et al., 2002). FGFs often signal directionally and reciprocally across epithelial-mesenchymal boundaries (Hogan, 1999). The binding (factor-receptor) causes two receptor molecules to dimerize, which activates their intracellular protein tyrosine kinase domains. The kinase activity initiates downstream intracellular signaling to finally activate transcription factors in the nucleus. The efficacy of FGFs-FGFRs binding is aided by the presence of specific heparan sulphate proteoglycans (HSPGs), which bind both to the FGFR and to the FGFs, increasing the concentration of FGFs at the receptor and stabilizing FGFs against thermal denaturation and proteolysis (Spivak-Kroizman, et al., 1994).

The different subfamilies of FGFs tend to have a similar expression pattern and some of them such as FGF3, FGF4, FGF8, FGF15, FGF17 and FGF19 are expressed exclusively during embryonic development, whereas others are expressed in embryonic as well as in adult tissues. Because FGFs within a subfamily have similar receptor-binding properties and overlapping patterns of expression, functional redundancy is likely to occur (Ornitz, et al., 2001).

1.4.*1*-Gene Organization of FGFs

In order to discuss genetic inactivation of different FGFs, which is part of the present work, it is necessary to shortly summarize their genomic structures.

The prototypical FGF gene contains three coding exons, with exon 1 containing the initiation methionine, although several FGF genes (as FGF2 and FGF3) have an additional 5′ transcribed sequence that is initiated upstream from the CUG codon. Exon 1 is subdivided into 1-4 alternatively spliced subexons, but a single initiation codon (ATG) in exon 1A is

used. This organization is conserved in human, mouse and zebrafish. Several FGF genes are clustered within the genome. FGF3, FGF4 and FGF19 are located in humans on chromosome 11q13 separated by only 40 and 10 kb, respectively. These gene locations indicate that the FGF gene family was very likely generated both by gene and chromosomal duplications and translocations during evolution (Ornitz, *et al.*, 2001).

Because of the functional redundancy that occurs among FGF family members, ascertaining a precise role for individual FGFs is difficult (Karabagli, *et al.*, 2002). Therefore, a combination of mutated FGFs alleles has to be generated to overcome redundancy.

1.4.*2*-FGFs During Inner Ear Development

Several secreted factors have been described as otic inducers in a variety of organisms. With one exception they all belong to the FGF family. The expression patterns of several members of the FGF family, including FGF2, FGF3, FGF8, FGF10 and FGF19 (in chicken) together with experimental manipulations have shown the implication of these factors during different stages of inner ear formation (Baker, 2001, Rinkwitz, et al., 2001, Noramly, *et al.*, 2002). In different species FGFs are reported to be implicated in otic formation such as FGF3 and FGF8 in fish (Reifers, *et al.*, 1998, Phillips, *et al.*, 2001, Maroon, *et al.*, 2002, Liu, et al., 2003), FGF2 and FGF3 in amphibians (Lombardo, *et al.*, 1998), FGF3, FGF19 and Wnt8c in birds (Wilkinson, *et al.*, 1989, Represa, *et al.*, 1991, Ladher, et al., 2000, Vendrell, et al., 2000), and FGF3 and FGF10 in mammals (Mansour, et al., 1993, Pirvola, et al., 2000, Brown, *et al.*, 2003, Pauley, et al., 2003).

1.4.*2.1*-Fibroblast Growth Factor 2

In chicken and mice, FGF2 is expressed in otic placode and vesicle (Frenz, *et al.*, 1994, Vendrell, *et al.*, 2000) and during later embryogenesis it is also found in the developing inner ear (Pickles, et al., 1997, Pickles, 2001). After birth it is detected in chicken in the sensory epithelium (Pickles, et al., 1997) and supporting cells (Lee, *et al.*, 1996). For instance, in chicken FGF2 has been proposed to participate in stimulating cell differentiation in inner ear epithelia (Oesterle, *et al.*, 2000). Moreover, FGF2 has been shown to induce formation of otic tissue in *Xenopus* (Lombardo, *et al.*, 1998). However, overexpression of FGF2 by viral infection on chicken ectoderm shows no capacity of otic induction (Vendrell, *et al.*, 2000). In contrast, Adamska *et al.*

showed ectopic patches of cells expressing otic markers by applying FGF2-soaked beads (Adamska, *et al*., 2001). The role of FGF2 in the otic development remains still unclear.

1.4.*2.2*-Fibroblast Growth Factor 3

FGF3 has been postulated as the earliest candidate to play a role during early inner ear induction, based on its expression in the developing hindbrain next to the forming inner ear (Wilkinson, *et al*., 1988), which is conserved among species including avian (Mahmood, *et al*., 1995), amphibians (Lombardo, *et al*., 1998), and fish (Phillips, *et al*., 2001). At E8.5 FGF3 is expressed in the cranial surface ectodermal domain that includes the otic placode and pharyngeal endoderm of the second and third arches (Mahmood, *et al*., 1996). At E9.5 the expression of FGF3 is detected in the hindbrain adjacent to the developing otic structures. At E10.5 FGF3 appeared in the otic vesicle, in the area destined to form the sensory organ of the vestibular system. At E17.5 FGF3 was expressed in the developing sensory regions, both in sensory hair and supporting cells (Table 1.2). Due to this pattern of expression FGF3 was suggested to have two distinct roles in the formation of the inner ear: as a morphogenetic signal coming from the hindbrain and later as a factor involved in sensory cell differentiation and/or innervation (Wilkinson, *et al*., 1988, Wilkinson, *et al*., 1989, Mahmood, *et al.,* 1996).

An FGF3 mouse mutant, in which the coding region was interrupted by a neomycin resistance gene via homologous recombination (Mansour, *et al.,* 1993), showed defects in the morphogenesis and differentiation of the inner ear, but not during otic induction, thus arguing against an early inductive role of FGF3. However, the mutant phenotype had reduced penetrance and expressivity. Therefore, the consequences of a loss of FGF3 function for mouse inner ear development may not have been fully explored.

In chicken embryos FGF3 is expressed in the hindbrain (r4 and r5) and in the developing pharyngeal endoderm but not in the otic vesicle (Mahmood, *et al.*, 1995). The overexpression of FGF3 via viral infection in the head and trunk ectoderm resulted in the formation of ectopic otic vesicles, which expressed otic markers (Table 1.2) (Vendrell, *et al.*, 2000). In the same species, FGF3 expression was induced by another FGF family member, FGF19, which together with Wnt8c and possibly FGF3 itself, act as synergistic signals to induce the otic placode (Ladher, *et al.,* 2000). In *Xenopus,* the capacity of FGF2 and FGF3 to induce ectopic otic vesicles has been reported (Lombardo, *et al.,* 1998).

In zebrafish, FGF3 was also implicated in otic placode induction and epithelial organization of the otic vesicle redundantly with FGF8 (Phillips, et al., 2001, Maroon*, et al.*, 2002, Liu, et al., 2003).

1.4.*2.3*-Fibroblast Growth Factor 8

Another member of the FGF family that is involved in otic development in different species is FGF8. In zebrafish FGF8 is coexpressed with FGF3 in the hindbrain and they play redundant roles in otic induction. Upon injection of either FGF3 or FGF8 antisense morpholinos as well as in the FGF8 mutant (*acerebellar*) a reduction of early placodal markers and of the size of the otic vesicle was observed. The loss of both FGFs resulted in a block of otic vesicle induction (Phillips, et al., 2001, Maroon, et al., 2002). Later in the developing otocyst FGF3 and FGF8 are coexpressed in zebrafish in utricular macula (Leger*, et al.*, 2002) (Table 1.2).

In chick, FGF8 is expressed during early stages in mesoderm and the primitive streak. Interestingly for otic induction, FGF8 is expressed in the mesoderm underlying r2 to r6 at the HH 8+ (Shamim*, et al.*, 1999); in the pharyngeal endoderm of the branchial arch around stage HH 10 (Stolte*, et al.*, 2002); within the otic placode (Adamska, *et al.*, 2001); and transiently in the cells of the otocyst, which delaminate to form the otic ganglia (Hidalgo-Sánchez*, et al.*, 2000) (Table 1.2). In chick, the ectopic application of FGF8 via soaked beads led to an increased expression of otic markers such as *Nkx5-1 or SOHo1* suggesting its role in otic patterning (Adamska, *et al.*, 2001).

In mice, expression of FGF8 has been found in the developing head, in the pharyngeal region (pouches, arches and grooves) which give rise to many components of the face including middle and outer ears. At E8 is detected in the foregut endoderm, overlaying endoderm and intervening lateral mesoderm in the proximity of the developing otic placode.(Crossley*, et al.*, 1995). Later, in the developing mouse inner ear, FGF8 is expressed in the otic epithelium and delaminating neuroblasts at E13.5 (Pirvola*, et al.*, 2002), at E14.5 in the developing labyrinth (Crossley, *et al.,* 1995) and at E16.5 in IHCs (Pirvola, *et al.,* 2002) (Table 1.2). Unfortunately, FGF8 null mutant mice die around E9.5 due to severe gastrulation defects prior to otic development (Meyers, et al., 1998). Therefore, the functions of FGF8 during inner ear development have not been assessed.

In comparison to the evidence present for FGF3 being an important early otic inducer, an inductive role of FGF8 is not well documented in higher vertebrates. Conditional inactivation

of FGF8 in mice or loss-of-function experiments in other species could clarify the role of FGF8 during otic induction.

1.4.*2.4*-Fibroblast Growth Factor 10

FGF10 has been also implicated in inner ear formation. FGF10 is expressed early during embryonic development in the ectoderm before otic vesicle formation, suggesting a role in otic induction (Noramly, *et al*., 2002). In mice, FGF10 is detected early in mesenchyme adjacent to the otic placode and in the hindbrain next to the area where the otic placode and vesicle develop (Alvarez, *et al*., 2003, Wright, *et al*., 2003). FGF10 appears later in the otic cup and its neuronal derivatives (Pirvola, *et al*., 2000) as well as later in the cochlear anlage, the three canal crista sensory epithelia and all sensory neurons (Pauley, et al., 2003) (Table 1.2). The phenotype of mice carrying an FGF10 null mutation confirmed a role of FGF10 during otic development, since FGF10 deficient mice show morphogenetic and innervation abnormalities of the developing otocyst (Ohuchi, *et al*., 2000, Pauley, et al., 2003). Both FGF10 and FGF3 are known to activate the IIIb isoform of the FGFR2 receptor, which is also expressed during early otocyst formation (Pirvola, *et al.*, 2000) and alternatively the FGFR1b (Ornitz, *et al*., 1996, Beer, *et al*., 2000, Pirvola, *et al*., 2002).

The expression of these factors coincides spatially and temporally with otic induction and morphogenesis So far FGF3, FGF8 and FGF10 seem to be involved in different processes during otic formation in different species. Importantly, the expression of FGF3 and FGF10 are overlapping in otic domains as well as FGF3 and FGF8 suggesting possible redundancy between these factors. The Table 1.2 summarizes the endogenous expression of FGFs and evidences that implicate FGF signaling in otic formation.

Table 1.2: Summary of gene expression patterns and existing mutants for FGF3, FGF8 and FGF10.

		FGF3	FGF8	FGF10
EXPRESSION	Hindbrain	_In chicken, mice, zebrafish and *Xenopus* between r3-r6. *(Wilkinson, et al., 1988, Mahmood, et al., 1995, Lombardo, et al., 1998, Phillips, et al., 2001)*	**Zebrafish** _Coexpressed with FGF3 in the hindbrain (r4) *(Phillips, et al., 2001)*	**Mice** _Hindbrain close to the developing otic placode and OV. *(Alvarez, et al., 2003)*
	Mesoderm or Endoderm	**Chicken** _Pharyngeal endoderm and mesoderm. *(Mahmood, et al., 1995)* **Mice** _Pharyngeal endoderm of the second and third arches (Mahmood, *et al.*, 1996)	**Chicken** _Mesoderm underlying r2 to r6 at the 6ss *(Shamim, et al., 1999)* _Pharyngeal endoderm of the branchial arches (2 and 3) *(Stolte, et al., 2002)* **Mice** _Foregut endoderm, adjacent ectoderm and mesoderm. *(Crossley, et al., 1995)*	**Mice** _Anterior and ventral mesenchyme. *(Alvarez, et al., 2003, Wright, et al., 2003)*
	Otic Placode	**Mice** _In otic placode *(Mahmood, et al., 1996, McKay, et al., 1996)*	**Chicken** _In otic placode *(Adamska, et al., 2001).*	**Mice** _Ectoderm before OV formation. *(Noramly, et al., 2002)*
	Otic Vesicle (OV)	**Mice** _Anterior otocyst. _Cells delaminating to form the otic ganglion. *(Mahmood, et al., 1996, McKay, et al., 1996, Pirvola, et al., 2000)*	**Chicken** _Cell delaminating to form otic ganglia *(Hidalgo-Sánchez, et al., 2000, Adamska, et al., 2001)*	**Mice** _Otic cup and OV (anterior, ventrolateral and medial wall) _Migrating neuronal derivatives. *(Pirvola, et al., 2000).*
	Developing Inner Ear	**Zebrafish** _Nascent utricular macula. *(Leger, et al., 2002)* **Mice** _Sensory regions (semicircular canals, utricle, saccule and cochlea) *(Wilkinson, et al., 1988, Wilkinson, et al., 1989)* _IHCs *(Pirvola, et al., 2000)*	**Zebrafish** _Nascent utricular and saccular macula and cristae. *(Leger, et al., 2002)* **Mice** _Otic epithelium and delaminating neuroblasts *(Pirvola, et al., 2002)* _Developing labyrinth and IHCs *(Crossley, et al., 1995, Pirvola, et al., 2002)*	**Mice** _Cochlear anlage, migrating neurons, cochleovestibular ganglion. *(Pirvola, et al., 2000)* _The three patches which form the canal crista, and sensory vestibular epithelia *(Pauley, et al., 2003).*
GAIN-OF-FUNCTION		**Chicken** _Ectopic OV by ectodermal viral infection *(Vendrell, et al., 2000)* **Described in this work** (chicken)	**Chicken** _ Expanded OV and expression of otic markers by bead implantation: *(Adamska, et al., 2001)* **Described in this work** (chicken)	**Described in this work** (Chicken)
LOSS-OF-FUNCTION		**Mice** _*Fgf3neo*: defects in inner ear morphogenesis and differentiation *(Mansour, et al., 1993).* **Zebrafish** _Morpholino- injection. Reduced OV and otic marker expression. *(Liu et al., 2003a; Maroon et al., 2002; Phillips et al., 2001; Reifers et al., 1998)* **Described in this work** (mice and chicken)	**Mice** _Null mutants die prior to otic development *(Meyers, et al., 1998)* **Zebrafish**: _Morpholino- injection and Hypomorphic mutation. Reduced OV and otic marker expression. *(Reifers, et al., 1998, Phillips, et al., 2001, Maroon, et al., 2002, Liu, et al., 2003)* **Described in this work** (mice)	**Mice** _Null mutation. Agenesis of the posterior canal and crista, altered anterior and lateral crista and reduced canals and altered utricular macula, innervation abnormalities *(Ohuchi, et al., 2000, Pauley, et al., 2003).* **Described in this work** (mice)

1.5-Genetically Modified Organisms (GMOs)

To analyze developmental processes we have taken advantage of different tools in order to change temporally or permanently the gene expression of an organism. In general, two approaches are appropriated to elucidate gene function during development: gain- or loss-of-function approach (Griffiths, *et al*., 1999). In the present work different techniques including manipulations of chick and mouse embryos have been used.

1.5.*1*-Transgenic Mice

One typical example for a gain-of-function approach is the creation of a transgenic mouse lines by injecting modified DNA constructs into fertilized mouse eggs. The injected DNA may be integrated into the genomic DNA and thus may find its way into germ-line cells. The effect of the expression of the genes introduced via this construct can then be analyzed in the progeny (Griffiths, et al., 1999).

Knockout approaches have been very successful in recent years to study gene function during development by either removing the whole coding sequence or interrupting the gene to produce a non-functional protein. In mice the so-called knockout (ko) technique or gene targeting involves the introduction of a mutation by homologous recombination replacing the endogenous gene with a modified non-functional copy in embryonic stem (ES) cells (Griffiths, et al., 1999).

Conditional ko: Some conventional ko mutations cause lethality during embryogenesis and therefore are not useful for studying gene function due to early embryonic death. To overcome this problem, methods that inactivate expression of a target gene at certain time point and/or in only some selected cells have been developed. Thus the animal can survive and the effect of the ko gene can be studied in a tissue or cell type of interest (Griffiths, et al., 1999). This is possible by directing the expression of a recombinase in a specific tissue of interest using a tissue-specific promoter or enhancer. Thus far, the established Cre-*loxP* and Flp-*FRT* system have been widely used to inactivate genes in a temporal or tissue-specific manner (Sauer, 1998, Zuo, 2002). The natural function of Cre recombinase is to mediate recombination between two *loxP* sequences that are in the same orientation. As a result, the sequence in flanked by *lox-P* sites is excised. Another used recombinase is Flp which also mediates recombination by recognizing two *FRT* sites. To illustrate the conditional ko strategy we explain next the creation of the FGF8 mutant generated by Cre- and Flp-mediated

recombination (Meyers, et al., 1998). This ko was used in the present work to study inner ear development.

To produce an FGF8 allele that can be modified by both Cre- and Flp-mediated recombination, a construct containing the following insertion was created: one *loxP* site inserted in the intron upstream of exon 2 and another one in the 3´-unstranslated region (UTR) to "flox" (**fl**ank with l**ox**P sites) the *Fgf8* coding region in the exons 2 and 3; a neomycin-resistance (*neo*) expression cassette **fl**anked by f**rt** sited "flrted" was inserted upstream of the 5´*loxP* site (Fig. 1.8) (Meyers, et al., 1998). Mice carrying the targeted allele, $Fgf8^{neo}$ (Fig 10) can be mated to Cre and Flp transgenic mice to generate animals containing the "floxed" allele or the $Fgf8^{\Delta 2,3}$ null allele (Fig.1.8). For example, the *Foxg1 (BF1-Brain Factor 1)-Cre* transgenic line can be used to inactivate FGF8 during early stages of inner ear development in mice (Meyers, et al., 1998, Hebert, et al., 2000). The strategy described above is also shown in Figure 1.8 in detail.

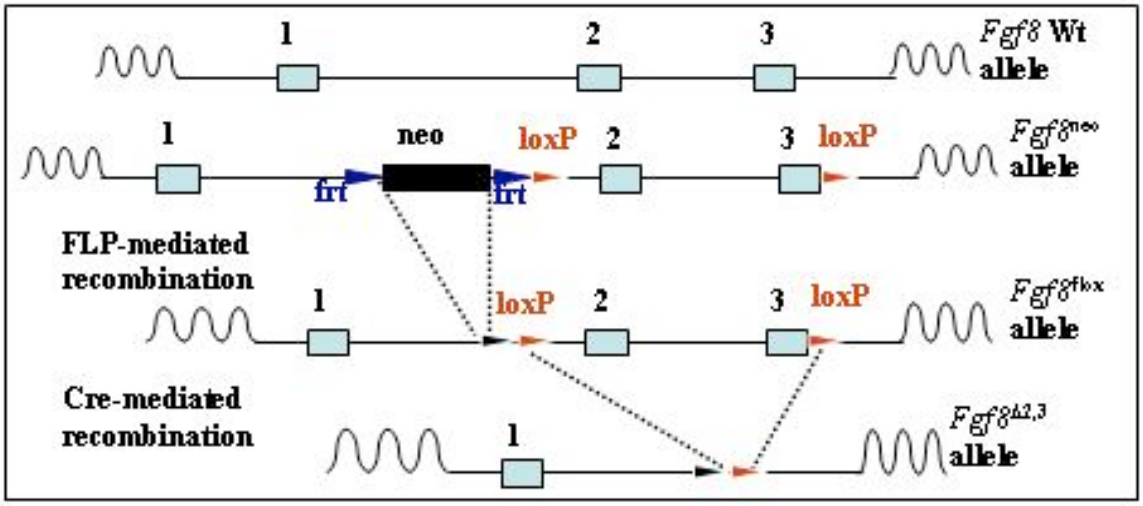

Figure 1.8: *Fgf8* mouse mutant. The first line shows the wt *Fgf8* allele and the second line the targeted allele, $Fgf8^{neo}$. After mating with Flp transgenic mice, an hypomorphic mutant is created in which *neo* is removed (Meyers, *et al.*, 1998). After crossing with Cre transgenic mice, the null allele $Fgf8^{\Delta 2,3}$ is obtained. (Scheme from Meyers et al., 1998)

1.5.*2*-Manipulating Chick Embryos: *In ovo* Electroporation

In chicken embryos, several techniques have been successfully used to transfer foreign genes to somatic cells including viral vectors, *in ovo* lipofection, microparticle bombardment and electroporation (Muramatsu, *et al.*, 1997). The great advantage of the chicken embryo is its easy accessibility from pregastrulation throughout all developmental stages, offering the possibility

for *in ovo* manipulations. Maramatsu *et al.* (1997) first showed that electroporation could induce misexpression of certain genes in chick embryos (Muramatsu, *et al.*, 1997). Later the conditions were established for efficient ectopic expression of genes (Nakamura, *et al.*, 2000).
Gene expression by electroporation is a straightforward method, requiring only a plasmid carrying the desired cDNA under the control of a suitable promoter. Electroporation is more effective and quicker than viral infection or lipoinfection since it obviates the need for preparation of high titers of virus particles. In addition, while electroporation has initially been technically difficult in very early stage embryos, the use of flat electrodes and a new culture system has made it possible to transfer genes to embryos at the primitive streak stage (Takeuchi, *et al.*, 1999, Yasuda, *et al.*, 2000, Kobayashi, *et al.*, 2002, Sugiyama, *et al.*, 2003).

1.5.*2.1*-Antisense Morpholinos in Chicken

Recently morpholino antisense oligonucleotides, that have proven to be very effective in zebrafish embryos, have been shown to efficiently silence gene expression in chick embryos (Kos, *et al.*, 2001, Kos, *et al.*, 2003, Sheng, *et al.*, 2003, Sugiyama, *et al.*, 2003). These oligos are termed morpholino because they are assembled from four different Morpholino subunits, each of which contains one of the four genetic bases (Adenine, Cytosine, Guanine, and Thymine) linked to a 6-membered Morpholino ring. They must be conjugated with FITC (Fluorescein Isothiocynate) to be positively charged before they can be transferred by electroporation. Since morpholinos only interfere with protein translation, antibodies against the molecule of interest for evaluation of gene silencing are required.

1.5.*2.2*-Small Interference RNA (siRNA)

Today a very promising tool is the application of double-strand RNA (dsRNA). It was shown that dsRNA triggers homologous gene silencing by a mechanism termed RNA-mediated interference (RNAi), and has been successfully tested as a powerful gene silencing tool in *Caenorhadbitis elegans* and *Drosophila*. Recently, gene silencing by the introduction of a siRNA expression vector via electroporation has become possible (Katahira, *et al.*, 2003).
The basic mechanism of RNAi is thought to be a multi-step process that takes place intracellulary. siRNA are 21 to 23 nucleotide long oligonucleotides with 3´overhanging ends which are generated by a ribonuclease III called Dicer (Fig. 1.9). siRNA binds to an

enzymatic complex called RNA Induced Silencing Complex (RISC) to induce the degradation of RNA homologous to the short sequences that have been recognized by siRNA (Fig. 1.9). In mammals, however, dsRNA provokes a strong cytotoxic response (Baglioni, *et al.*, 1983, Williams, 1999), which can be overcome by using synthetic short 19- to 21-nucleotides interfering RNA (siRNA) (Fig. 1.9) (Elbashir, *et al.*, 2001). Recently, it was shown that short hairpin dsRNA (shRNA) exerts RNAi effects. A vector for shRNA expression, which has an RNA polymerase III promoter (the U6 or H1 promoter) has been developed (Svoboda, *et al.*, 2001, Brummelkamp, *et al.*, 2002, Paddison, *et al.*, 2002, Sui, *et al.*, 2002, Yu, *et al.*, 2002). The advantage of transfecting a vector instead of a short sequence of RNA is a longer duration of inhibition due to the maintenance of expression of the vector since the plasmid is not degraded as rapidly as simple RNA. Some guidelines have been defined to improve the efficiency of correct gene targeting (Elbashir, *et al.*, 2001, Khvorova, *et al.*, 2003, Semizarov, *et al.*, 2003). A BLAST search should be carried out to avoid binding to non-target mRNAs. Gene knockdown by vector-based siRNA introduced by *in ovo* electroporation in chick embryos has been performed (Katahira, *et al.*, 2003) and was shown to be effective for the study of gene expression cascades (Kimura, *et al.*, 2004).

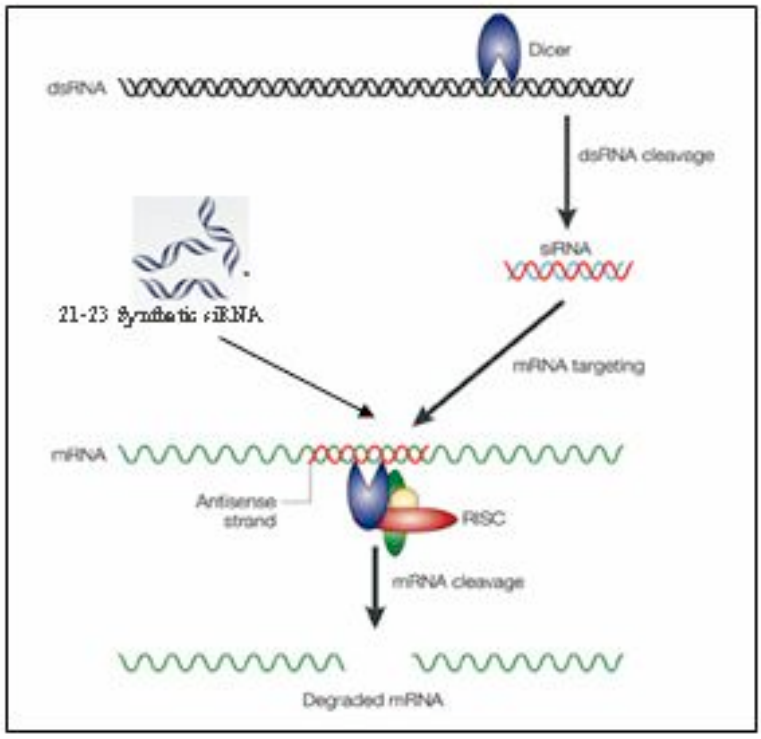

Figure 1.9: A model for RNA interference in mammalian cells. RNAi can be initiated by synthetic siRNAs or by dsRNA, which is cleaved into siRNAs by Dicer. The siRNAs are incorporated into the RISC complex. The antisense strand guides target recognition and cleavage of the target mRNA. (McManus, *et al.*, 2002)

1.6-Rationale and Hypothesis

Several members of the FGF family have been described to be involved in the inner ear formation in different species, but the exact role of these members and the molecular pathways acting to execute this developmental program are not fully understood.

FGFs such as FGF2, FGF3, FGF8 and FGF10 are known to be expressed during induction and morphogenesis of the inner ear. One of the aims of this study is to assess the role of these factors during inner ear development in mice and chicken. For this purpose, gain- and loss-of-function experiments are carried out on both species.

FGF3 expression pattern suggested its participation in the otic formation, to elucidate its *in vivo* function; *Fgf3* null mutant mice are analyzed in this study. FGFs are known to compensate for each other during organ development. Since *Fgf10* expression coincides partially with *Fgf3* expression in hindbrain and developing otocyst, the subsequent goal in this study is to investigate the otocyst development in double *Fgf3*/*Fgf10* mutants.

FGF8 is also expressed during inner ear formation, but the null *Fgf8* mutants die at early embryonic stages. Therefore, to study otic development, mice with a conditional inactivation of this gene in the otic placode and vesicle are studied. Partially overlapping expression of FGF3 and FGF8 occurs at different stages of the inner ear development indicating redundant functions between these two factors. To test this possibility double *Fgf3*/*Fgf8* mutants are investigated.

Additionally, to ascertain the participation of FGF3, FGF10 and FGF8 during inner ear formation in avian and to establish possible conserved mechanism between birds and mammals, gain- and loss-of-function experiments are performed by using *in ovo* electroporation in chicken embryos.

II-RESULTS

2.1-Loss-of-Function Approach in Mice

The importance of FGFs has been revealed by analyzing mice lacking different FGF or FGFR genes such as *Fgf3, Fgf10, Fgfr2IIIb or Fgfr1*, which exhibit defects in the patterning and differentiation of the inner ear (Mansour, *et a*l., 1993, De Moerlooze*, et al.*, 2000, Ohuchi, *et al*., 2000, Pirvola, *et al.*, 2000, Pirvola, *et al.*, 2002). The function of different members of the FGF family in mice by creating single and compound null mutants and combining them to test possible redundant functions between members of the FGF family was analyzed further in the present study.

2.1.*1*-Analysis of Mice Lacking the Entire *Fgf3*-Coding Region

Fgf3 homozygous mutants have been already reported to have defects in tail formation and differentiation of the inner ear (Mansour, *et al.,* 1993). The creation of the *Fgf3* mutant strain described in the mentioned analysis has been based on $Fgf3^{neo}$ mutant mice, in which the neo^{r} gene had been inserted into exon 1b several codons downstream from the signal peptide-coding sequence (Mansour, *et al.*, 1993). However, the analysis of these mice has been complicated by the fact that fewer than 50% of the expected homozygous mutants were recovered postnatally, and that the observed inner ear phenotype showed variation in both penetrance and expressivity. Most importantly, the expression of *Fgf3* could not entirely be excluded (Mansour, *et al.*, 1993). Therefore, the results may be explained by leaky expression of the mutant *Fgf3* allele.

In order to define further the *in vivo* function of FGF3 and to avoid any interference caused by remnants of its coding region, a new mutant *Fgf3* allele devoid of all *Fgf3*-coding sequences was generated in our lab before I joined the research group. A *Fgf3* null mutant has been created in our lab by homologous recombination, where the sequences contained in exons 1b, 2 and 3 of the *Fgf3* gene were replaced by a cDNA encoding *Fgf3* and a neomycin resistance gene (neo^{r}) flanked by *loxP* sites (Fig. 2.1). Subsequently, the cDNA and the neo^{r} gene were removed by Cre-mediated deletion between the external *loxP*-sites (deletion type I, Fig. 2.1) present in the targeted locus to create heterozygous $Fgf3^{+/\Delta}$ animals. By crossing heterozygous $Fgf3^{+/\Delta}$ mice homozygous $Fgf3^{\Delta/\Delta}$ mutant embryos were produced which lacked *Fgf3* expression as assayed through whole-mount RNA in situ

hybridization (data not shown). Another type of deletion (deletion type II) was obtained after Cre-mediated deletion between the *loxP*-sites flanking the *Fgf3* cDNA. In these mutants the *neo*^{r} gene replaces the *Fgf3* gene (see Fig. 2.7). Fidelity of the targeting event in embryonic stem cells and subsequent Cre-mediated excision was demonstrated by Southern blots and PCR (data not shown) (Alvarez, *et al.*, 2003).

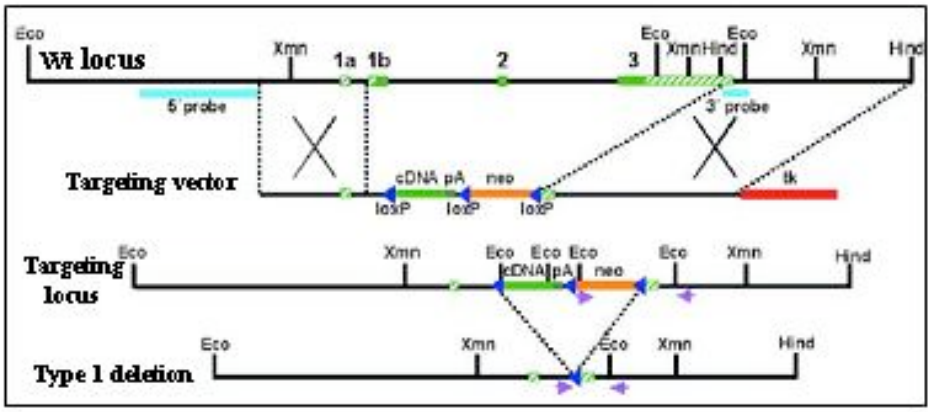

Figure 2.1: Deletion of the *Fgf3*-coding region in mice. The genomic locus with the exons and coding regions of the *Fgf3* gene is indicated. The coding region was replaced by a *Fgf3* cDNA and a *neo*^{r} gene flanked by *loxP*-sites by homologous recombination and removed by Cre-mediated excision to obtain two kinds of deletion: Type I (*Fgf3*$^{-/-}$) indicated in the figure above and Type II (*Fgf3* $^{neo/neo}$).

Fgf3$^{-/-}$ mice lacking the entire coding region for *Fgf3* were found to be viable and fertile. Phenotypically they could be distinguished due to their shortened, thickened and curved tail (see details in Fig. 2.2) observed from E11 onwards, which was also reported for *Fgf3* ^{neo} (Mansour, *et al.,* 1993).

Figure 2.2: Wild-type (wt) and mutant *Fgf3*$^{-/-}$ adult mice. The *Fgf3*$^{-/-}$ mice are clearly distinguishable from the wt animal due to the curved tail. This defect is due to the disruption of *Fgf3* expression in the primitive streak region which gives rise to the tail bud and forms the posterior vertebrae. The last vertebrae are fused in these mutants.

.

For further analysis of the inner ear, a detailed histological analysis of the developing inner ear during embryogenesis from the otic vesicle stage until adulthood of these mutants was performed. The structures were visualized by Toluidine Blue staining, a metachromatic blue nuclear stain (see methods 5.8.1.*1*). In the *Fgf3*$^{-/-}$ mutant embryos (*n*=40) (Table 2.1), the otic vesicle appeared slightly smaller than the otocyst of comparable age-matched littermates at E10.5 (Fig.2.3A). However, upon analysis of older embryos (E11.5 and E13.5), differences of the otic vesicle in comparison with the wt littermates were not found (Fig.2.3B, C). At E13.5 it is possible to identify all the structures present in a wt developing inner ear such as the endolymphatic duct, posterior and lateral canals, utricle, saccule and cochleovestibular ganglia (Fig. 2.3C).

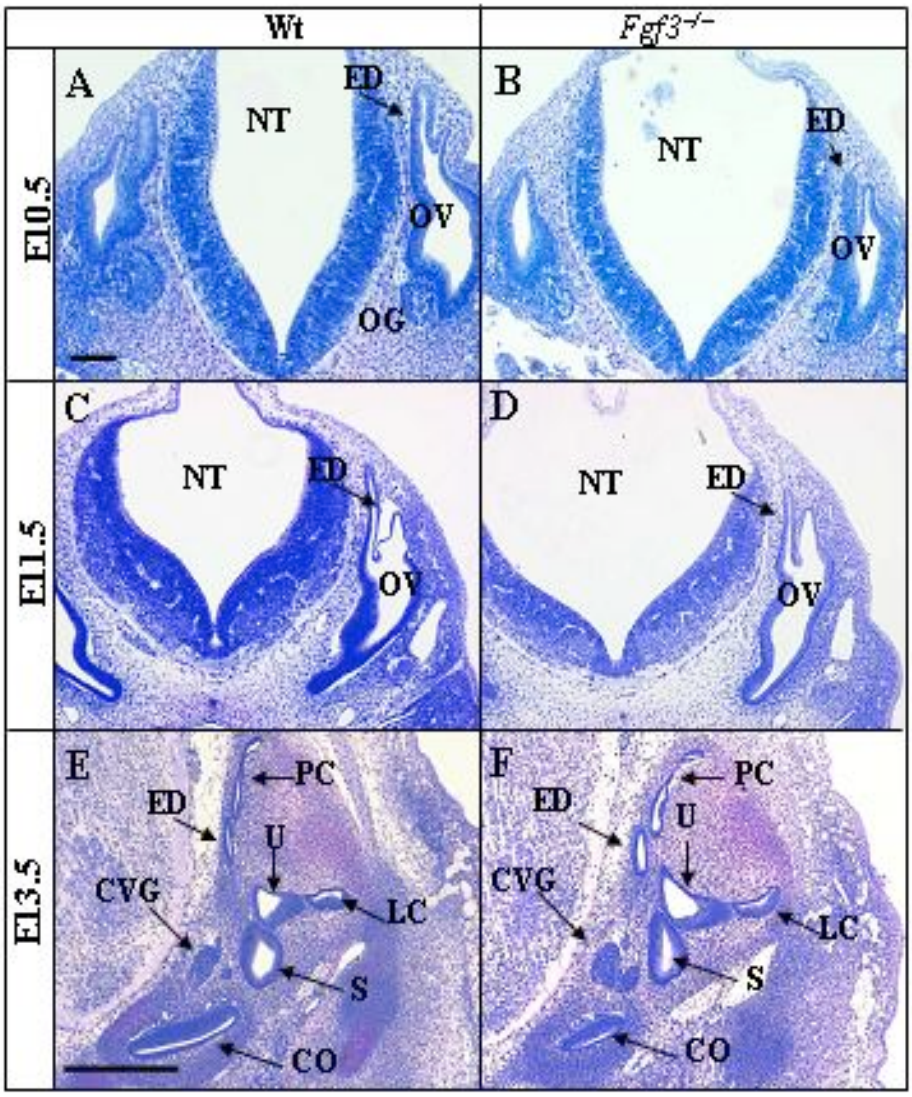

Figure 2.3: Sections of the developing inner ear of wt and *Fgf3*$^{-/-}$ mutant mice at different stages stained with Toluidine Blue. **A** (wt) and **B** (*Fgf3*$^{-/-}$) Embryos at E10.5. In B the mutant shows a slightly smaller otocyst in comparison with A. **C** (wt) and **D** (*Fgf3*$^{-/-}$) Embryos at E11.5 and **E** (wt) and **F** (*Fgf3*$^{-/-}$) at E13.5 showing normally developed inner ears. Observe in F that all the inner ear

structures present at this stage are normal. **CO:** cochlea; **CVG:** cochleovestibular ganglia; **ED:** endolymphatic duct; **LC:** lateral semicircular canal; **NT:** neural tube; **OG:** otic ganglia; **OV:** otic vesicle; **PC:** posterior semicircular canal; **S:** saccule; **U:** utricle. Scale bar in A=200 µm for A-B; bar in E=200 µm for E and F.

Furthermore, to investigate whether all the structures of the inner ear were present and normally developed at the three dimensional level, the white latex paint-filling technique (see methods 5.8.2) was used. After dissection of adult inner ears white latex paint was injected into the ears of wt and mutant mice (*n*=8). The contrast created by the paint allows us to analyze the whole shape of the bony cavity. Major defects in the *Fgf3*$^{-/-}$ mutant when compared with the wt (for details see Fig. 2.4) were not observed.

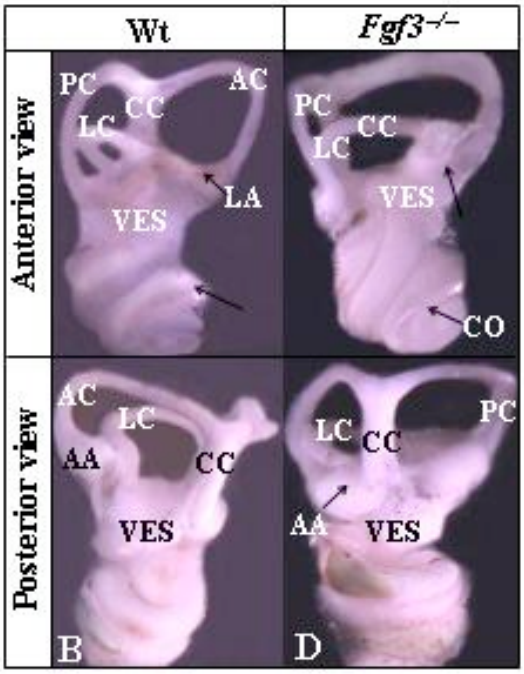

Figure 2.4: Paint-filled wt (**A,B**) and *Fgf3*$^{-/-}$ (**C**,**D**) adult inner ear. Compare the anterior and posterior view of the mutant ears with the wt inner ear. Canals, vestibule and cochlea are present in the wt. **AA:** anterior ampulla; **AC:** anterior semicircular canal; **CC:** common cross; **CO:** cochlea; **LA:** lateral ampulla; **LC:** lateral semicircular canal; **PC:** posterior semicircular canal; **VES**: vestibule.

Since the endolymphatic duct could not be visualized by paint filling in adult inner ear, the same technique was applied to inner ears from E14 mutant embryos. The endolymphatic duct was found to be normally developed in the *Fgf3*$^{-/-}$ mutants (Fig. 2.5).

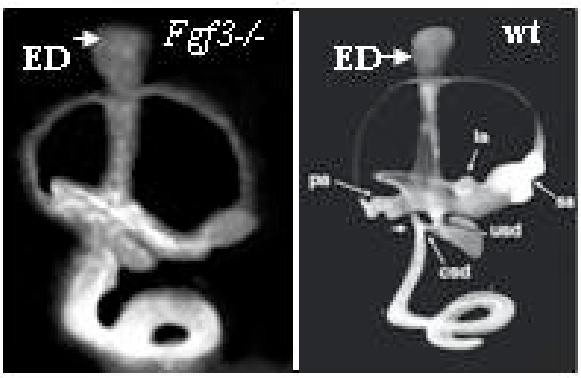

Figure 2.5: Paint-filling of developing otocyst at E14. (**A**) Observe the presence of the endolymphatic duct in the *Fgf3*$^{-/-}$ mutant. (**B**) Control paint filling (Morsli, *et al.*, 1998).

Next, the mutants were tested for Preyer´s reflex and by audiometry (see methods 5.12). All the mutants that have been tested had a normal Preyer´s reflex and normal hearing (data not shown). A histological analysis of the mutant adult inner ears (*n*=10) was performed. This analysis revealed a normal histological architecture of the whole inner ear and the presence of all cellular structures within the organ of Corti; vestibule and semicircular canals (see details in Fig. 2.6).

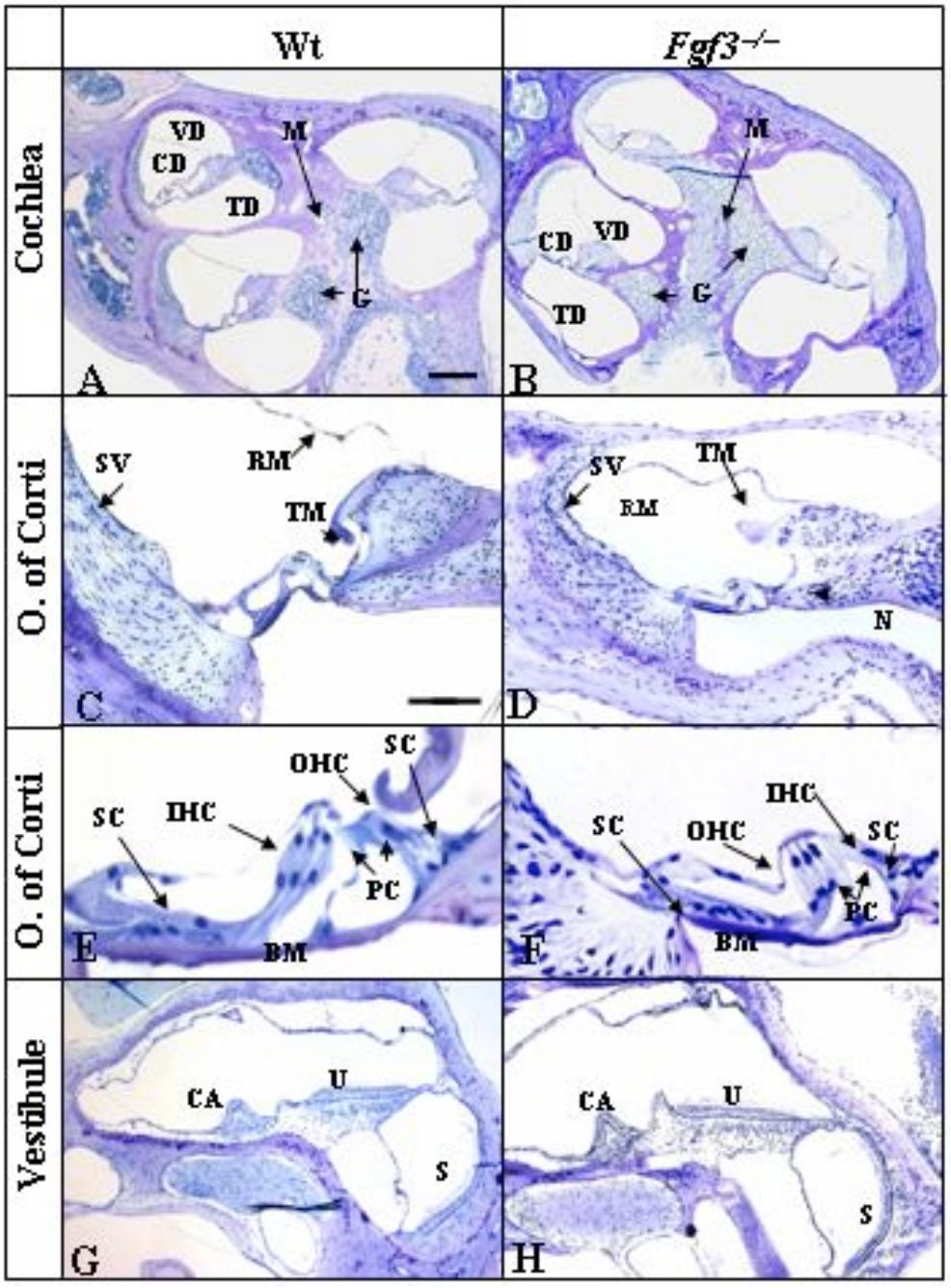

Figure 2.6: Sections of inner ears of a wt and *Fgf3*$^{-/-}$ adult littermates. (**A**, **B**) Sections of the cochlea across the modiolus. The whole cochlea in the mutant is normal in structure and size. Observe in the mutant the presence of the three cavities: vestibular **(VD)**, tympanic **(TD)** and cochlear duct **(CD)**, the modiolus **(M)** and the cochlear ganglion **(G)**. (**C**, **D**) Organ of Corti.

Observe the presence of the entire organ of Corti and membranes such as Reissner´s membrane **(RM)**, tectorial membrane **(TM)**, nerve fibers **(N)**, and *stria vascularis* **(SV)** in the mutant. (**E**, **F**) Organ of Corti at higher magnification where the **IHC** and **OHC**, pillar cells **(PC)**, supporting cells **(SC)** and basilar membrane **(BM)** are correctly located in the mutant. (**G**, **H**) Section across the vestibule. Here it is possible to distinguish the *crista ampullaris* **(CA)** from the ampulla of the lateral semicircular canal, the utricle **(U)** and saccule **(S)** are correct located in the mutant. Scale bar in A=200 µm for A, B, G and H; bar in E=100 µm for E and F, in C=100 µm for C and D.

2.1.*2*-A *neo*^{r} Gene in the *Fgf3*-Coding Region Leads to Inner Ear Alterations

As described above, another type of deletion (deletion type II) was obtained after Cre-mediated recombination between the *loxP*-sites that removed the *Fgf3* cDNA but not the *neo*^{r} gene (Fig. 2.7). This mutant was analyzed in order to clarify possible influences of the *neo*^{r} gene on the inner ear phenotype similar to those described in the *Fgf3* mutant by Mansour *et al.* (Mansour, *et al*., 1993).

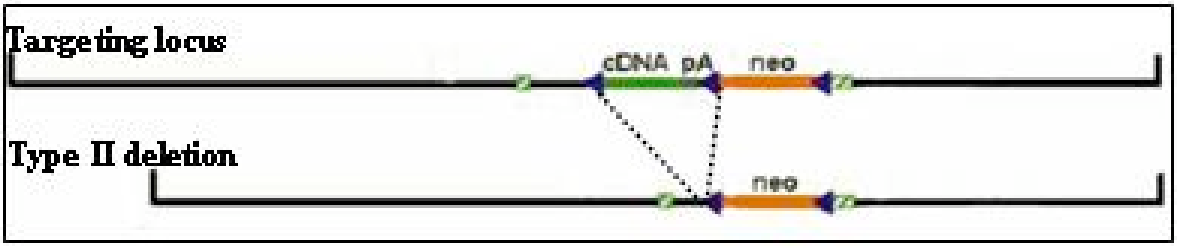

Figure 2.7: Type II deletion where the *neo*^{r} gene replaces the Fgf3 coding region.

Loss of expression of *Fgf3* was confirmed in the *Fgf3*$^{neo/neo}$ mutants by whole-mount in situ hybridization analysis (data not shown). Several of these mutants (12%) (Table 2.1) displayed an inner ear phenotype as suggested by their circling behaviour. However, the expressivity and penetrance of the phenotype were variable. Next, developing inner ears of these mutants at embryonic stages and adulthood were analyzed. Histological analysis of embryos (*n*=20) (Table 2.1) at stages 10.5, 11.5 and 13.5 was performed. Some embryos (20%) (Table 2.1) presented a slightly delayed otic vesicle formation at the mentioned stages but embryos with apparently unaffected otic vesicles were found as well (for details see Fig. 2.8).

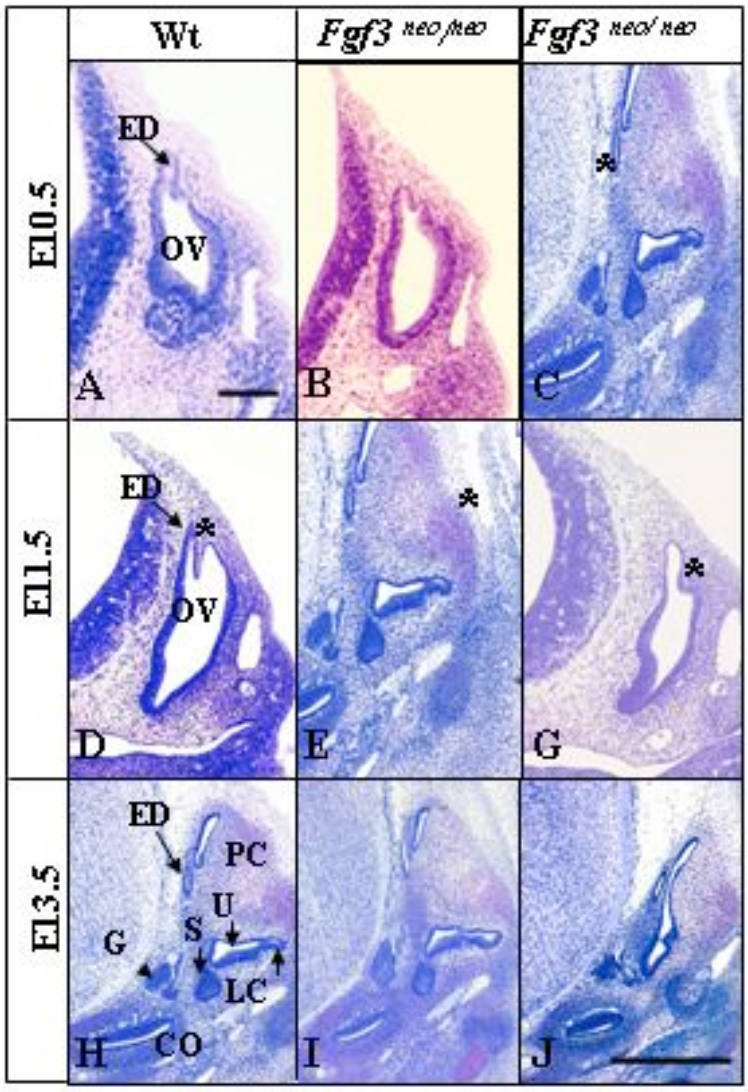

Figure 2.8: Transversal sections of developing inner ear of wt and *Fgf3*$^{neo/neo}$ mutant littermates at different stages stained with Toluidine Blue. (**A**) wt otic vesicle showing the developing otic structures. (**B**) Normal developing otocyst in an *Fgf3*$^{neo/neo}$ mutant. (**C**) Delayed otocyst is seen in an *Fgf3*$^{neo/neo}$ mutant in comparison to the wt otocyst, notice that in **C** the endolymphatic duct (*asterisk*) is not as visible as in the wt otic vesicle. (**D**) Wt otocyst. (**E**) *Fgf3*$^{neo/neo}$ mutant showing an otic vesicle without apparent abnormalities. (**G**) Delayed *Fgf3*$^{neo/neo}$ otocyst at E11.5. Compared to the wt otic vesicle, here it is possible to see a little delay in the developing semicircular posterior canal (compare the *asterisk* in **D, E** and **G**). (**H**) Wt developing inner ear at E13.5. all the structures distinguishable at this stage are indicated in the figure. (**I**) *Fgf3*$^{neo/neo}$ mutant shows a normally developing inner ear in comparison with the inner ear of the wt littermate. (**J**) Delayed developing inner ear in a *Fgf3*$^{neo/neo}$ mutant is seen, notice here the less developed lateral semicircular canal (*asterisk*) in comparison with the wt and the normal mutant inner ear in I. **CO:** cochlea; **ED:** endolymphatic duct; **G:** cochleovestibular ganglion; **LC:** lateral semicircular canal; **OV:** otic vesicle; **PC:** posterior semicircular canal; **S:** saccule; **U:** utricle. Scale bar in A= 200 μm for A-G; bar in H=200 μm for H-J.

In order to define the inner ear defects of the *Fgf3*$^{neo/neo}$ mice, adult mutants (*n*=8) were investigated. First, paint-filling of inner ears from three months old wt and mutant mice was performed. Two groups of mutants were found. One group of mice displayed unaffected inner ears and normally developed structures, and another group of mutants contained defective inner ears. The major abnormalities in the affected ears appeared in the semicircular canals, where the posterior semicircular canal was malformed, widened and shortened compared to the normal inner ear. Remember that at E11.5 a delayed development of the posterior semicircular was observed (see Fig. 2.9C). The lateral semicircular canal appeared smaller and the ampulla was not properly developed. The formation of the lateral semicircular canal was also found to be delayed at E13.5 (Fig. 2.9J). The common cross was not identified in the mutants but it was not clear whether it was completely missing or fused with the posterior semicircular canal. Finally, the cochlea of *Fgf3*$^{neo/neo}$ mutants was not properly coiled (Fig. 2.9B,D). The defects in the ears of *Fgf3*$^{neo/neo}$ mutants were often unilateral. All the mutants presenting turning behaviour showed defects at least in one of the inner ears. Additionally, audiometric analysis of the *Fgf3*$^{neo/neo}$ mutants showed reduced hearing thresholds in the affected inner ears (data not shown).

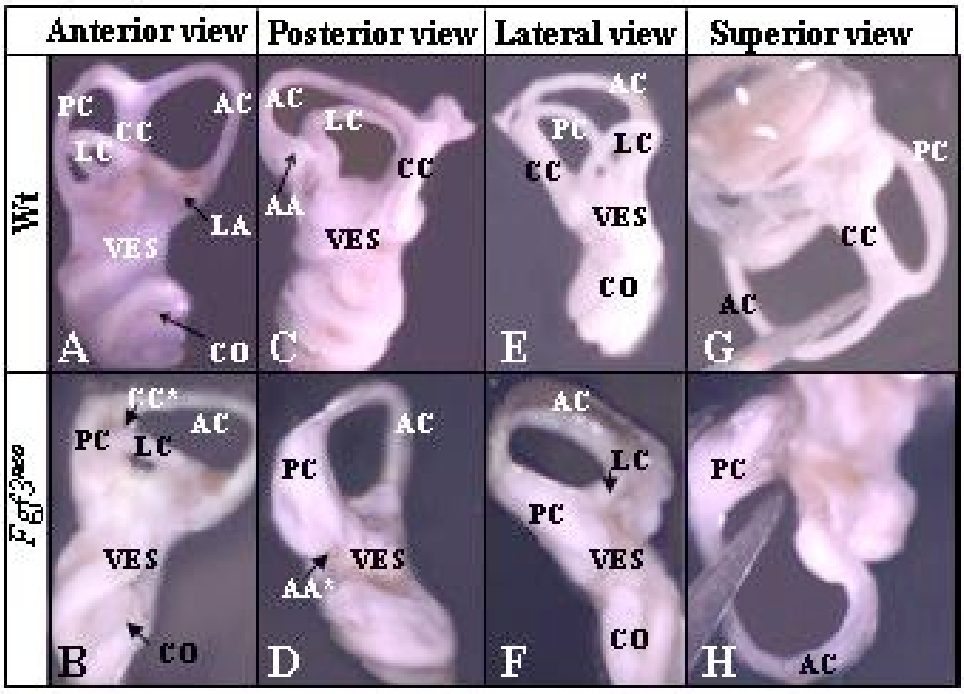

Figure 2.9: The upper panel (**A,C,E,G**) shows different views of a wt paint-filled adult inner ear in order to compare with the mutant. The lower panel (**B,D,F,H**) shows the same views of a *Fgf3*$^{neo/neo}$ paint-filled adult inner ear (**A**) The three semicircular canals are perfectly distinguished in the wt inner ear but the mutant (**B**) shows atrophy in the posterior semicircular canal and the common cross is not visible (CC*). The lateral canal in the same view appears highly reduced when

compared with the wt and the cochlea shows an abnormal coiling (B). (**C,D**) In the posterior view the widened posterior semicircular canal is easily seen in the mutant inner ear (**D**), the ampulla is not visible (AA*****), and the vestibular portion is reduced. (**E,F**) The lateral view shows a highly reduced lateral canal and the improperly coiled cochlea (**F**). (**G,H**) In the superior view in H the absence of the common cross and again the widened posterior semicircular canal is seen. **AA:** anterior ampulla; **AC:** anterior semicircular canal; **C:** cochlea; **CC:** common crus; **LA:** lateral ampulla; **LC:** lateral semicircular canal; **PC:** posterior semicircular canal; **VES**: vestibule.

Secondly, the histological analysis of the adult inner ears of *Fgf3*$^{neo/neo}$ mutants as described previously for *Fgf3*$^{-/-}$ mice was carried out. The mutant mice with a normal behaviour showed normal inner ear histology (data not shown); while asymmetrically affected inner ears were found in the mutants with vestibular phenotype. In Figure 2.10 two inner ears (left and right) which belong to the same adult mutant are compared with a wt mouse. In this panel it is possible to appreciate the affected structures of the inner ears of *Fgf3*$^{neo/neo}$ mutants. In this case the mutant presented a right inner ear which was more affected than the left inner ear (see the details in Fig. 2.10).

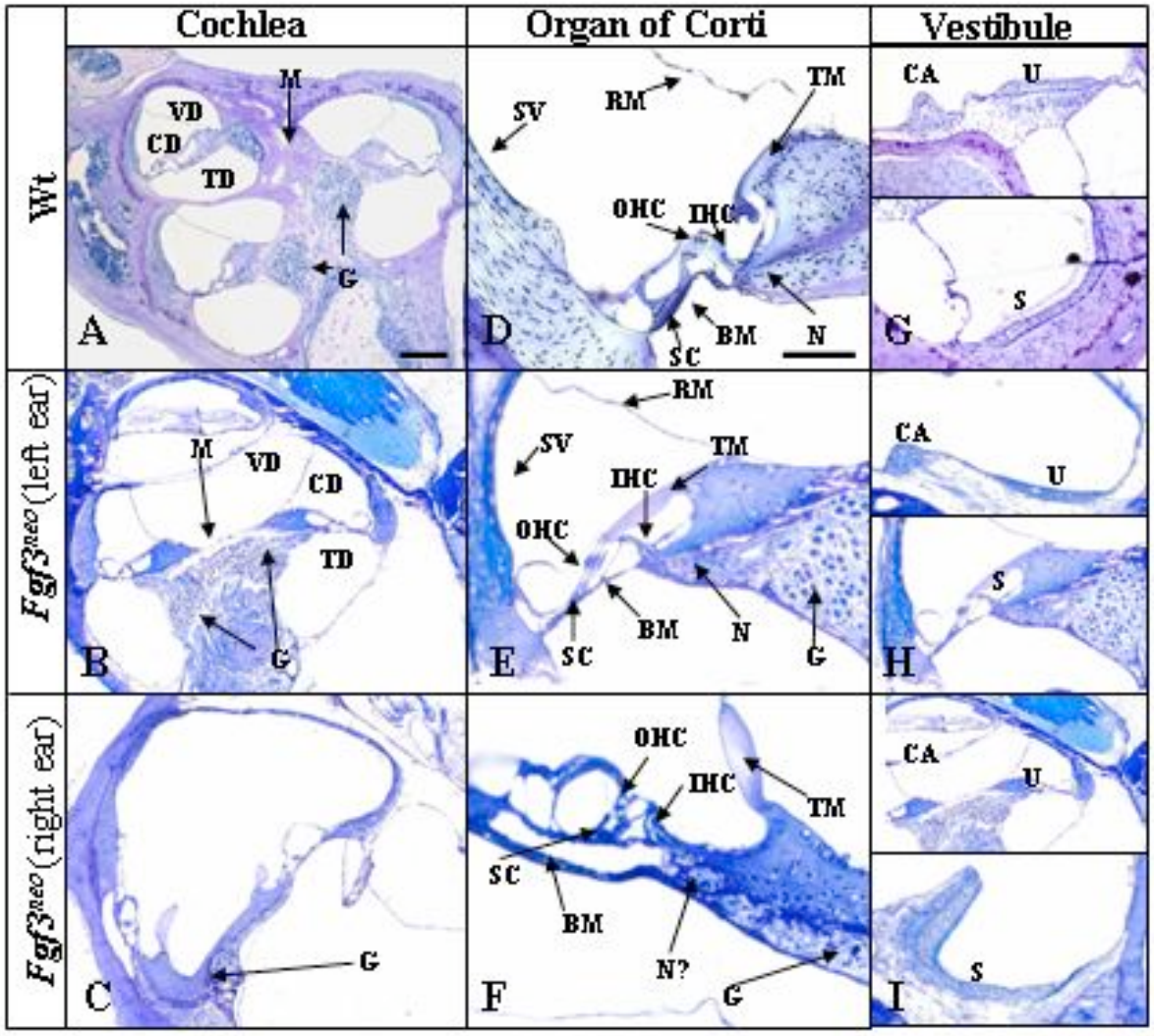

Figure 2.10: (**A,D,G**) Sections of wt inner ears. Sections of the left (**B,E H**) and right (**C,F,I**) inner ear of an *Fgf3*$^{neo/neo}$ mutant. The cochlea shown in **B** is not properly coiled, but the cavities are still visible. In **C** the cochlea is more severely affected showing incomplete turns, the modiolus (**M**) is not formed and the different ducts inside the cochlea are not well separated as vestibular (**VD**), and tympanic duct (**TD**), but remnants of the cochlear ganglion (**G**) are still visible. In **E** a high magnification of the cochlea at the level of the organ of Corti is shown where it is still possible to see an organized epithelium and the presence of IHC, OHC, supporting cells (**SC**), Reissner´s membrane (**RM**); basilar membrane (**BM**), tectorial membrane (**TM**), nerve fibers (**N**) and *stria vascularis* (**SV**). In **F** the phenotype is more severe and a high disorganization of the organ of Corti is seen. The ganglion and nerves fibers are reduced. The epithelium shows disorganized OHCs and IHCs. In **H** the *crista ampullaris* (**CA**), the utricle (**U**) and the saccule (**S**) appear reduced. In **I** the *crista ampullaris* and the utricle are highly reduced and also the epithelium shows some disorganization. In **I** the saccule appears severely altered. Scale bar in A=200 µm for A-C and G-I, bar in D=100 µm for D, E, and F.

Finally, molecular aspects which lead to the functional abnormalities, such as circling behavior, were aimed to be revealed. One of the critical molecular markers of the functional inner ear is the potassium voltage-gated channel KCNQ4, which is expressed in the basal membrane of the hair cells in the organ of Corti and the type I hair cells in the vestibular organ (Kharkovetts *et al.,* 2000). They maintain the right concentration of potassium in the endolymph. Indeed, *Fgf3*$^{neo/neo}$ mutants with circling behavior showed a reduced number of KCNQ4 positive cells, as determined by immunohistochemistry (Fig. 2.11)

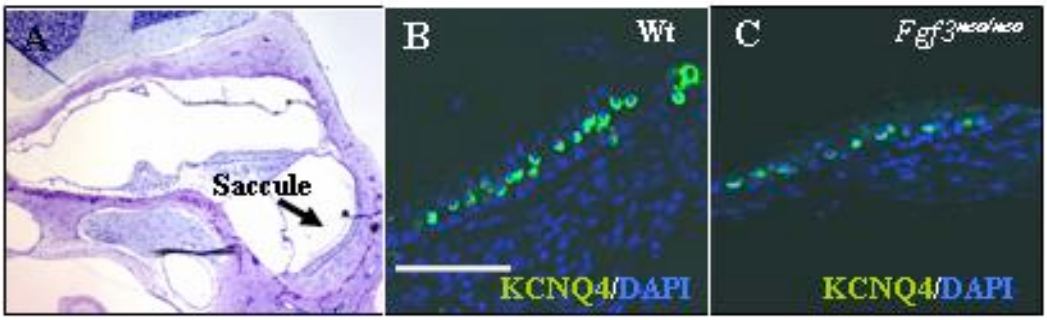

Figure 2.11: (**A**) Section across the vestibule showing the saccule of the wt inner ear stained with Toluidine Blue in order to visualize the structures in B and C. (**B**, **C**) Cryosections of adult inner ear of wt and *Fgf3*$^{neo/neo}$ mice at the level of the vestibule. (**B**) The green staining indicates the normal expression of KCNQ4 in hair cells of the saccule of a wt inner ear. The blue color is a DAPI nuclear stain. (**C**) Saccule of *Fgf3*$^{neo/neo}$ inner ear which shows reduced expression of KCNQ4. Scale bar in B=50 μm for B, C.

The majority of the analyzed *Fgf3*$^{-/-}$ animals showed no evidences that deletion of the whole *Fgf3*-coding region has consequences on viability or on function of the inner ear. However, 12 % of *Fgf3*$^{neo/neo}$ mutants presented an inner ear phenotype with variable expressivity and penetrance. This may suggest that the inner ear phenotype in *Fgf3* mutants is possibly partially due to the presence of the *neo*^{r} gene rather than to the absence of the *Fgf3*-coding region.

2.1.*3*-Double FGF3 and FGF10 Mutants Develop Severely Affected Otic Vesicle

The expression of FGF3 and FGF10 in the developing hindbrain during formation of the otic placode and vesicle suggested their potential involvement in functioning as neural signals during this process (Mahmood, *et al*., 1996, Alvarez, *et al*., 2003, Wright, *et al.*, 2003)

However, as described in the present work, FGF3 mutant mice carrying a deletion of the whole coding region of the gene show an apparently normal formation of the inner ear. The *Fgf3* mutant mice generated in our lab, in which the *Fgf3* coding region is replaced by *neo*^{r} gene or the already described *Fgf3*$^{neo/neo}$ mutants (Mansour *et al.,* 1993) display defects that affect only the differentiation of the otic vesicle but induction is unaffected. Furthermore, *Fgf10* mutant mice form otic vesicles, although their size appears reduced and later differentiation of the inner ear is affected (Ohuchi et al., 2000; Pauley et al., 2003).

To explore the possibility that FGF3 and FGF10 may act as redundant factors during early inner ear development, we created mice carrying mutations for both of these genes. To obtain double mutants, *Fgf3* mutant mice were mated with heterozygous *Fgf10* mutant mice generated by Sekine *et al*. (Sekine, *et al*., 1999). In the FGF10 mutant the exon encoding the ATG translational start site has been replaced by a *neo*^{r} cassette (Sekine, *et al*., 1999). The offspring from double heterozygous *Fgf3* and *Fgf10* mice resulted in all combinations of the expected genotypes at the expected Mendelian ratios at E9 and E12, but no *Fgf3*$^{-/-}$/*Fgf10*$^{-/-}$ mutant embryos were recovered from E12.5 onwards. Next, the embryos at early stages (n=26) were analyzed to examine otic vesicle formation. All *Fgf3*$^{-/-}$/*Fgf10*$^{-/-}$ mutant embryos examined showed severe loss of otic tissue. At otic placode (E8) and vesicle (E9) stage, the *Fgf3*$^{-/-}$/*Fgf10*$^{-/-}$ embryos showed a severe reduction or absence of otic marker genes such as *Dlx5* and *Pax2* (Fig. 2.12). At E9 and E10, *Fgf3*$^{-/-}$/*Fgf10*$^{-/-}$ mutants had formed reduced sized otic vesicles. The histological analysis of the mutant embryos showed a ventralized smaller otocyst, which showed a complete lack of the cochleovestibular ganglion (Fig. 2.12). The inner ear phenotype exhibited variable expressivity between mutant embryos and also between the two vesicles of the same embryo.

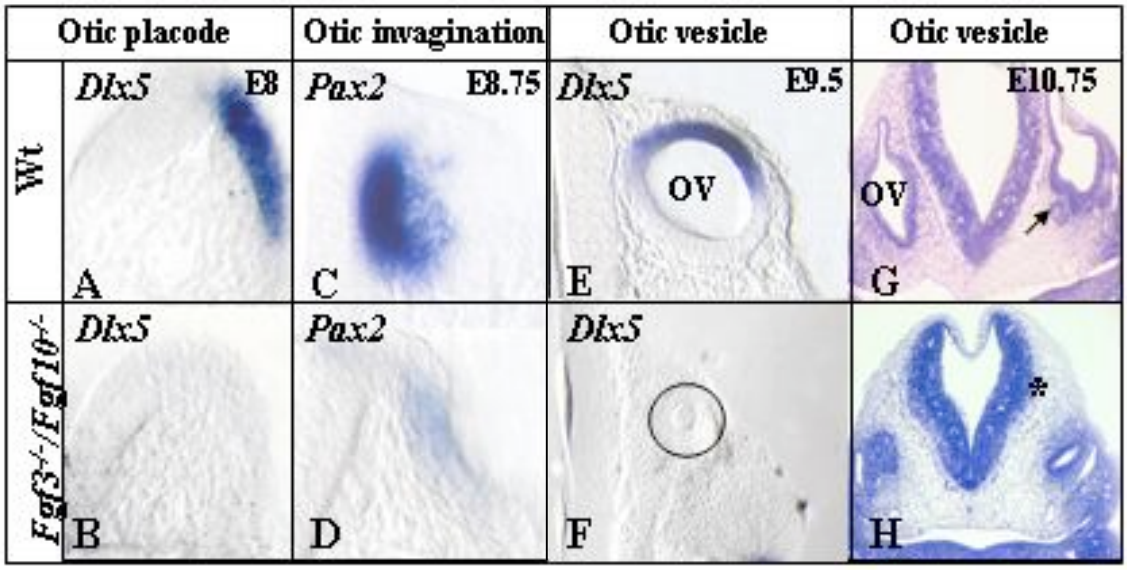

Figure 2.12: Defective inner ear formation in the *Fgf3*$^{-/-}$*/Fgf10*$^{-/-}$ double mutants. (**A-F**) Whole-mount RNA *in situ* hybridization with the indicated probes. (**A,B**) Sections at the level of the otic placode hybridized with *Dlx5* probe. Note the absence of *Dlx5* staining in B. (**C.D**) Sections at the level of the invaginating placode which have been hybridized with *Pax2*. The invagination in the mutant embryo is delayed and shows weaker expression of *Pax2* in comparison with the wt in C. (**E,F**) Sections at the level of the otic vesicle of embryos hybridized with *Dlx5*. Notice the absence of *Dlx5* in the microvesicle of the mutant embryo (*circle*). (**G,H**) Toluidine Blue stained sections through the otic vesicle of a wt and an *Fgf3*$^{-/-}$*/Fgf10*$^{-/-}$mutant littermate at E10.75. Note the absence of the cochlear ganglion in the mutant (*indicated by an arrow in the wt animal*) and a more ventralized position of the vesicle relative to the border of the neural tube (*marked by asterisks*). **G:** ganglion; **OV:** otic vesicle. Scale bar in A=40 µm for A-F; bar in H=200 µm for G, H; Figure parts from Alvarez *et al.,* 2003, with permission of Victor Vendrell.

Although the formation of the otic placode and vesicle is severely disturbed in the *Fgf3*$^{-/-}$*/Fgf10*$^{-/-}$ mutants, expression of otic genes such a *Pax2* and *Dlx5* is observed in a subset of embryos (data not shown). An embryo which was able to develop until E12.5 contained remnant otic tissue, such as cochlea, vestibule and ganglion, revealed by histological analysis (Fig. 2.13). Thus all the initial steps in the morphogenesis of the inner ear are not affected in this embryo.

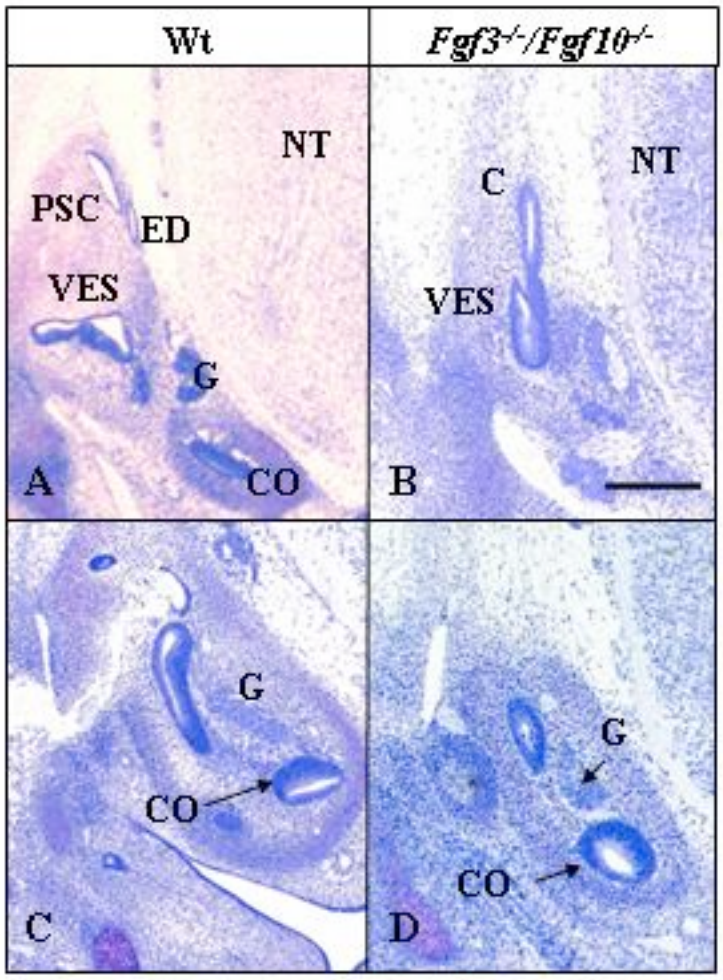

Figure 2.13: Inner ear at E12.5 of wt and *Fgf3*$^{-/-}$/*Fgf10*$^{-/-}$ double mutant embryos. (**A,B**) Transversal section of embryos at the level of the inner ear (more rostral) stained with Toluidine Blue. Notice the rudimentary otic tissue that may correspond to parts of the vestibule and a canal in the mutant embryo (B). (**C,D**) Transversal section of embryo at the level of the inner ear (more caudal). A remnant cochlea and ganglion are seen in the mutant. **C**: canal; **CO:** cochlea; **ED:** endolymphatic duct; **G:** ganglion; **NT**: neural tube; **PSC:** posterior semicircular canal; **V:** vestibule. Scale bar in B=200 μm for A-D.

2.1.*4*-The Mutation of One *Fgf10* Allele in a Background of the *Fgf3* Null Mutation Lead to the Formation of Severely Affected Inner Ear

To try to elucidate the individual role of FGF3 and FGF10, homoheterozygous animals with mutant allele combinations of FGF3 and FGF10 have been analyzed. Interestingly, some of the homozygous adult mutants for *Fgf3* carrying one mutated *Fgf10* allele (26%) (Table 2.1) moved in circles and showed a severe inner ear phenotype. The mutants were analyzed at embryonic stages and adulthood. First, to identify the defects in the developing

otocyst, histological analysis of the embryos at E10 and E11.5 (*n*= 15) (Table 2.1) was performed. It was found that 45% of the *Fgf3*$^{-/-}$*Fgf10*$^{+/-}$ mutant embryos presented abnormalities in the developing otic vesicle. The otic vesicles were in most of the cases smaller, ventralized, and lacked the ganglion (Fig. 2.14). The defects in the ears and otic vesicles were mostly unilateral.

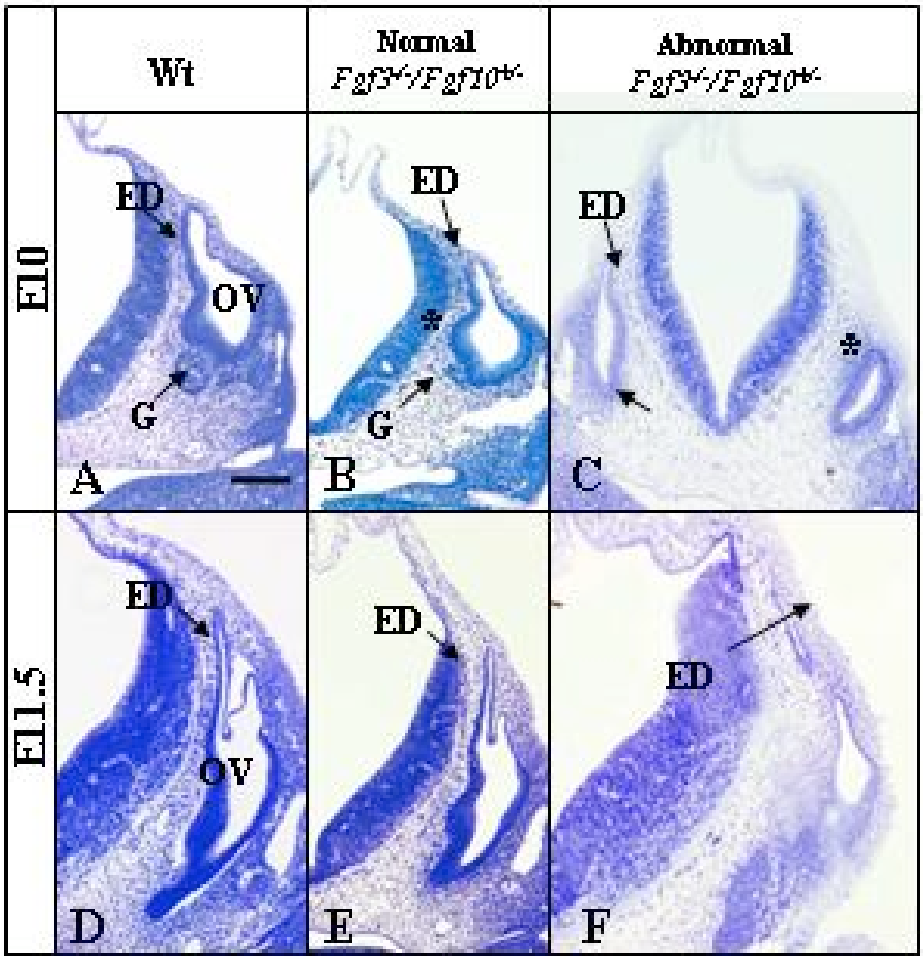

Figure 2.14: Transversal sections at the level of the developing otocyst of *Fgf3*$^{-/-}$/*Fgf10*$^{+/-}$ mutant embryos and wt stained with Toluidine Blue. (**A-B**) Sections of E10 embryos. In B a mutant with a normal developing otocyst is shown. In C a mutant shows affected otic vesicles. One OV is more affected than the other. Observe the smaller and more ventralized otic vesicle. Compare with the wt the distance between the otocyst and the neural tube (*asterisk*) and the lack of ganglion (*arrows*). (**D-F**) Sections of E11.5 embryos. In E the mutant embryo shows a relatively normal otocyst but in F the otocyst appears again more ventralized and smaller. **ED:** endolymphatic duct; **G:** cochleovestibular ganglion; **OV:** otic vesicle. Scale bar in A=200 μm.

The defects in adult inner ears of *Fgf3*$^{-/-}$/*Fgf10*$^{+/-}$ mutants were next investigated by performing paint-filling of inner ears adult mutants (*n*=7). Many structures as the lateral semicircular canal and common cross were missing, and other structures as anterior and

posterior semicircular canal, vestibule and cochlea were severely malformed (see details in Fig. 2.15). All the mutants that presented turning behavior showed affected inner ears.

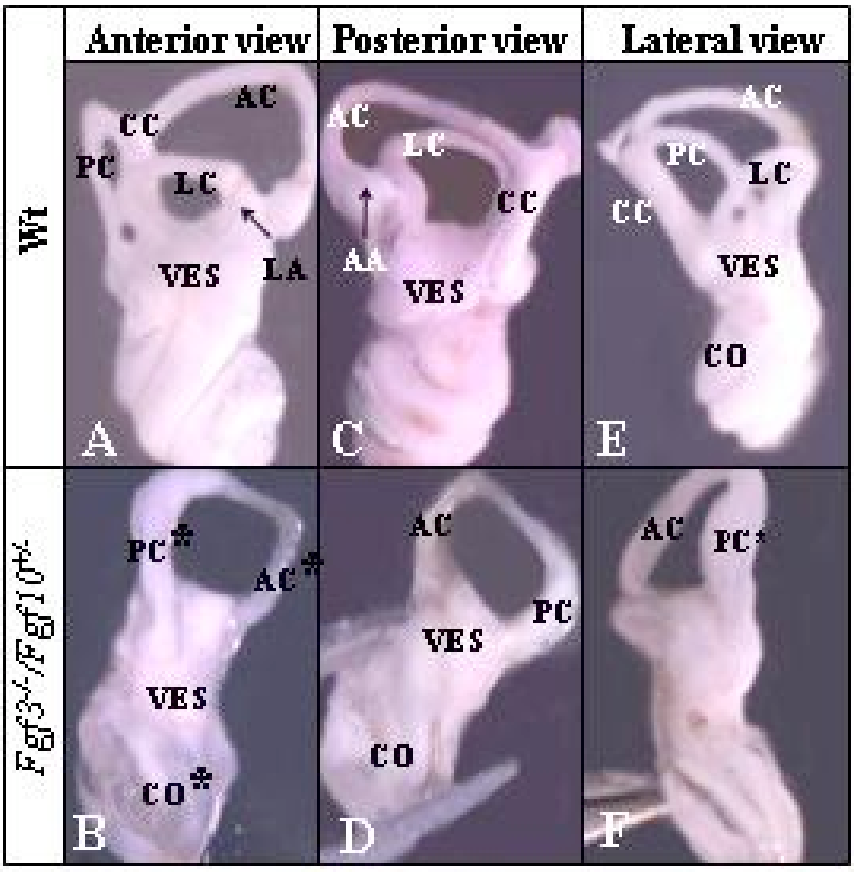

Figure 2.15: Paint-filled inner ears of adult wt and *Fgf3*$^{-/-}$*/Fgf10*$^{+/-}$ mice. (**A,B**) Anterior view of the paint-filled ears. In B a severely malformed inner ear is shown, the lateral semicircular canal and the common cross are not visible, the anterior semicircular canal is reduced (*asterisk*), the posterior semicircular canal is shortened and widened (*asterisk*), the vestibule is malformed and the cochlea incompletely coiled (*asterisk*). (**C,D**) Posterior view of the same ears shown in A and B. Notice in D the smaller mutant inner ear and the malformed cochlea as well as the lack of the anterior ampulla. (**E,F**) Lateral view of the same ears. The widened and shortened posterior semicircular canal (*asterisk*), the lack of the lateral canal, and the malformed vestibule can be observed. **AA:** anterior ampulla; **AC:** anterior semicircular canal; **CO:** cochlea; **CC:** common crus; **LA:** lateral ampulla; **LC:** lateral semicircular canal; **PC:** posterior semicircular canal; **VES**: vestibule.

To analyze closer the sensory epithelia of the adult inner ear, histological analysis of *Fgf3*$^{-/-}$*/Fgf10*$^{+/-}$ mutants was performed. As described before the structures were stained with Toluidine Blue to visualize the different cell types in the sensory organ of the inner ear.

The result of this analysis is shown in Figure 2.16. *Fgf3*$^{-/-}$/*Fgf10*$^{+/-}$ mutant developed an incompletely coiled cochlea (as shown by paint-filling analysis), disorganized organ of Corti and reduced vestibular epithelium (Fig. 2.16).

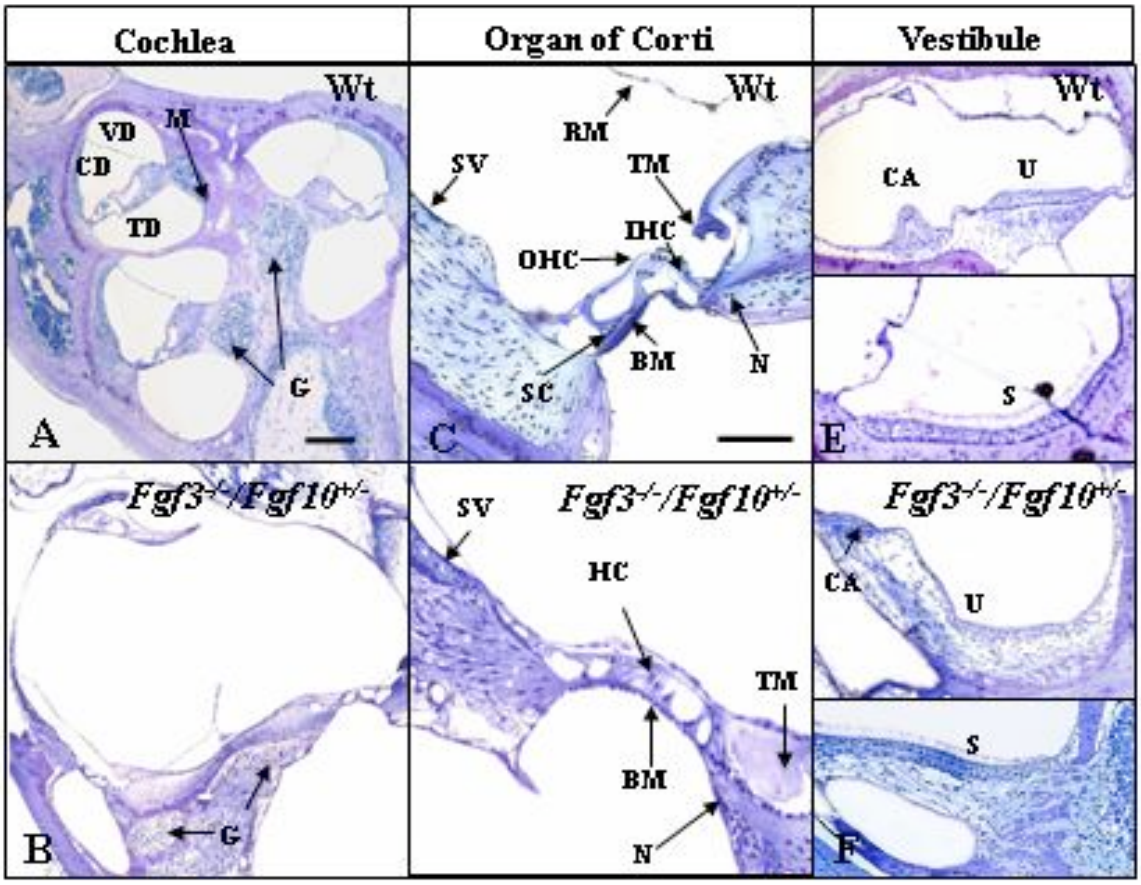

Figure 2.16: Section of the cochlea through the modiolus. The mutant inner ear shows an incompletely coiled cochlea and the different cavities are not distinguishable (B). In the mutant, the ganglion is still visible but reduced. (**C,D**) High magnification of the organ of Corti. The mutant shows a disorganized epithelium in which inner or outer hair cells can not be distinguished. The nerve fibers and the *stria vascularis* are reduced in comparison with the wt organ of Corti (D). (**E,F**) Section through the vestibule. The *crista ampullaris* is highly reduced in the mutant as well as the epithelium of the utricle and saccule which are thinner (F). **BM**: Basilar membrane; **CA**: *crista ampullaris*; **CD:** cochlear duct; **G:** ganglion; **HC**: hair cells; **IHC:** inner hair cells; **N:** nerve fibers; **OHC:** outer hair cells; **RM:** Reissner´s membrane; **S:** saccule; **SC:** supporting cells; **SV:** *stria vascularis*; **TM:** tectorial membrane. Scale bar in A=200 μm for A, B, E and F, bar in C= 100 μm for C and D.

Next, to test the functionality of the structures still present in the mutant mice two different markers were used: One of the markers is a voltage-gated potassium channel, member 1 of the KQT-like subfamily, (KCNQ1) which is expressed in the cochlea in the dark cells of

the stria vascularis and KCNQ4, which has been described to be expressed in the saccule (Kharkovets, 2000). Both are necessary for recycling of potassium by secreting it into the endolymph (Sakagami, 1991). After immunostaining a high reduction of the KCNQ4 expressing cells in the saccule and KCNQ1 in the stria vascularis was observed (Fig. 2.17).

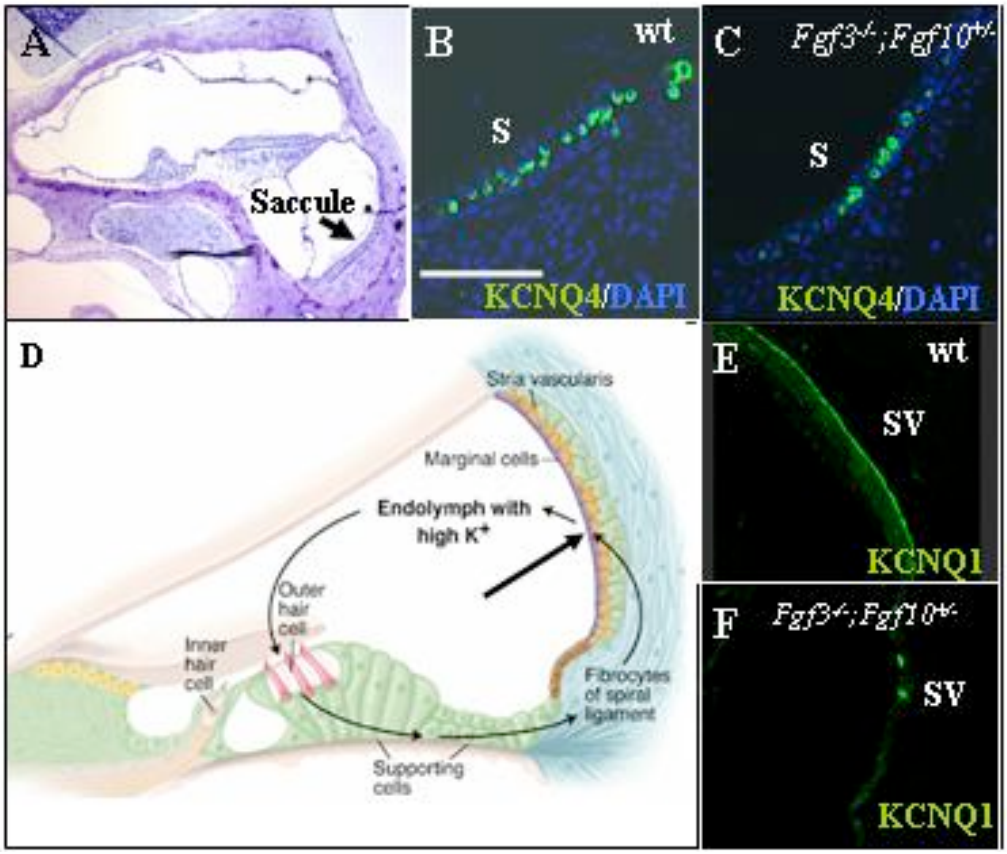

Figure 2.17: Immunostaining of the inner ear of wt and *Fgf3*$^{-/-}$/*Fgf10*$^{+/-}$ mice using the indicated antibodies. (**A**) Section at the level of the vestibule to show the localization of the structures stained in B and C. (**B,C**) KCNQ4 immunostaining in the saccule of wt and mutant mice, notice in C the reduced number of cells stained with the antibody in comparison with the wt in B. (**D**) Scheme of the cells expressing KCNQ1 in the *stria vascularis* to visualize the structure stained in E and F (Steel, 1999). (**E,F**) KCNQ1 immunostaining in the cochlea of wt and mutant mice. Sections at high magnification showing the *stria vascularis*. Notice a dramatic loss of dark cells stained by the antibody in the mutant (F). **S:** saccule; **SV:** *stria vascularis*. Scale bar in B=50 μm for A, B, C, E and F.

Mutants homozygous for FGF10 and heterozygous for FGF3 (*Fgf3*$^{+/-}$/*Fgf10*$^{-/-}$) (n=6) were analyzed as well. These mutants did not survive until adulthood; therefore, we only analyzed embryonic stages. At E10 the otic vesicles of *Fgf3*$^{+/-}$/*Fgf10*$^{-/-}$ mutants appeared slightly smaller but the endolymphatic ducts as well as the ganglions were present (Fig.

2.18A,B). At E11.5 a clearly delay in otocyst formation could be observed. The otic vesicles were much smaller than a wt otocyst and the ganglion was not properly developed (Fig. 2.18C,D). However, this phenotype was not 100 % penetrant, but observed only in 20% of embryos.

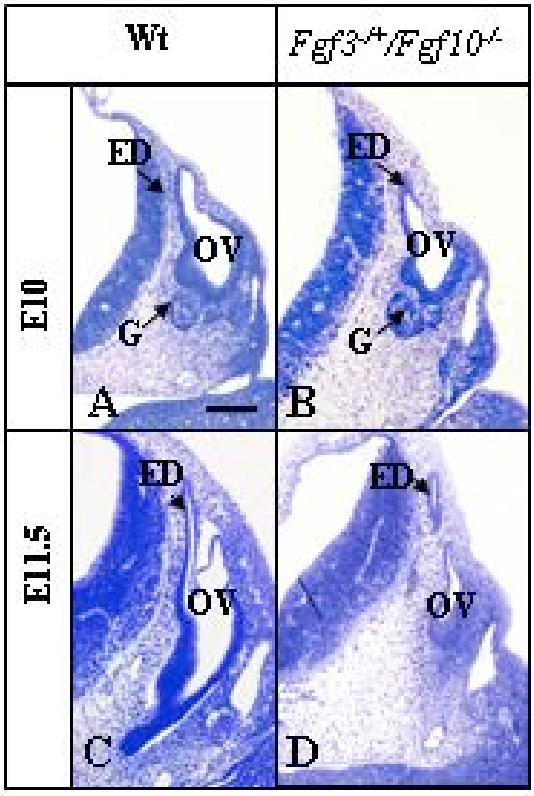

Figure 2.18: Developing otocyst in *Fgf3*$^{+/-}$*/Fgf10*$^{-/-}$ mutants. (**A,B**) Sections of embryos at the level of the developing otocyst at E10. Notice the smaller but well developed otocyst in the mutant (B). (**C,D**) Otocyst at E11.5. The mutant shows a severe reduction of the size of the otocyst (D). Scale bar in A=200 µm.

Whereas the majority of our single *Fgf3*$^{-/-}$ null mutants did not show any apparent defects in the formation of the inner ear, the homoheterozygous *Fgf3*$^{-/-}$*/Fgf10*$^{+/-}$ mouse mutants showed severe defects during this process, and although some mutants were normal, 26% of them presented an abnormal otic development. FGF3 and FGF10 may share redundant functions with other FGF family members since the initial steps of inner ear induction are undisturbed in *Fgf3*$^{-/-}$*/Fgf10*$^{-/-}$ mouse mutants. Based on the expression pattern of another member of the FGF family, FGF8, the involvement of this factor during formation of the inner ear was further investigated.

2.1.5-FGF8 May Play a Role in the Formation of the Inner Ear

According to the results in this work, FGF3 is not essential for otic induction and the combined loss of FGF3 and FGF10, although affecting severely the normal formation of

the otocyst, does not inhibit the initial program, since remnant otic tissue is found in the double FGF3 and FGF10 mutants. Therefore, the role of another member of the FGF family was addressed further in this study. Homozygous null mutants for FGF8 are lethal in mice by E10.5 due to failure in gastrulation, therefore the otic formation can not be addressed in these mutants (Meyers, *et al*., 1998, Sun*, et al.*, 1999). For this reason, the importance of FGF8 during inner ear development has been tested in this study by specific inactivation of FGF8 using *Foxg1* (Fork head box) or (BF1) (Brain Factor)-*Cre* mice (Hebert, *et al*., 2000). In *Foxg1-Cre* mice, Cre recombinase is targeted to the *Foxg1* locus. *Foxg1* is expressed in early embryonic stages in discrete head structures (Kaestner, *et al.,* 2000), indeed Cre recombination in *Foxg1-Cre* mice has been reported to occur in domains which are coincident with *Fgf8* expression such pharyngeal endoderm, ectoderm-derived head structures including otic placode, and otic vesicle (Hebert, *et al*., 2000).

2.1.*5*.1-FGF8 Single Mutation Does Not Severely Affect the Formation of the Inner Ear

To examine the effects of FGF8 on inner ear development mice containing a $Fgf8^{flox}$ allele (Meyers, Lewandoski & Martin 1998; *see introduction* 1.6.*1.2*) have been used in this study. In these mutants exon 2 and 3 of the *Fgf8*-coding region are flanked by *loxP*-sites and are therefore susceptible to undergo specific recombination. The $Fgf8^{flox}$ mutants were crossed with *Foxg1-Cre* deleter mice (Hebert, *et al.*, 2000). To identify the specific cells and precise timing in which *Cre* was expressed a *ROSA26* reporter mouse (Soriano, 1999) was used. In this mouse strain (ROSA26-**loxP**-Stop **-loxP**-*LacZ*) a *lacZ* gene is constitutively silent, but can be activated upon deletion of the *floxed* Stop sequence by crossing the ROSA26 *LacZ* reporter with a mouse line expressing Cre recombinase (Soriano, 1999). The ROSA locus is expressed ubiquitously from the preimplantation stage in the embryos. Offspring of the breedings between the *Foxg1-Cre* mice and the ROSA26 *LacZ* reporter mice were analyzed for *LacZ* expression. The expression of *Foxg1-Cre* was indeed observed to coincide temporally and spatially with the endogenous expression of *Fgf8* at E8 in the mesoderm, endoderm and surface ectoderm adjacent to the otic placode and otic vesicle (unpublished data supported by Dr. Alvarez).

Next, FGF8 mutants carrying the *floxed* or the null allele $\Delta 2,3$ and the *Foxg1-Cre* transgene were created ($Fgf8^{flox}/Fgf8^{\Delta 2,3}$*; Foxg1-Cre* or $Fgf8^{flox}/Fgf8^{lox}$*; Foxg1-Cre* mice), in

which one Fgf8 allele is inactive and the other one or both are susceptible to recombination by *Cre* driven by the *Foxg1* promoter. *Fgf8*^{flox}/*Fgf8*$^{\Delta 2,3}$; *Foxg1-Cre* mutants (n=15) (Table 2.1) were phenotypically distinguishable from their normal littermates. They were smaller and showed clear craniofacial abnormalities lacking the embryonic mesoderm, endoderm and neural crest-derived structures at E10 (Fig. 2.19A,B). However, the histological analysis of the mutant embryos revealed a normal development of the inner ear. *Fgf8*^{flox}/*Fgf8*$^{\Delta 2,3}$; *Foxg1-Cre* mice were analyzed at different embryonic stages and at birth. The mutant embryos and the developing otocyst appeared smaller and delayed compared to wt littermates, but no apparent specific defects in the developing inner ear was found. The structures normally present in a wt inner ear could be identified in the mutant embryonic inner ear (Fig. 2.19E,G,I).

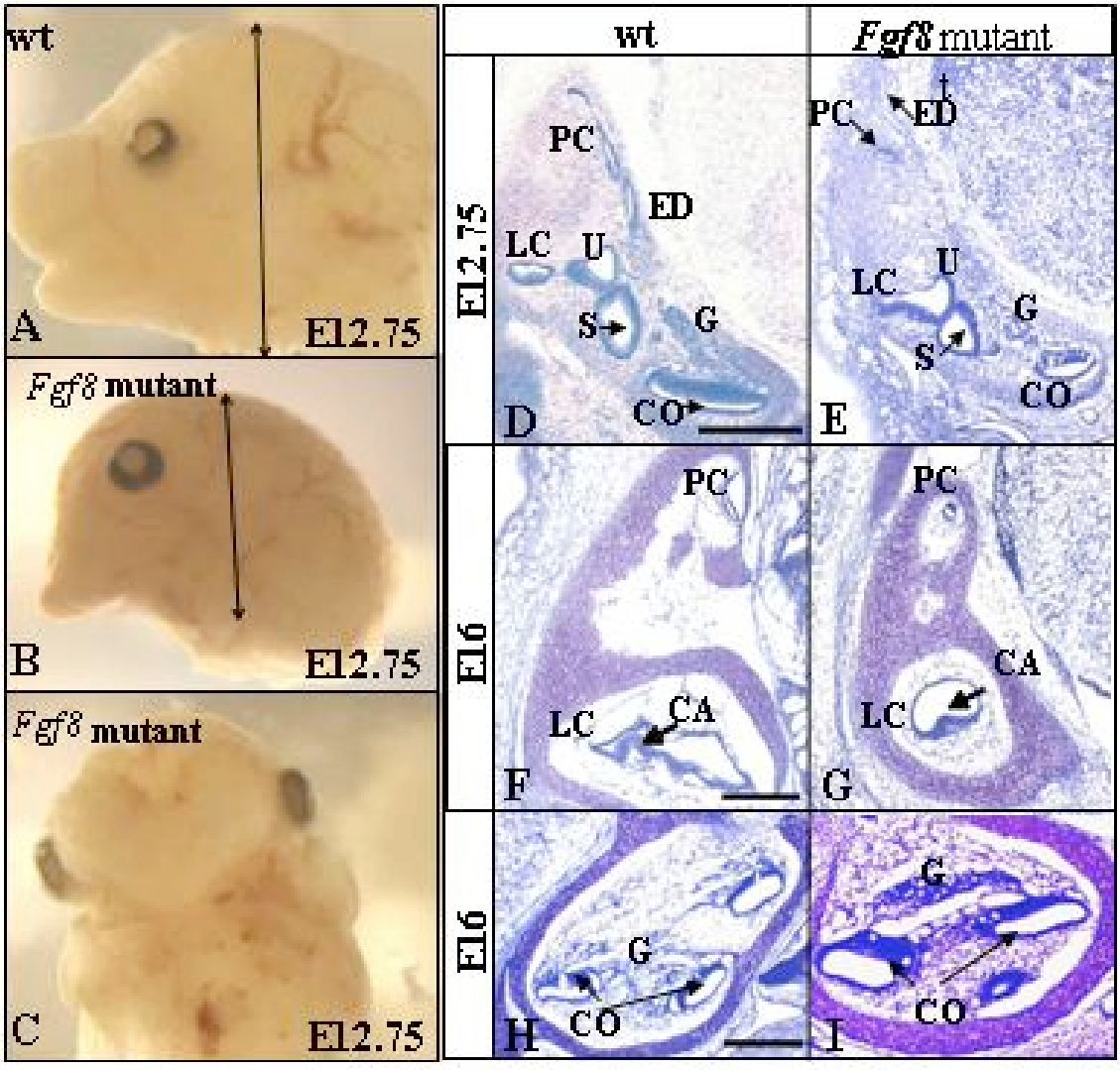

Figure 2.19: General malformations in the FGF8 mutants. (**A-C**) Wt and FGF8 mutant heads of embryos at E12.75. Note the lack of embryonic mesoderm and neural crest-derived structures in the face and a compression of the head at the level of the ears of the mutant (*arrows*). (**D,E**)

Transversal sections of embryos at E12.75 at the level of the developing inner ear. The FGF8 mutant inner ear (E) appears smaller and less developed in comparison with the wt but structures such as posterior semicircular canal (**PC**), endolymphatic duct (**ED**), lateral semicircular canal (**LC**), utricle (**U**), saccule (**S**), cochlea (**CO**), and ganglion (**G**) are distinguishable in the mutant. (**F-I**) Inner ears at E16. Although the mutants have smaller inner ears, the PC, LC and corresponding *crista ampullaris* (**CA**), CO and G are found. Scale bar in D=200 μm for D-I, bar in F= 140 μm for F and G, bar in H= 100 μm for H and I.

Since FGF8 is expressed during late embryogenesis stages in the developing inner ear, newborn FGF8 mutants were analyzed to monitor the consequences of a lack of FGF8 in the inner ear (n=6) (Table 2.1). After application of paint-filling in the inner ear of wt and mutant mice, smaller mutant inner ears were seen but the structures present in the wt inner ear were also observed in the mutants (see details in Fig. 2.20).

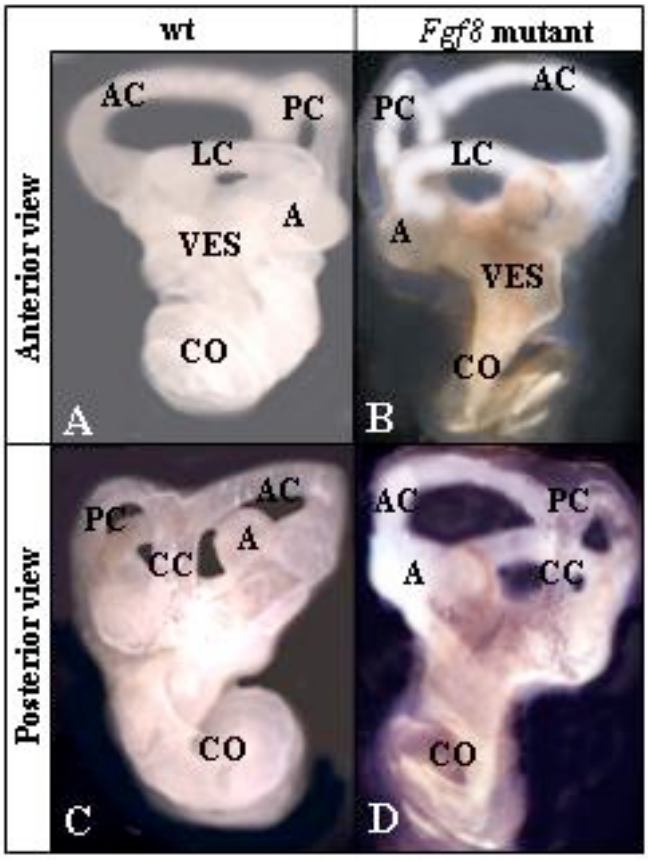

Figure 2.20: Paint-filling of wt and mutant inner ears of newborn mice. (**A,B**) Anterior view of the paint-filled ears. Observe the presence of the vestibule (**VES**), coiled cochlea (**CO**) lateral (**LC**), posterior (**PC**) and anterior semicircular canals (**AC**) and the respective ampulla (**A**). (**C,D**) Posterior view of the painted ears. The common cross (**CC**) and the structures mentioned before are clearly visible in the mutant.

FGF8 is expressed specifically in the IHCs of the organ of Corti at birth (Pirvola, *et al.*, 2002). To look for possible defects in this organ a more detailed analysis at the cellular level was performed in these mutants. The different cell types of the organ of Corti were visualized by nuclear staining with Toluidine Blue. The histological analysis revealed a normal cochlear and vestibular epithelium. In the organ of Corti the hair, supporting and pillar cells were perfectly visualized, as well as the tectorial and basilar membrane (Fig. 2.21).

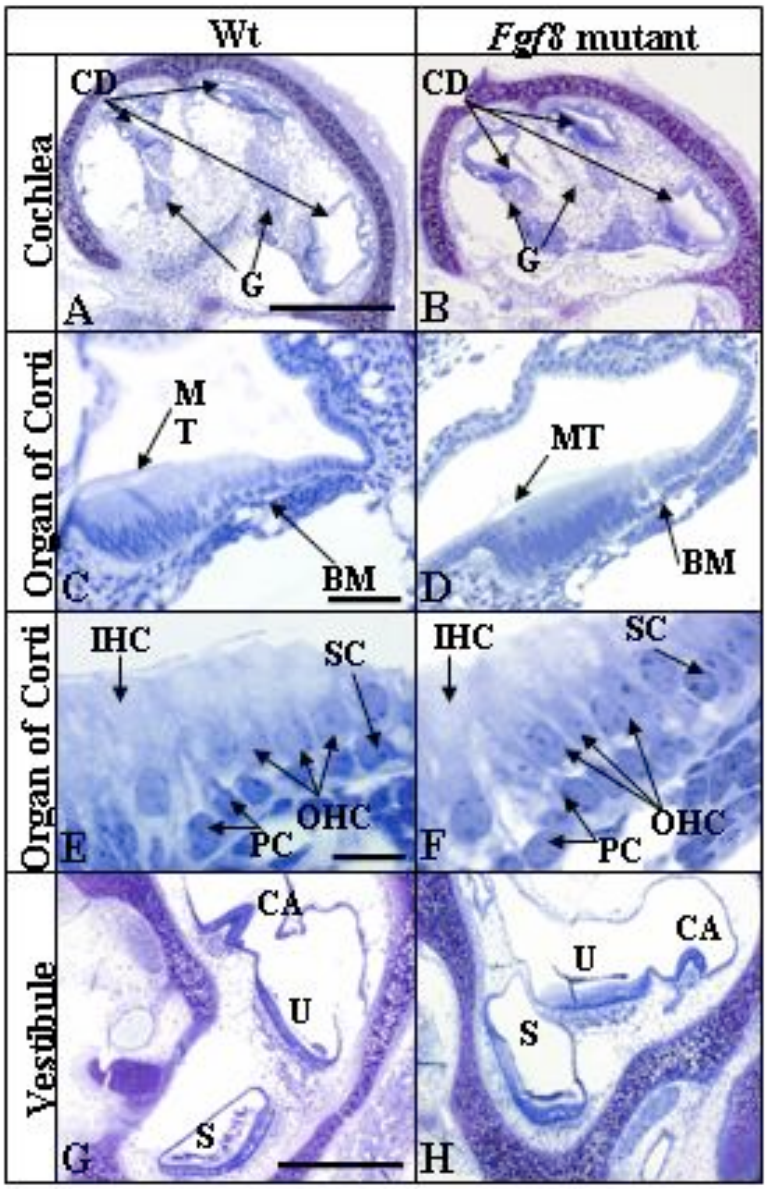

Figure 2.21: Histological analysis of the inner ear of newborn FGF8 mutants. (**A,B**) Wt and mutant cochlea. The FGF8 mutant shows a smaller cochlea in comparison with the wt, but the cochlear duct is visible as well as the cochlear ganglion (**G**). (**C,D**) Cochlear duct. In the mutant the organ of Corti presents a normal architecture. (**E,F**) The Organ of Corti in the mutant inner ear appears normal and the epithelium contains IHC, OHC, pillar (**PC**) and supporting cells (**SC**). (**G,H**) The vestibular epithelium shows also normal morphology; observe the *crista ampullaris* (**CA**), utricle

(**U**) and saccule (**S**). Scale bar in A=120 μm for A and B, bar in B=40 μm for C and D, bar in E= 10 μm for E and F.

FGF8 has been reported to be expressed at E13.5 in delaminating neuroblasts which form the otic ganglion (Pirvola, *et al*., 2002). The next question was whether the otic ganglion develops properly in the *Fgf8* mutant. To answer this question, the development of the otic ganglion was investigated by using anti-neurofilament (NF) 160 as a neural marker. Immunostaining of inner ears of wt and *Fgf8* mutant inner ears at E18 revealed a slightly reduced number of nerve fibers directing themselves towards the cochlea in the mutant (Fig. 2.22D,F;H) as well as a reduced innervation of the hair cells in the organ of Corti (Fig. 2.23B) was visualized. Moreover, the vestibular epithelium showed an apparent reduction of innervation of the hair cells of the crista ampullaris (Fig. 2.23D).

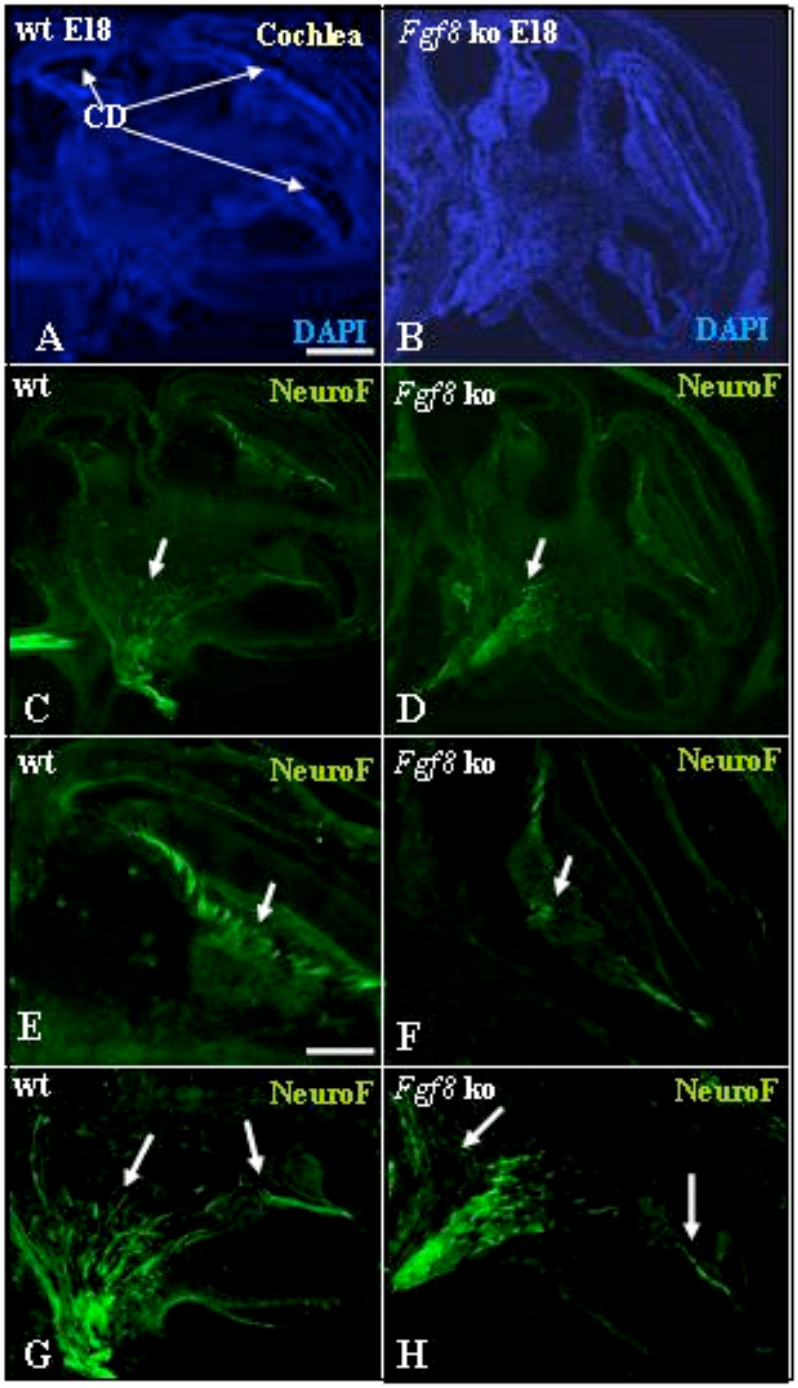

Figure 2.22: Impaired formation of otic ganglion in FGF8 mutants. (**A H**) Immuno-staining of cochleas of wt and FGF8 mutants using anti-NF 160 as a marker. The DAPI staining in A and B shows the structure of the cochlea which is shown in a fluorescent field in C and D, notice the cochlear ducts (**CD**). The mutant cochlea in D shows slightly reduced innervation, which can be observed at high magnification in F and H (*arrows*). Scale bar in A= 80 μm for A-D, bar in E=40 μm for E-H.

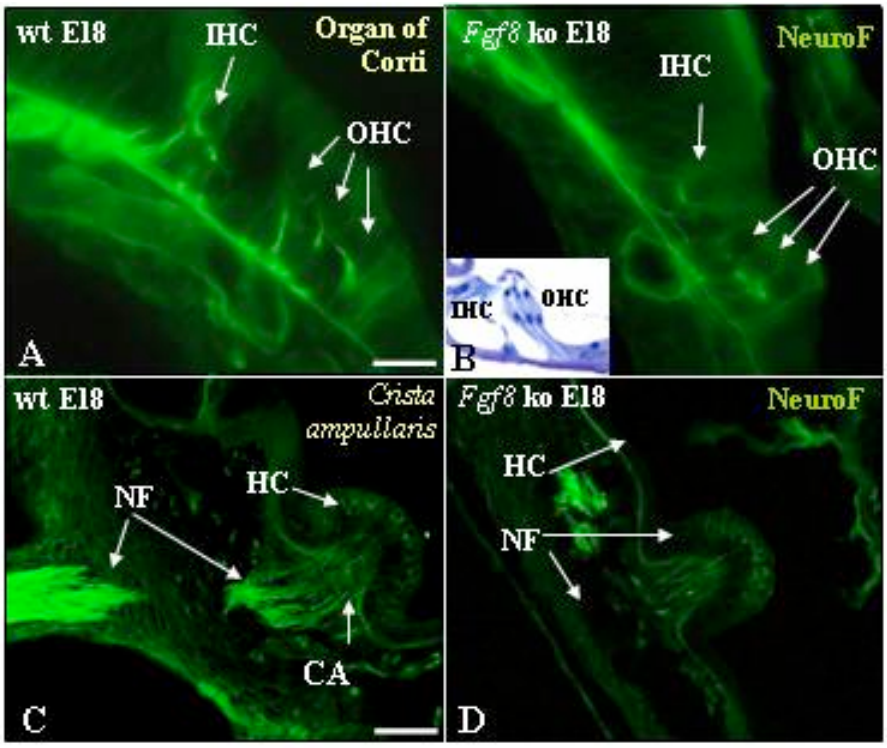

Figure 2.23: Altered innervation of hair cells in FGF8 mutants. (A,B) Notice in the Organ of Corti less NF staining underneath hair cells in the mutant (B) in comparison with the wt in (A). The morphology of IHC and OHC is indicated by a Toluidine stained section depicted in the lower part of the figure B. (C,D) Crista ampullaris. Observe in the mutant (D) that less nerve fibers (NF) appear to innervate the hair cells (HC) in the *crista ampullaris*. **CA:** *crista ampullaris,* **IHC**: inner hair cells, **OHC**: outer hair cells. Scale bar in A= 15 μm for A and B, bar in C=40 μm for C and D.

In zebrafish, FGF8 has been reported to play an essential role redundantly with FGF3 for otic induction (Liu *et al.,* 2003a; Maroon *et al*., 2002; Phillips *et al*., 2001; Reifers *et al*., 1998). However, the set of experiments described above does not support FGF8 as an essential factor for inner ear formation in mice. Interestingly, in mice, FGF3 is expressed before and during otic placode formation (E7-8) in the developing neuroectoderm in a broad area adjacent to the developing otic placode finally concentrating in r5 and r6 of the hindbrain (Alvarez, et al., 2003). At E8.5 FGF3 is expressed in the otic placode and pharyngeal endoderm of the second and third arches (Mahmood, *et al.*, 1996). Later during otocyst formation FGF3 is found in sensory regions and delaminating neuroblasts in the otic vesicle (Wilkinson, *et al*., 1988, Wilkinson, *et al*., 1989, Mahmood, *et al*., 1996, McKay, *et al.,* 1996,

Pirvola, *et al*., 2000). At birth FGF3 is detected in differentiating IHCs. In turn FGF8 is expressed at E7-8 in the pharyngeal endoderm proximal to the developing otic placode, and at E8 in the otic ectoderm and adjacent endoderm as mentioned before. Later it is found to be expressed in the IHCs of the otic epithelium and delaminating cells forming the otic ganglion (Crossley, *et al*., 1995, Pirvola, *et al*., 2002). The expression of FGF3 and FGF8 coincide temporally and spatially at different stages of otic formation suggesting redundancy between FGF3 and FGF8 to execute the otic program.

To test this possibility, mice carrying mutations for both FGF3 and FGF8 have been analyzed.

2.1.*5.2*-FGF8 and FGF3 Coordinate the Normal Development of the Mouse Inner Ear

To obtain *Fgf3*/ *Fgf8* double mutants first, $Fgf3^{-/-}$ null mutants were crossed with the Foxg1-Cre deleter mice. The null $Fgf3^{-/-}$; Foxg1-Cre mutants were subsequently crossed with mice carrying *Fgf8* mutant alleles to create mice containing the following genotype $Fgf3^{-/-}$; $Fgf8^{flox}/Fgf8^{\Delta 2,3}$; *Foxg1-Cre* or $Fgf3^{-/-}$; $Fgf8^{flox}/Fgf8^{flox}$; *Foxg1-Cre*. These mutants were considered as double mutants *(Fgf3+8)* and selected for analysis to study otic development. The inactivation of FGF8 by Foxg1-Cre as explained above, was supposed to occur in the endoderm, mesoderm and adjacent otic placode ectoderm at E8 when Cre is active.

Fgf3+8 mutants were first analyzed histologically at different embryonic stages. At E11 the double mutant embryos showed a normally developing otocyst but from this stage onwards, the otic vesicle appeared delayed and malformed (Fig. 2.24). In the mutants the developing inner ear appeared aberrant at E14 and the expected otic structures were not formed. Normally separated cavities forming the vestibule, saccule, cochlea and semicircular canals appeared in the inner ear at this stage but the mutants presented instead a continuous cavity with rudimentary structures. A rudimentary crista and canal were found, as well as a cochlea but the ganglion could not be distinguished (Fig. 2.24D,F,H).

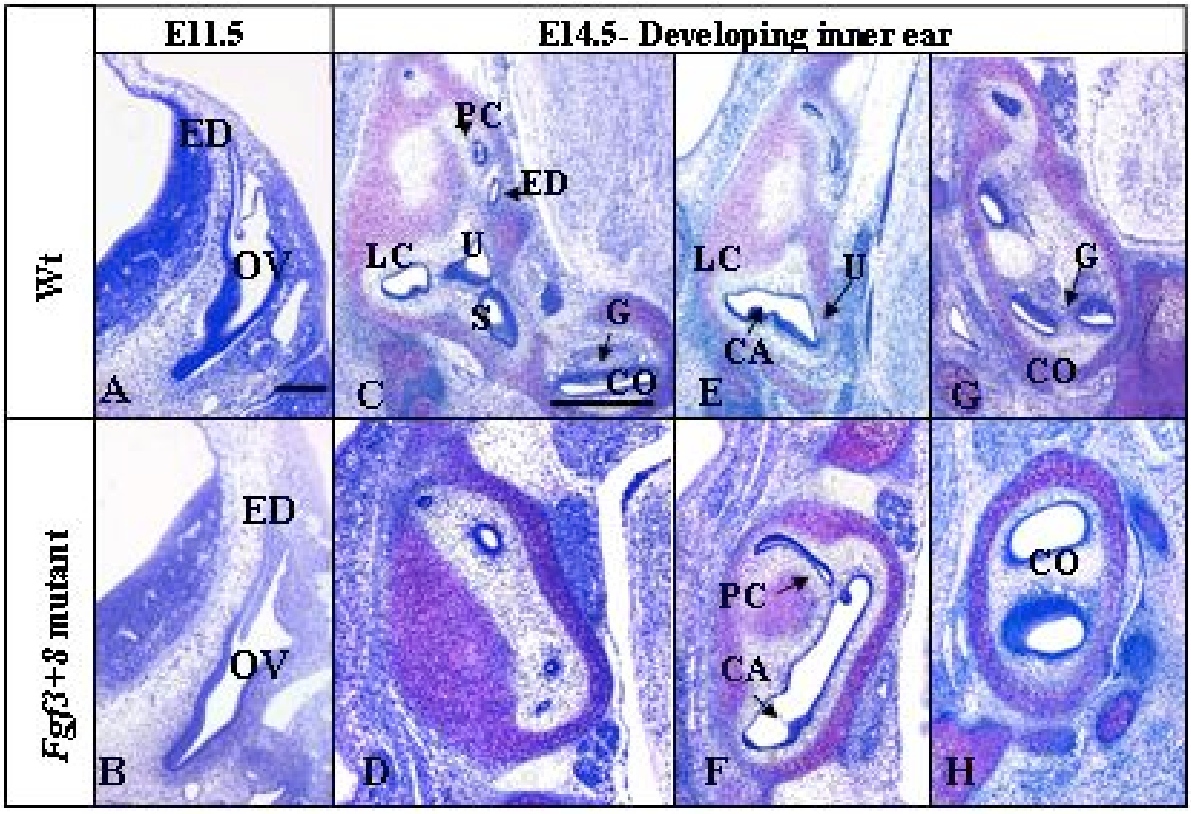

Figure 2.24: Developing inner ear in *Fgf3+8* double mutant embryos at E11 and E14.5. (A,B) Comparison of the developing otocyst at E11 of a wt and mutant embryo, notice the apparently normally developing otocyst and growing endolymphatic duct in the mutant. (C-H) E14.5 developing otocyst of a double mutant. The mutant in D shows some canal-like structures, which are far less developed in comparison with the wt, where the epithelia of utricle, saccule and cochlea were visible as well as the semicircular canals and endolymphatic duct. In F it is possible to distinguish a rudimentary *crista ampullaris* and canal (*arrows)* but the utricle and saccule could not be distinguished. In H a rudimentary cochlear epithelium is seen but the ganglion has not been formed. **CO:** cochlea; **ED:** endolymphatic duct; **G:** ganglion; **LC:** lateral semicircular canal; **OV:** otic vesicle; **PC:** posterior semicircular canal; **S:** saccule; **U:** utricle. **CA:** *crista ampullaris*. Scale bar in A=200 μm for A, B; bar in C=200 μm for C-H.

Fgf3+8 double mutants at E18 were next collected for posterior histological analysis. The inner ears of the mutant embryos showed a completely disorganized structure and the different cavities inside the cochlear duct and vestibule were not formed. The cochlear duct was lined by an undifferentiated epithelium and the organ of Corti was not properly formed (Fig. 2.25A-D). Vestibular and cochlear ganglions were not found. The sections at the level of the vestibule displayed a malformed epithelium as well. The vestibular chamber

was lined by undifferentiated cells and no *crista ampullaris* or macula were distinguished (Fig. 2.25E-H).

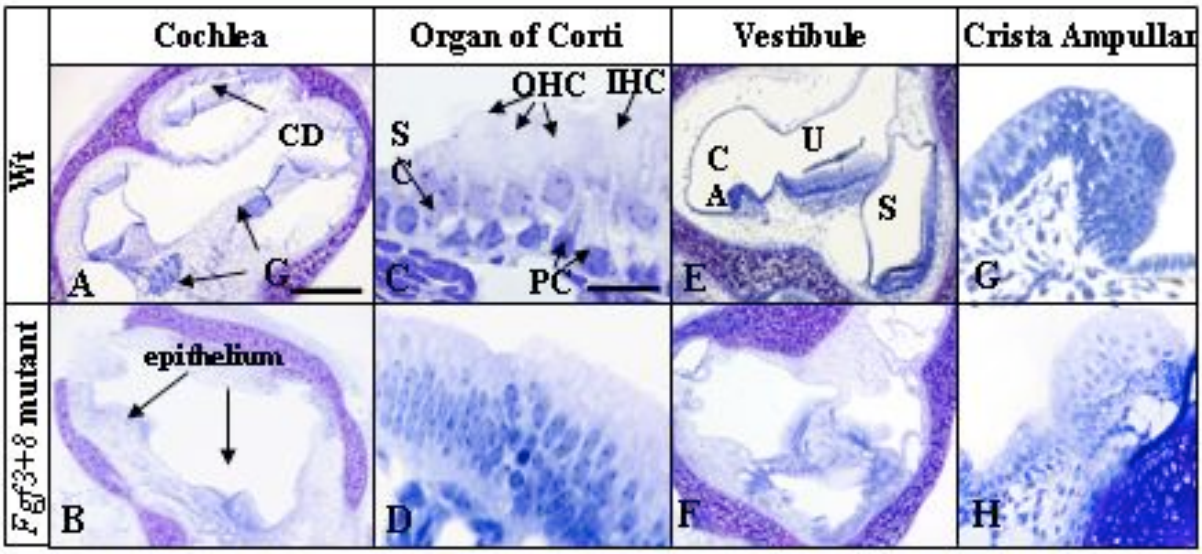

Figure 2.25: *Fgf3+8* double mutant inner ear at E18 (**A,B**) Wt and mutant cochlea. A normal cochlear epithelium is not formed in the mutant inner ear but rather a disorganized epithelium is found (B) and the cochlear ganglion is not formed. The *arrow* in B indicates the organ of Corti. (C,D) The Organ of Corti in the mutant (D) appears as a group of undifferentiated cells while in the wt it is possible to see the different cell types. (**E,F**) The vestibular epithelium was not properly formed in the mutant inner ears. Observe the mutant in F showing a compartment lacking a define epithelium. In H a group of cells which are lining the vestibule is seen at high magnification; they do not form neither a proper *crista ampullaris* nor a macula, compared with the proper developed *crista ampullaris* of the wt inner ear. **CA:** *crista ampullaris*; **CD:** cochlear duct; **G:** ganglion; **IHC:** inner hair cells; **OHC:** outer hair cells; **PC**: pillar cells; **S:** saccule; **SC:** supporting cells; **U:** utricle. Scale bar in A=100 μm for A, B, E and F; bar in C=10 for μm C, D, G and H.

To reveal the cause of the alterations of the inner ear in the double mutants from E11 onwards, apoptosis was examined. Since the inner ear malformations appeared shortly after E11 the presence of apoptotic cells of mutant embryos at E12 by TUNEL (see methods) was investigated. Interestingly, the number of apoptotic cells at E12 was slightly increased in the otocyst of the *Fgf3+8* double mutant embryos and especially ventrally where the ganglion starts to form by delamination of neuroblasts (Fig. 2.26B). However, at E18 it was not possible to detect any apoptotic cells in the mutants in contrast to the wt developing inner ear, which presented some apoptotic cells (Fig. 2.26D).

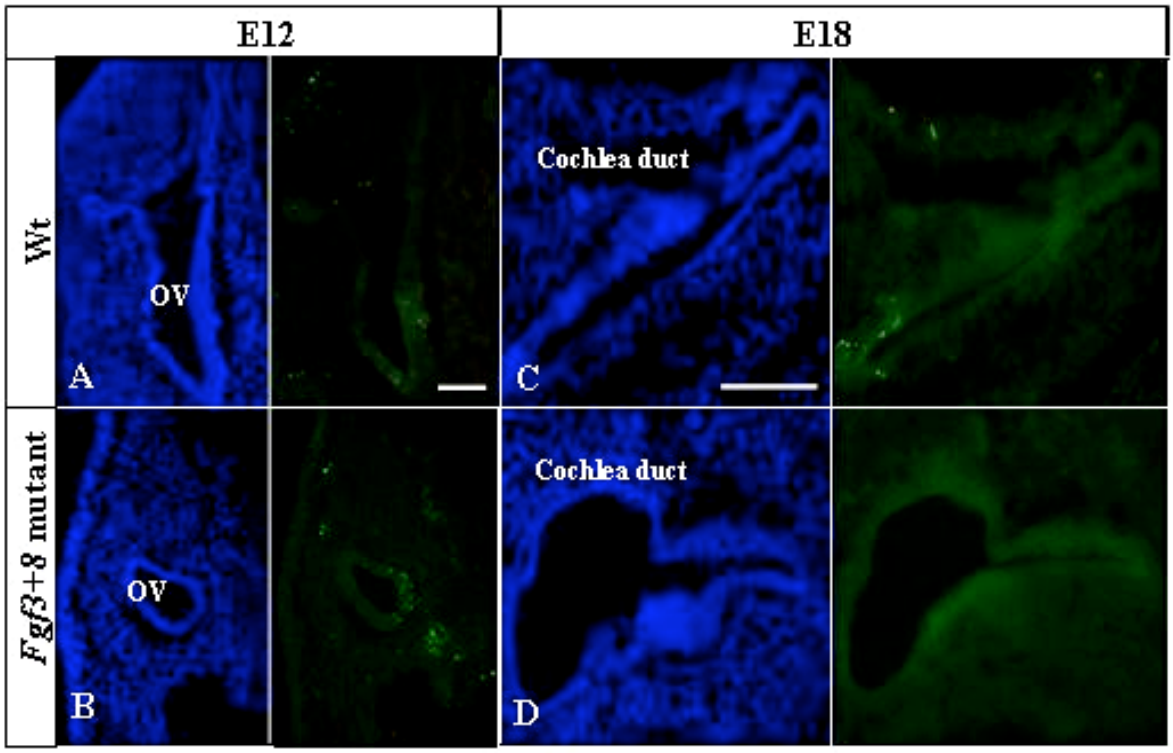

Figure 2.26: Apoptotic cells visualized by TUNEL (*green dots*) in wt and *Fgf3+8* mutant otocysts. The DAPI staining (*blue*) helps to see the structures present in the neighboring sections. (**A,B**) Apoptotic cells in the otocyst at E12. Observe in B, that the mutant shows a smaller otic vesicle with slightly increased cell death in the ventral part and in the region where the future ganglion is formed. (**C,D**) Cochlear duct of inner ears of embryos at E18. While the wt (C) cochlea shows some apoptotic cells, the mutant cochlea does not present apparent cell death. Scale bar in A=200 μm for A and B, bar in C=40 μm for C and D.

The question that arose next was whether the appearance of the inner ear phenotype observed in the double mutants can be correlated with *Fgf8* expression shortly before the onset of the phenotype. To answer this question *in situ* hybridization on sections of E12.5 embryos was performed to analyze the endogenous *Fgf8* expression at this stage. In parallel, *Fgf8* expression was compared with the expression of *Fgf3* by analyzing mice carrying a *lacZ* reporter construct under the control of a *Fgf3* enhancer sequence (Powles, *et al.*, 2004). In this reporter *Fgf3*-expressing cells can be detected by *lacZ* staining (see methods).

Fgf8 was detected in the vestibule and saccule of the developing inner ear at the mentioned stage (Fig. 2.27C-F). Furthermore, a clear *Fgf3* signal was seen in the sensory epithelium

of the utricle and ganglion between E12-E16 (Fig. 2.27G,H and data not shown). However, the expression of *Fgf3* in the utricle is broader than the expression detected with *Fgf8*.

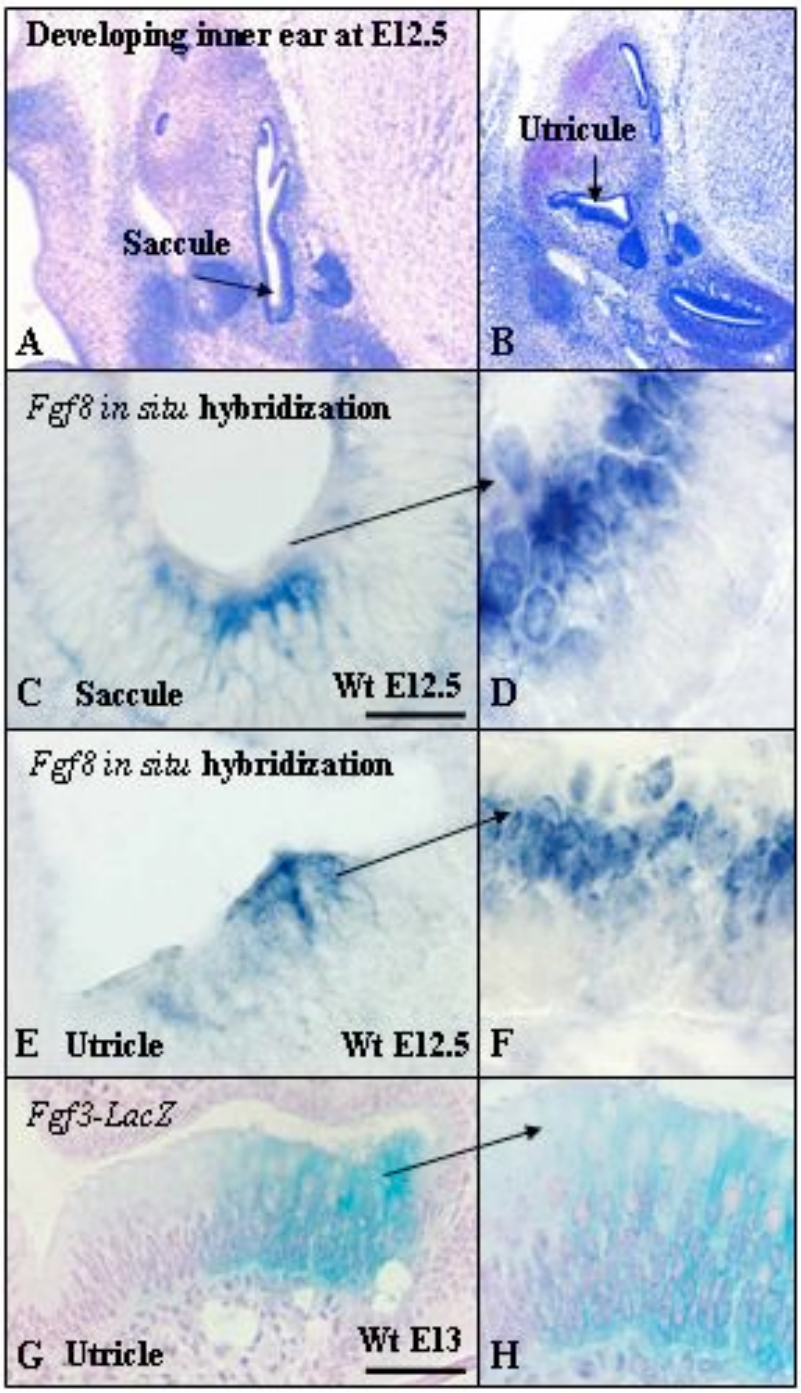

Figure 2.27: *Fgf8* and *Fgf3* expression in the sensory regions of the developing inner ear of a wt embryo at E13-13.5. (**A,B**) Transversal section of a developing otocyst at E12.5 to show the localization of the structures stained in C-H. (**C**,**D**) Transversal section of the developing otocyst at E13.5 shows the expression of *Fgf8* in the saccule. Observe the cells at higher magnification in D. (**E**) Cells of the utricle expressing *Fgf8*. (**F**) Higher magnification of the cells expressing *Fgf8* in E. (**G**) Transversal section of an otocyst at E13.5 expressing the *Fgf3-lacZ* transgene reporter, observe *Fgf3* expression in the prospective utricle. (**H**) High magnification of the picture in G showing the

Fgf3-expressing cells, notice the wider expression of *Fgf3* in comparison with *Fgf8* in the same structure (F). Scale bar in C=20 μm for C-E; bar in G=40 μm.

Together these data indicate that FGF3 and FGF8 contribute to the formation of the otocyst in a redundant manner and furthermore that they are essential for the proper otic formation. Expression of FGF8 has been found to partially overlap with the expression of FGF3 in the developing utricle suggesting that they could compensate each.

2.1.*6*-FGF2 is not Essential for Inner Ear Formation in Mice

Furthermore the role of FGF2 for development of the inner ear was analyzed This member of the FGFs family is expressed early during otic development in the otic placode and otic vesicle in mice and chicken (Frenz, *et al*., 1994, Vendrell, *et al*., 2000). Mouse embryonic cochlear cultures treated with FGF2 showed a significant increase in the number of pillar cells and a small increase in the number of inner hair cells in explants cultures (Mueller, *et al*., 2002). FGF2 together with FGF1 were reported to play important roles in the migration and initial differentiation of cochlear ganglion neurons in the mouse (Hossain, *et al*., 2000) but the participation of FGF2 during otic development in mice was not reported. Thus, in this study the *in vivo* role of FGF2 during development of the inner ear in mice was addressed. This mouse mutants in which FGF2 was inactivated by homologous recombination (Dono, *et al*., 1998, Ortega, 1998) were analyzed. In these mutants the complete first *Fgf2*-coding exon and parts of the 5´- and 3´-flanking intronic sequences were replaced by the neo^r gene (Dono, *et al*., 1998, Ortega, 1998).

The cochlear and vestibular sensory organs of the inner ear of the $Fgf2^{-/-}$ mutants were examined and no obvious defects compared with the wt control were revealed (Fig. 2.28). Likewise, no cellular loss or defects were observed upon more detailed inspection of the cochlear sensory epithelium, the organ of Corti and the vestibular sensory epithelium (Carnicero 2004) (Fig. 2.28).

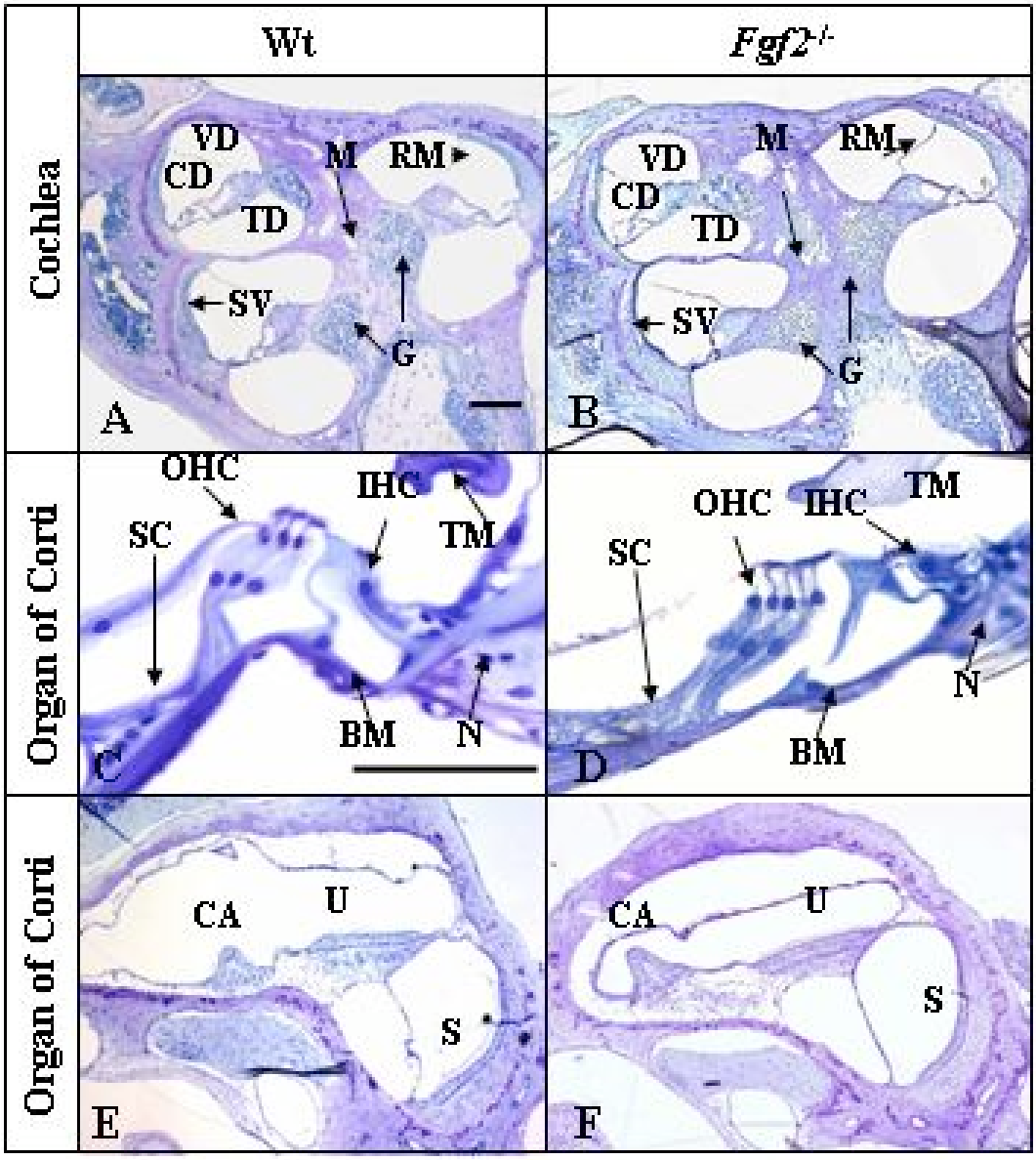

Figure 2.28: Sections of adult inner ears at the level of the cochlea and vestibule of wt and *Fgf2*$^{-/-}$ mutants. (**A,B**) Sections of the cochlea show a normal histological architecture in the mutants (B). (**C,D**) Comparison of the organ of Corti between wt and mutant. No cellular abnormalities are observed in the mutant (D). (**E,F**) The vestibular system of the mutant mice is normal when compared with the wt. **BM**: Basilar membrane; **CA**: *crista ampullaris*; **CD:** cochlear duct; **G:** ganglion; **HC**: hair cells; **IHC:** inner hair cells; **N:** nerve fibers; **OHC:** outer hair cells; **RM:** Reissner´s membrane; **S:** saccule; **SC:** supporting cells; **SV:** *stria vascularis*; **TM:** tectorial membrane. Scale bar in A=200 μm for A,B,E and F; bar in C=100 μm for C and D.

To examine further the functional integrity of the auditory structures, three different markers were used, which are important for maintaining the potassium concentration in the endolymph of the cochlear duct. These antibodies were directed against potassium voltage-

gated channels, KCNQ4 which has been described to be expressed in the basal membrane of the hair cells in the organ of Corti (Kharkovets, 2000), the K-Cl cotransporter Kcc4 and Barttin, an essential _-subunit for ClC-Ka and ClC-Kb chloride channels. In the inner ear Kcc4 is expressed in the organ of Corti in the supporting cells, stria vascularis and OHC, and it has been suggested to recycle potassium from the OHC to the Deiters´cells (supporting cells) (Boettger, 2002). Barttin is expressed in the cochlea and in the basolateral membrane of the potassium-secreting cells of the stria vascularis (Estevez, 2001). Thus they are good candidates to test the functionality of the inner ear epithelium. Finally, KCNQ4, Kcc4, and Barttin showed a normal pattern of expression in the *Fgf2*$^{-/-}$ mutant in comparison with the wt (Carnicero, 2004) (Fig. 2.29).

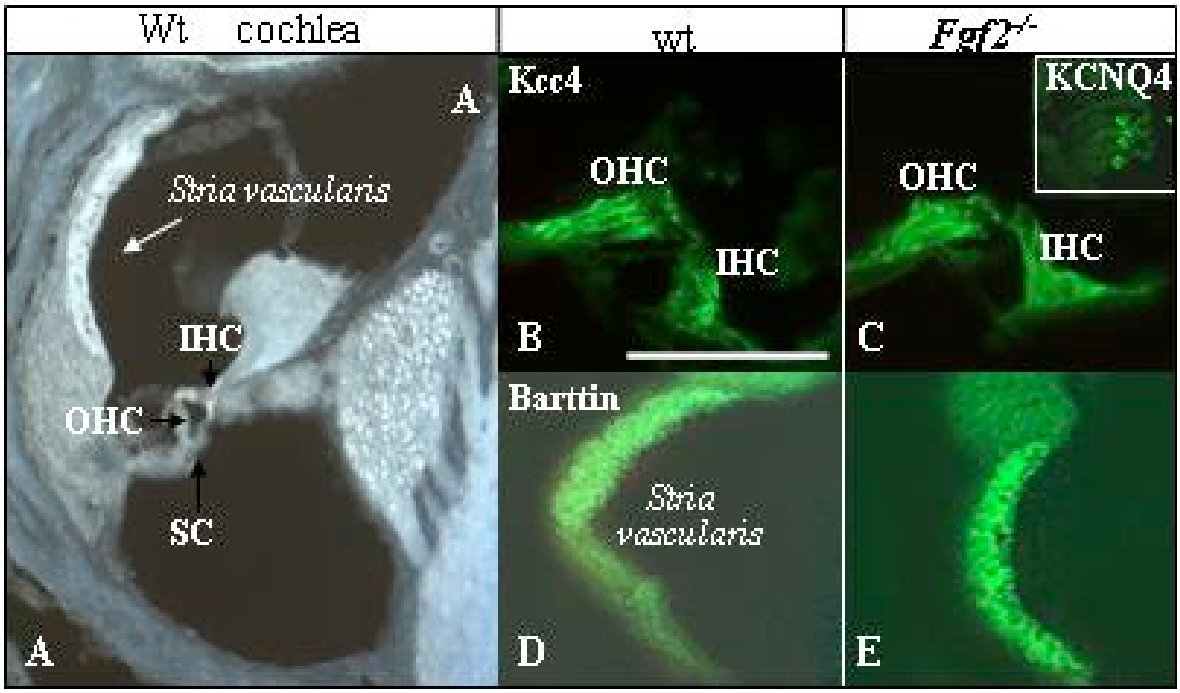

Figure 2.29: Expression of inner ear markers in *Fgf2*$^{-/-}$ mutant mice. (**A**) Section through the inner ear at the level of the cochlea indicating the relevant structures for the immunostainings in B-E. (**B,D**) Sections of wt adult inner ear indicating the normal expression of the used markers. (**C,E**) Sections through a *Fgf2*$^{-/-}$ mutant inner ear showing a normal staining in comparison with the wt for all the used markers. **IHC:** inner hair; **OHC:** outer hair cells; **SC:** supporting cells; Scale bar= 100 μm

The histological and functional analysis of the *Fgf2*$^{-/-}$ mutants showed no major defects in the inner ears indicating that FGF2 is not essential for otic vesicle formation in mice.

Table 2.1: Summary of the phenotypes found in the different analyzed mutants

Mice Mutants	Otic Phenotype	Percentage
Fgf3-/-	**Adults (5%):** -No otic phenotype -Few mutants with cochlear and vestibular defects. -Less coiled cochlea and disorganized OC. -Reduced vestibular epithelium and ganglion. -Reduced ASC.	**Adults:** n=80 (5 % presented otic phenotype) **Embryos**: n=40 (normal)
Fgf3neo	**Adults:** -Turning behavior -Asymmetrical otic defects -Widened and shortened PSC -Smaller LSC -Malformed ampulla -No common cross -Abnormal vestibular and cochlear epithelium **Embryos:** **-**Slightly delay otic vesicles	**Adults:** n=65 (12% moved in circles, otic phenotype) **Embryos:** n=20 (20% otic phenotype)
Fgf3-/- ***Fgf10-/-***	**Embryos:** -Highly reduced otic tissue	**Embryos:** n=34 (35% showed microvesicles, the rest present drastically reduced otic tissue)
Fgf3-/-; ***Fgf10+/-***	**Adults:** -Turning behavior -Asymmetrical otic defects -Missing LSC and common cross -Malformed ASC and PSC and vestibule -Incompletely coiled cochlea -Abnormal vestibular and cochlear epithelium **Embryos:** **-**Ventralized and smaller otic vesicle -Reduced otic ganglion	**Adults**: n=19 (26% moved in circles, otic phenotype) **Embryos:** n=15 (45% otic phenotype)
Fgf8-/-; ***Foxg1-Cre***	**Newborns:** -Slightly reduced otic innervation	**Embryos:** n=15 (100% normal developing otocyst) **Newborns:** n=6 (2 mutants exhibited reduced innervation)
Fgf3-/-;Fgf8-/- ***Foxg1-Cre***	**Embryos:** -General malformation of the otocyst from E11 onwards	**Embryos:** n=6 (100% of the mutants showed otic phenotypes after E11)

ASC: anterior semicircular canal; **LSC:** Lateral anterior semicircular**; PSC:** posterior anterior semicircular**; OC:** organ of Corti

2.2-Gain-of-Function Approach in Chicken Embryos

To complement the studies performed in mice in this work, the function of different members of the FGF family in chicken embryos was addressee.

In chicken, electroporation was used to perform gain- and loss-of-function approaches during early stages of chick development. To define the developmental stages of chicken embryos the table of Hamilton and Hamburger (HH) was used (Hamburger, 1951).

2.2.*1*-The Ectopic Expression of FGF3 and FGF10 in the Neural Tube of Chicken Embryos Induces the Formation of Ectopic Otic Structures in the Ectoderm

Electroporation into the neural tube of chicken embryos was performed to test the capacity of FGF3 and FGF10 to act as inducers of the otic placode in avian. The capacity of FGF3 to act as otic inducer when overexpressed in the ectoderm of chicken via virus infection was already reported (Vendrell, *et al.,* 2000). The goal of the experiments in the present work was to test the importance of the hindbrain as a source of FGF3 and other members of the FGF family to instruct the ectoderm to form an otic vesicle.

cDNAs for *Fgf3* and *Fgf10* from mouse were cloned into a pCS2 vector under the control of a cytomegalovirus (CMV) promoter (pCS2m*Fgf3* and pCS2m*Fgf10*). This plasmid together with a pEGFP-C1 reporter vector (Clontech), which encodes Enhanced Green Fluorescent Protein were electroporated into the neural tube of embryos at stages HH 8-9 (see methods 5.4). The embryos were incubated at 37° C until the desired stage had been reached and then prepared for electroporation. In this experimental setting, expression of GFP serves as a control marker for successful electroporation and serves as a reporter for the co-electroporated plasmid, which contains *Fgf3* or *Fgf10*. GFP expression was detectable as early as 2h after electroporation (Fig. 2.30). The GFP signal reached peak intensity around 12 h after electroporation. After this time it was still possible to detect GFP but the intensity decreased, which is consistent with episomal plasmid dilution due to mitotic division. Following electroporation of the GFP reporter gene, one side of the neural tube is GFP-positive, whereas the other side is GFP-negative and thereby serves as an excellent internal control (Fig. 2.30).

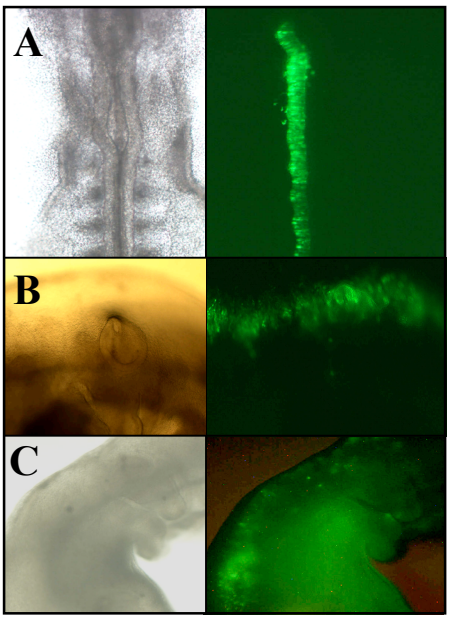

Figure 2.30: Embryos electroporated into the neural tube with a pEGFP reporter plasmid. Brightfield pictures of the embryos (left) and the expression of GFP (right) at different timepoints after electroporation are shown. (**A**) Embryo 2h after electroporation (**B**) Embryo 24h after electroporation, **C:** Embryo 36h after electroporation. The intensity of GFP expression decreases gradually, which is consistent with episomal plasmid dilution due to mitotic division.

After electroporation the embryos were incubated for 36h at 37°C and dissected for analysis. The survival average of the electroporated embryos was 76%. The overexpression of pCS2m *Fgf3* was confirmed by whole-mount *in situ* hybridization using a mouse antisense probe for *Fgf3*. The expression of *Fgf3* was clearly detected in the neural tube of the electroporated side. *Fgf3* was expressed in a broad area that included the hindbrain next to the area where the otic vesicle forms (Fig.2.31).

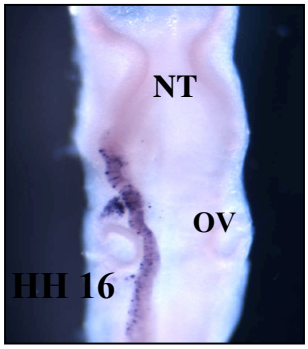

Figure 2.31: *Fgf3 in situ* hybridization of a pCS2m*Fgf3*-electroporated chicken embryo. The picture shows the expression of exogenous mouse *Fgf3*-RNA in the electroporated (left) part of the neural tube of an embryo at stage HH16. *Fgf3* was expressed in a broad area of the hindbrain posterior and anterior to place where the otic vesicle is formed. **OV:** otic vesicle, **NT:** neural tube.

The analysis of the embryos after electroporation revealed that the electroporation of pCS2m*Fgf3* into the neural tube (n=35) resulted in ectopic structures in the ectoderm close and posterior to the normal otic vesicle in 70% of the electroporated GFP-positive embryos (Table 2.2). Ectopic structures were never found far away from the normal otic vesicle. This observation is coincident in part with the reported large area of ectoderm with competence to form an otic placode, which comprises a broad stripe anteriorly and posteriorly to the otic vesicle (Vendrell, *et al.*, 2000). This competence decreases at stages HH 10-11 (12 somites). The structures found presented a vesicular shape and a single layer of epithelium could also be visualized (Fig. 2.32).

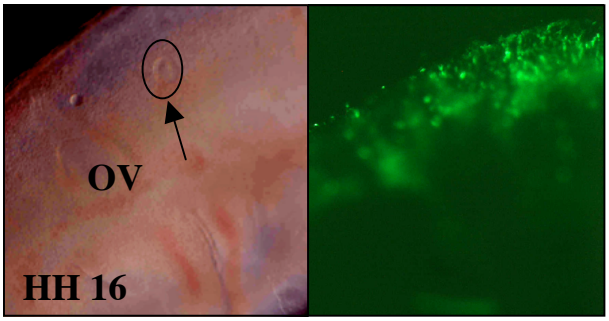

Figure 2.32: pCS2m*Fgf3*-electroporated embryo, after electroporation, at stage HH 16 showing an ectopic structure (*left-arrow and circle*) and the corresponding GFP expression (right). **OV:** normal otic vesicle.

In order to determine the nature of these ectopic structures, the embryos were subjected to RNA *in situ* hybridization with different otic markers. The *in situ* hybridization with a RNA probe against chicken LIM-homeodomain *Lmx1*, which is expressed dorso-laterally within the normal otic vesicle, showed a positive signal within the structure (Fig. 2.33).

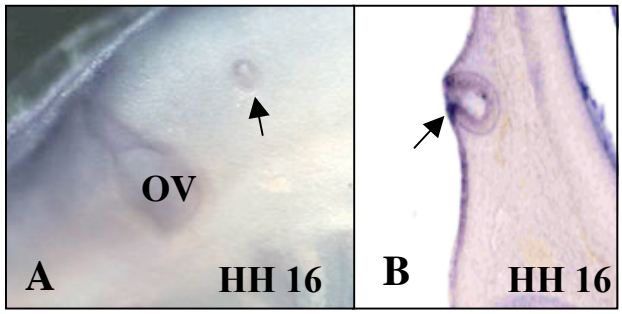

Figure 2.33: Chicken *Lmx1 in situ* hybridization in a pCS2m*Fgf3*-electroporated embryo. (**A**) Whole-mount *in situ* hybridization of an embryo showing an ectopic structure adjacent to the normal otic vesicle (*arrow*). (**B**) Transversal section of the same embryo shown in A. The ectopic structure expresses *Lmx1* (*arrow*). **OV:** otic vesicle.

Histological analysis of these structures was also performed to confirm their epithelial nature. To do so, another set of embryos were stained with Toluidine Blue. The analysis showed a very organized vesicular structure with an epithelium surrounding it (Fig. 2.34). Together these data support the capacity of FGF3 as a signal coming from the hindbrain and able to induce ectopic otic vesicles.

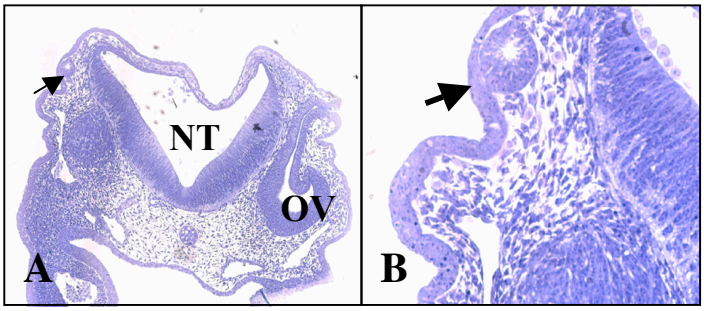

Figure 2.34: pCS2m*Fgf3* electroporated embryo. Transversal sections of an embryo with an ectopic vesicular structure (*arrow*). The sections are stained with Toluidine Blue. (**A**) Section shows the normal otic vesicle control (right side) and the little ectopic structure (electroporated left side). (**B**) Higher magnification of the ectopic structure shown in A. **NT:** neural tube, **OV:** otic vesicle.

The overexpression of *Fgf3* also affected the size of the normotopic otic vesicle (Fig. 2.35). Many embryos (20%) showed on the electroporated side an oversized otic vesicle in comparison to the normal otocyst on the non-electroporated side.

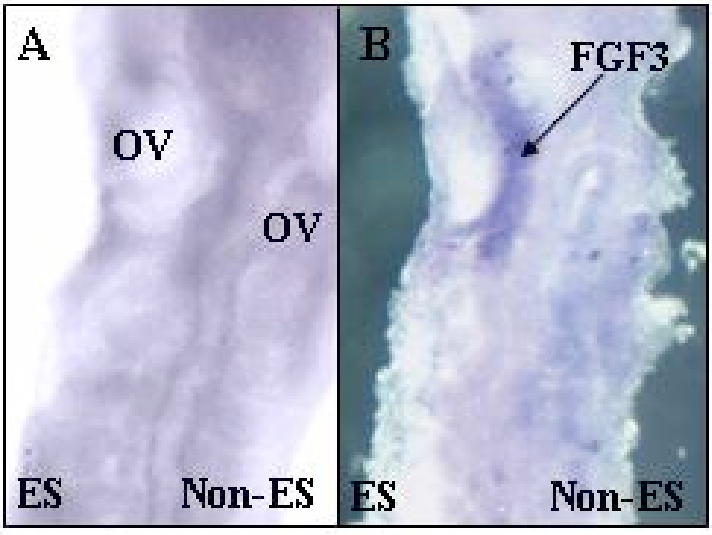

Figure 2.35: pCS2Fgf3 electroporated embryo. (**A**) An embryo showing an oversized otocyst on the electroporated side (left). (**B**) The same embryo showing expression of Fgf3 after in situ hybridization.

Since FGF10 has been reported to be involved in inner ear morphogenesis, differentiation, and sensory neuron survival in mice (Ohuchi, et al., 2000, Pauley, et al., 2003) and moreover shares the same receptor (FGFR2b) with FGF3, next the capacity of FGF10 to participate in inner ear formation was tested.

The results obtained by electroporation of *Fgf10* (n=91) also showed ectopic structures close to the normal otic vesicle, similar to those obtained with *Fgf3* electroporation. However, the percentage was much lower, approximately 5% as compared to the percentage for *Fgf3* (Fig. 2.36, Table 2.2).

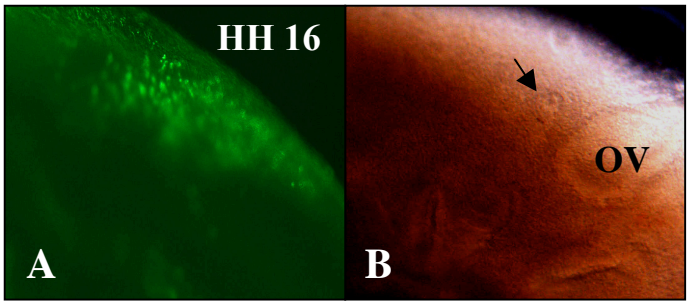

Figure 2.36: pCS2m*Fgf10* electroporated embryo. The embryo was electroporated at stage HH 9 and isolated 30 hours later for analysis. (**A**) GFP expression in the neural tube on the electroporated side. (**B**) Ectopic structure (*arrow*) on the electroporated side close to the normal vesicle. **OV:** otic vesicle.

After electroporation the expression of pCS2m*Fgf10* cDNA was confirmed by *in situ* hybridization on the electroporated GFP-positive side of the embryo (Fig. 2.37).

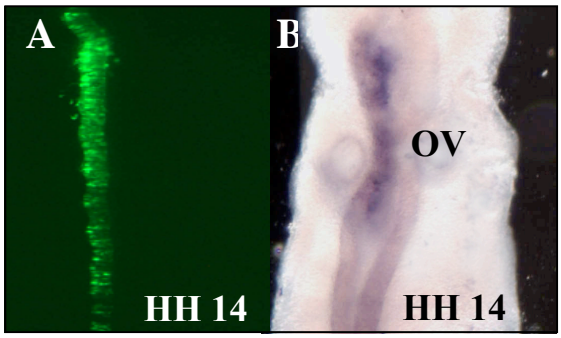

Figure 2.37: *Fgf10 in situ* hybridization of a pCS2m*Fgf10* electroporated embryo. (**A**) Embryo expressing GFP after electroporation. (**B**) Fgf10 expression in the electroporated half of the neural tube. *Fgf10* was detected in the hindbrain in an area located posteriorly and anteriorly to the normal otic vesicle**. OV:** otic vesicle.

In situ hybridization with different otic markers showed the expression of chicken *Lmx1, Pax2 and Cek8* in the ectopic structures. The regionalization of the expression of the different otic markers was not normal; instead all observed markers were uniformly distributed in the whole ectopic structure (Fig. 2.38).

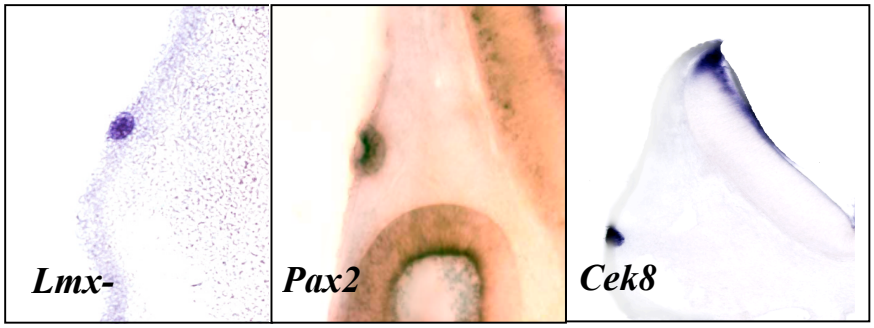

Figure 2.38: Embryos at stage HH 15-16, 24 hours after electroporation of *Fgf10.* The ectopic structures found on the electroporated side express different otic markers, which are shown in this panel. (**A**) *Lmx-1*, (**B**) *Pax-2*, (**C**) *Cek-8*

The capacity of FGFs to induce ectopic otic structures on the ectoderm upon electroporation into the neural tube has been shown. Next, to elucidate the mechanism of otic induction, the possible interactions between members of the FGF gene family was tested.

2.2.*2*-FGFs Can Affect the Expression of Other Members of the FGF Family

Interactions between different members of the FGF family are already known from other developing systems such as the vertebrate limb (Kawakami, *et al*., 2001). For instance, during chicken limb development FGF10 has been reported to induce FGF8 in limb buds (Ohuchi, *et al*., 1997, Xu, *et al*., 1998). In order to see whether a similar genetic interaction may also occur during inner ear development in the hindbrain, effects of overexpression of *Fgf10* in r3 and r5 of the hindbrain was analyzed. Therefore, a construct containing *Fgf10* was coelectroporated with a pEGFP repoter plasmid into the neural tube of chicken embryos at stages HH 8-9. 24 h later the embryos were analyzed. A set of embryos was processed for *Fgf10 in situ* hybridization (Fig. 2.39A) to monitor overexpression of *Fgf10* in r3 and r5. Another set of embryos was used to examine the expression of endogenous *Fgf8* by *in situ*

hybridization. In *Fgf10*-electroporated embryos ectopic expression of *Fgf8* in r3 and r5 was observed in a stage-dependent manner. The strongest ectopic expression of *Fgf8* was seen at early stages around HH 10. Expression then decreased at HH 11 first more caudal in r5 and later more anterior in r3 (Fig. 2.39B). Taken together, these results indicate that FGF8 can be induced by FGF10 in the chicken hindbrain.

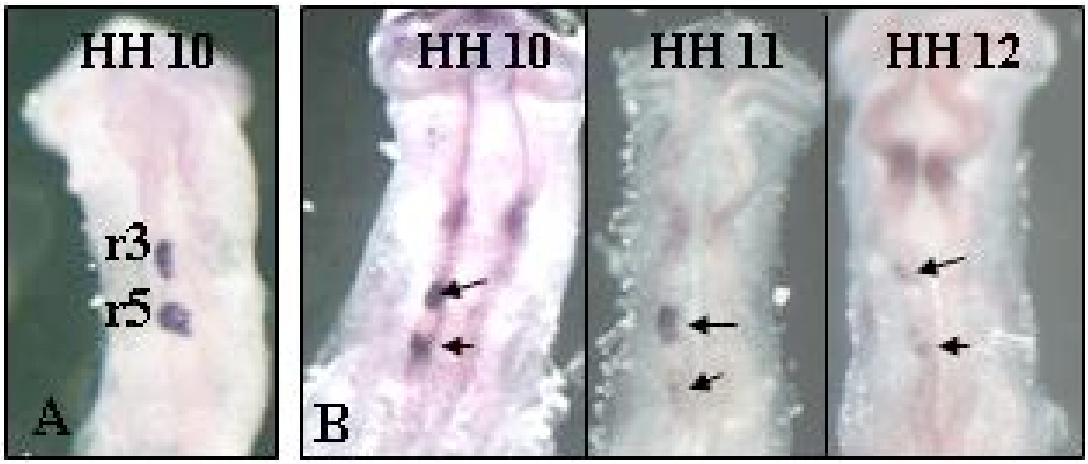

Figure 39: *Fgf10* expressing plasmid was used to electroporate chicken embryos. The embryos were electroporated at stage HH 8 and isolated after different timepoints (indicated on the top of each figure) to investigate the expression of *Fgf10* or *Fgf8*. (**A**) *Fgf10 in situ* hybridization in an *Fgf10*-electroporated embryo. Notice the ectopic expression of Fgf10 in rhombomeres 3 and 5 on the electroporated side. (**B**) *Fgf8 in situ* hybridization in *Fgf10*-electroporated embryos. The embryos show induction of *Fgf8* by *Fgf10* in a stage-dependent manner. The expression of *Fgf8* is strongest at stage HH 10 and decreases at stages HH 11 and HH 12 first in the posterior region and then most anterior.

2.2.*3*-Overexpression of FGF8 in the Neural Tube Leads to the formation of smaller Otocysts in Chicken Embryos

Another member of the FGF family, FGF8 has been shown to be important for otic placode induction as well as epithelial organization of the otic vesicle in zebrafish (Maroon, et al., 2002, Liu, et al., 2003). In chicken, there are evidences for FGF8 acting as a regulator of the otocyst patterning (Adamska, *et al.,* 2001). Therefore, the capacity of this factor to participate in early inner ear formation using electroporation was tested in the present work. The effect of ectopic expression of *Fgf8* in the neural tube by electroporation was explored. *Fgf8* cDNA was cloned into pCS2 (pCS2m*Fgf8*) and coelectroporated with an EGFP reporter vector into the neural tube of chicken embryos at stages HH 8-10. The success of

electroporation was confirmed by GFP expression and *Fgf8 in situ* hybridization, which confirmed the expression of *Fgf8* in the electroporated side of the neural tube (Fig. 2.40). Electroporation of *Fgf8* resulted in a reduced survival of embryos, compared to the embryos electroporated with *Fgf3* and *Fgf10*. As mentioned, normally the average survival rate was 76% in case of *Fgf3* and *Fgf10* electroporation, but when *Fgf8* was overexpressed the survival rate was only 30%. Malformations of the majority of embryos were also observed upon *Fgf8* overexpression. Specifically, the midbrain and hindbrain could not develop properly. Although the electroporated side was preferentially affected, the non-electroporated side was also often affected by these malformations.

Less malformed embryos were chosen for further analysis. Concerning the otic vesicle, the overexpression of *Fgf8* (n=52) resulted in a smaller and malformed otocyst on the electroporated side, which was found in 62% of the electroporated embryos expressing GFP. To determine the nature of the ectopic vesicle, morphological analysis of these embryos was performed. The otic vesicle on the electroporated side presented a clear malformation (Fig. 2.41). The analysis of *Pax2* expression by *in situ* hybridization showed a reduced expression of this gene in the otic vesicle of the electroporated side (Fig. 2.42).

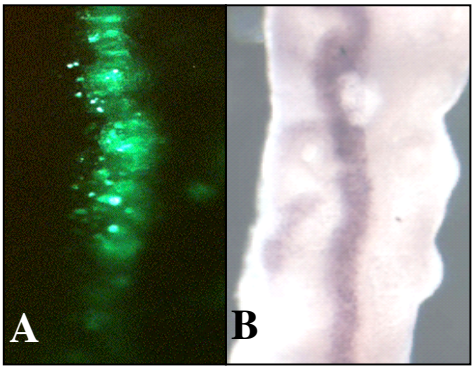

Figure 2.40: *Fgf8 in situ* hybridization in a pCS2m*Fgf8*-electroporated embryo. (**A**) HH15 embryo expressing GFP 24 h after electroporation. (**B**) *In situ* hybridization monitoring overexpression of *Fgf8*. *Fgf8* is expressed in the electroporated half of the neural tube, which coincides with GFP expression.

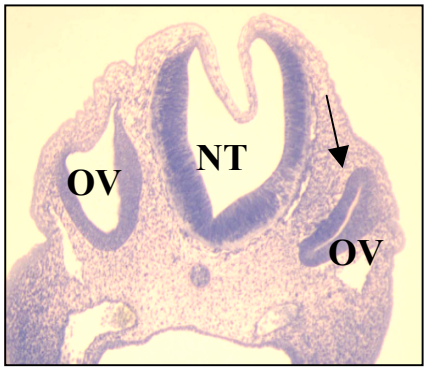

Figure 2.41: Transversal section of a pCS2m*Fgf8*-electroporated embryo stained with Toluidine Blue (right side: electroporated side). The otocyst on the electroporated side is smaller and malformed (*arrow*) in comparison with the normal otocyst on the control side. **OV:** otic vesicle, **NT:** neural tube.

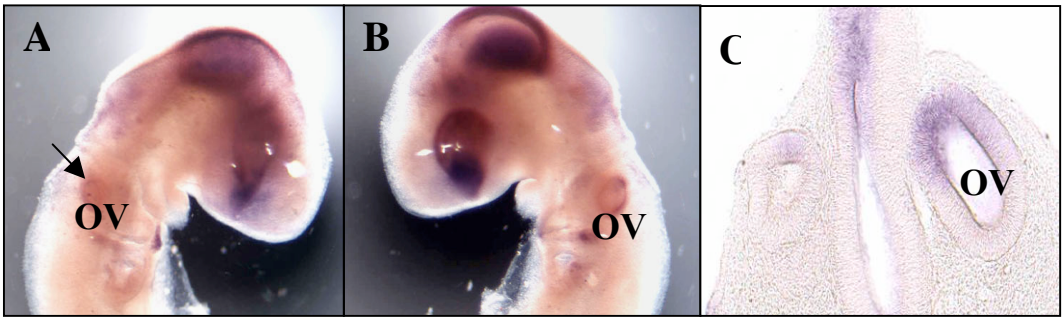

Figure 2.42: Upper panel: chicken *Pax2* whole mount *in situ* hybridization of a pCS2m*Fgf8*-electroporated embryo. (**A**) Electroporated side showing a reduced otic vesicle as well as reduced expression of *Pax2 (arrow*). (**B**) Non-electroporated side showing a normal otic vesicle and *Pax2* expression (**C**) Transversal sections of the same embryo comparing the expression of *Pax2* in both control and electroporated otocysts. The expression on the electroporated side is reduced in the otocyst. **OV:** otic vesicle.

2.3-Loss-of-Function Approach in Chicken Embryos

Using gain-of-function experiments the capacity of FGF3 and FGF10 to produce ectopic otic structures and the capacity of FGF10 to induce FGF8 have been shown. Further evaluation of the importance of these factors remains necessary to determine whether they are not only sufficient but also essential for inner ear formation. In order to do so, loss-of-function experiments using antisense-morpholinos and siRNA were carried out.

2.3.1-Electroporation of Morpholinos directed against FGF3 Results in Defective Morphogenesis of the Chicken Otocyst

Antisense morpholinos are antisense oligonucleotides that bind and inactivate selected RNA sequences by blocking the translation from messenger RNA into protein. Morpholinos have been designed to overcome the limitations of typical DNA oligonucleotides. They are more stable than conventional oligonucleotides (Heasman, 2002). Although morpholinos have been widely used in zebrafish and shown to interfere with gene expression, they have been used in only a few studies in chicken embryos (Kos, *et al*., 2001, Granata, 2003, Kos, 2003). In *Xenopus* and zebrafish embryos morpholinos are classically

delivered by intracellular injection in early stages, but this is not possible in chicken embryos (Bourikas, *et al.*, 2003). Therefore, electroporation is a feasible way to introduce morpholinos into chicken embryos.

In the present study, this approach was employed to block endogenous expression of *Fgf3*. Embryos at stages HH 8-9 were electroporated with 3´-fluorescein labelled morpholinos (see methods 5.3). Thereafter the embryos were incubated at 37°C for 36h to reach the required stage at which they were removed from the eggs to analyze their phenotype. Electroporated embryos were detected by monitoring fluorescein (Fig. 2.43A).

The analysis of embryos electroporated with *Fgf3*-morpholinos (n=80) (Table 2.2) revealed a clear phenotype that consisted of a failure of the otic vesicle to close properly (Fig. 2.43B). The otocyst on the control non-electroporated side (Fig. 2.43C) as well as the otocyst of embryos electroporated with control morpholinos was normal (data not shown).

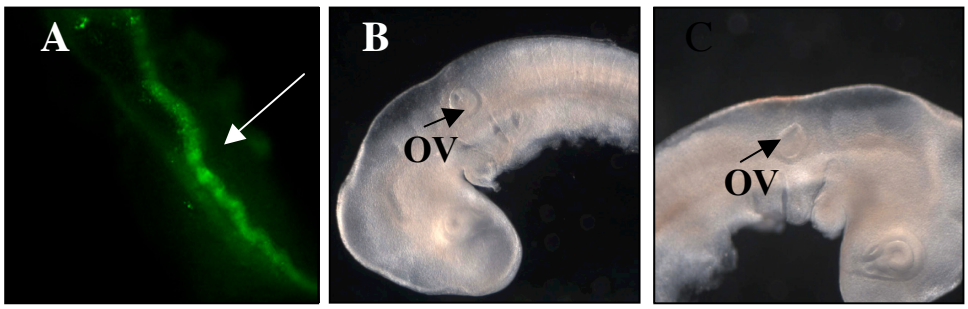

Figure 2.43: *Fgf3*-morpholino-(Fluorescein-labeled) electroporated embryos. (**A**) Fluorescein is seen in the electroporated side (*arrow*). (**B**) Electroporated side of an embryo 24 h after electroporation. Notice the delayed closure of the otocyst. (**C**) Non-electroporated control side of the same electroporated embryo in B where the otocyst has completed its closure. **OV:** otic vesicle

The otic vesicle misgenesis was confirmed histologically by sectioning embryos electroporated with FGF3 morpholino and staining with Toluidine Blue (Fig. 2.44).

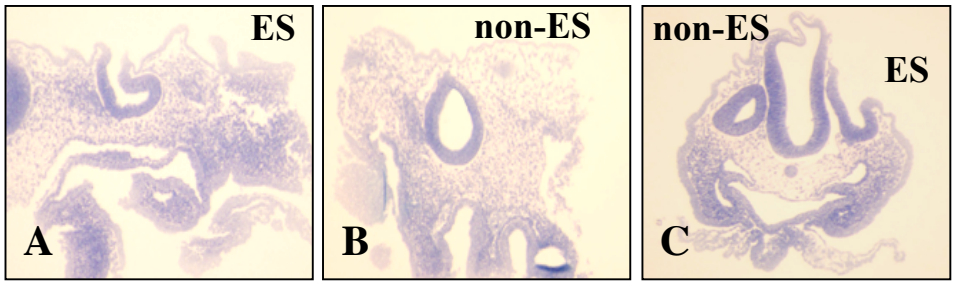

Figure 2.44: Sections of *Fgf3*-morpholino-electroporated embryos stained with Toluidine Blue . (**A,B**) Sagittal section of an electroporated embryo, (**A**) electroporated side (**ES**) showing an open

otic vesicle, (**B**) non-electroporated side (**non-ES**). (**C**) Transversal section of an electroporated embryo (an open vesicle is seen on the right electroporated side).

Subsequently, *in situ* hybridization with otic markers was carried out to determine whether the retarded otocyst presented abnormal expression of otic genes, but no differences could be found in the expression of *Lmx1, Cek8* (Fig. 2.45) and *Pax2* (data not shown) compared to the non-electroporated side.

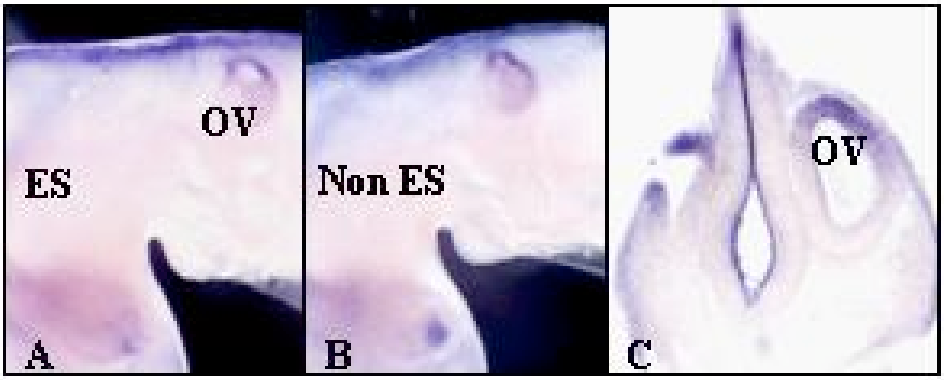

Figure 2.45: (**A,B**) *Lmx1 in situ* hybridization of *Fgf3* morpholino-electroporated embryos. (A) Electroporated side. The otic vesicle appears smaller but the expression of *Lmx1* is not altered. (B) Non-electroporated side with a normal otocyst. (**C**) *Cek8 in situ* hybridization in a *Fgf3* morpholino -electroporated embryo. Transversal section showing the open vesicle on the electroporated side with unchanged *Cek8* expression. **ES:** electroporated side; **Non-ES**: non-electroporated side; OV: otic vesicle.

Because the morpholino acts at the translation step, mRNA expression of FGF3 is not affected, therefore it is impossible to use RNA *in situ* hybridization to evaluate the effect of the morpholino. To overcome this problem a different technique to downregulate gene expression in a manner which allows its monitoring by RNA *in situ* hybridization was established. Electroporation of siRNA, a relatively new technique that has not been used widely in chicken embryos was thus tested.

2.3.2-Electroporation of siRNA against FGF3 Inhibits the Closure of the Otic Vesicle

RNAi offers a couple of advantages in comparison with other loss-of-function approaches, which include improved stability and a sustained silencing of protein production. In this study the GeneSuppressor IMG-800 (Biocarta) plasmid based system to generate siRNA intracellularly has been used. The GeneSuppressor IMG-800 (pSuppressorNeo) plasmid

was used to clone three different short sequences of the FGF3 chicken cDNA. The inserts cloned into this vector express RNAs under the control of the U6 promoter (see methods 5.2).

A mix of plasmids containing three different sequences derived from the chicken *Fgf3* cDNA and the pEGFP plasmid were coelectroporated into the neural tube of chicken embryos at stages HH 8-9. At these stages *Fgf3* is expressed in chicken embryos in the hindbrain at the level of the developing otic placode (Mahmood, *et al.,* 1995), which was aimed to be blocked. Six hours after electroporation the embryos were removed from the eggs, analyzed for GFP marker expression (Fig. 2.46) and fixed in 4% PFA for subsequent analysis by RNA *in situ* hybridization.

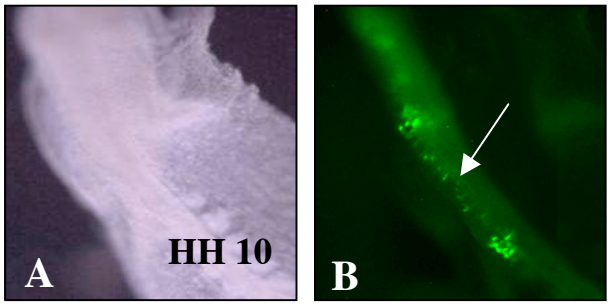

Figure 2.46: Embryos coelectroporated with plasmids expressing EGFP and *Fgf3* siRNA into the neural tube at stage HH 8. Six hours after electroporation embryos were isolated and analyzed for GFP expression. (**A**) Electroporated embryo in a bright field view (HH 10). (**B**) Electroporated embryo under fluorescent view showing expression of GFP in the electroporated side (*arrow*).

During the analysis of the expression of *Fgf3* after electroporation a complete block of *Fgf3* expression upon RNAi electroporation was not seen but rather a high reduction. By electroporating siRNA against *Fgf8* Ladher *et al.* have shown a downregulation of *Fgf8* expression in electroporated chicken explants (Ladher, *et al.*, 2005), supporting the idea that it is difficult to obtain a complete block of gene expression by siRNA. *In situ* hybridization revealed a reduction of *Fgf3* mRNA in the electroporated side of the neural tube at the level of the rhombomeres 4 and 5, where *Fgf3* is normally expressed (Fig. 2.47A,B). As a control for specificity, embryos were transfected with *Fgf8* siRNA sequences (see methods). They showed no changes in the expression of *Fgf3* (Fig. 2.47C), which confirms the specificity of *Fgf3* downregulation.

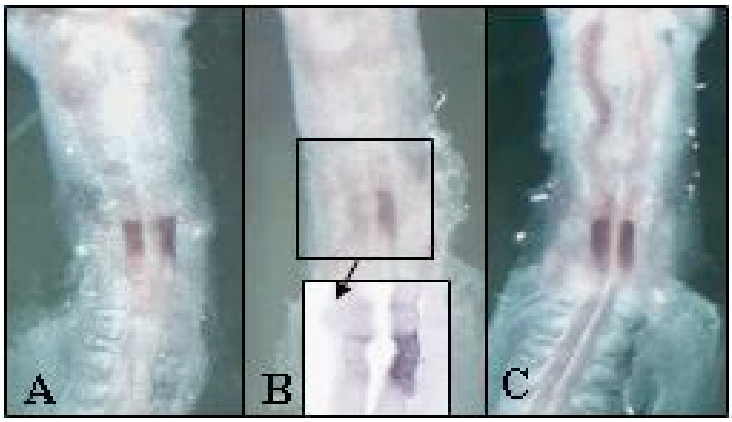

Figure 2.47: *Fgf3 in situ* hybridization of control (A), *Fgf3*siRNA (B) and *Fgf8*siRNA (C) electroporated embryos. (**A**) Normal expression of *Fgf3* in a non-electroporated embryo (HH 10+). (**B**) *Fgf3* siRNA-electroporated embryos showing reduction of *Fgf3* left electroporated side of the neural tube. High magnification of a dorsal section in the insert shows cells expressing *Fgf3* on both sides of the neural tube and the clear difference between control and electroporated side (*arrow*). (**C**) Embryo electroporated with *Fgf8*siRNA sequences does not show a difference between control and electroporated side. The electroporation was confirmed by GFP expression in all embryos.

Furthermore, the siRNA-electroporated embryos were analyzed histologically. They presented an open otocyst on the electroporated side, similar to the experiments performed with the morpholino against *Fgf3* (see above). In some cases, the electroporation with *Fgf3* siRNA resulted in a more severe phenotype consisting only in the formation of an otic placode (Fig. 2.48).

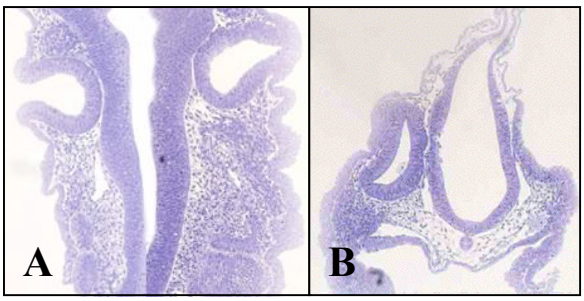

Figure 2.48: *Fgf3* siRNA electroporated embryos stained with Toluidine Blue. The embryos were electroporated at stage HH 8 and removed from the eggs after 24 h of incubation at stage HH 14. (**A**) Dorsal section showing an open otocyst on the electroporated side (left). (**B**) Transversal sections of an embryo presenting an otic placode on the electroporated side (right) while the non-electroporated side presents a normally developed otocyst.

The expression of *Pax2* in embryos electroporated with siRNA directed against *Fgf3* was not affected (Fig. 2.49).

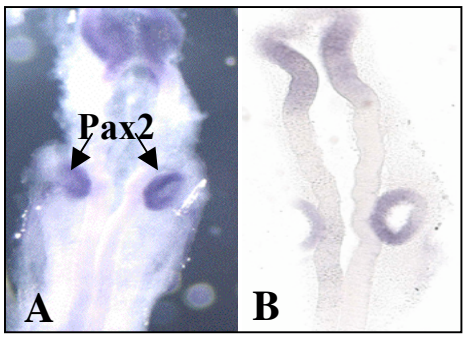

Figure 2.49: *Pax2* in situ hybridization of *Fgf3* siRNA electroporated embryos. (**A**) Whole-mount showing the expression of *Pax2* in the otocyst on both electroporated and non-electroporated sides. (**B**) Dorsal section of the embryo shown in A. Notice that the open otocyst on the left electroporated side does maintain the normal expression of *Pax2.*

By blocking *Fgf3* expression we have seen that the otocyst fails to form and sometimes remains at the placodal stage. These data confirm our previous results using morpholino antisense oligonucleotides and suggest that FGF3 is essential for otic vesicle formation in chicken.

Table 2.2: Average of electroporated embryos and phenotypes found

	Embryos GFP or fluorescein positive	**GFP positive embryos with phenotypes**	**Tested otic markers**
FGF3cDNA	80% (n=35)	71% (Ectopic structures) 20% (Oversized otic vesicles)	Lmx1
FGF10cDNA	82%, (n=91)	5% (Ectopic structures)	Lmx1; Cek8; Pax2
FGF8cDNA	81% (n=52)	62.5% (Reduced otic vesicle)	Pax2
FGF3 morpholino	64% (n=80)	62.1% (Open otic vesicle)	Lmx1; Cek8; (Pax2 data not shown)
siRNA-FGF3	63% (n=76)	33% (Open otic vesicle)	Pax2 (Lmx1 data not shown)

(n) Corresponds to a 100% of embryos used in the experiment

III-DISCUSSION

3.1-FGF3 is not Essential for Otic Induction in Mice

The role of FGF3 as an otic inducer appears to be conserved amongst fish, amphibians, avian and mammals (Wilkinson, *et al*., 1988, Represa, *et al*., 1991). In all species examined, FGF3 is expressed in the hindbrain, consistent with classical studies showing that the hindbrain is a source of otic-inducing factors (Wilkinson, *et al*., 1989, Mahmood, *et al*., 1995, Mahmood, *et al*., 1996, Lombardo, *et al*., 1998, Phillips, *et al*., 2001, Riley, 2003). The capacity of FGF3 as an inducer was demonstrated in chicken (Vendrell, *et al*., 2000) and zebrafish (Phillips, *et al*., 2001, Maroon, *et al*., 2002). A later role for FGF3 signaling in inner ear formation was postulated given that homozygous *Fgf3* ko mice, in which a *neo*^{r} cassette had been inserted in the exon 1b of the *Fgf3*-coding region (*Fgf3*^{neo}), showed normal otic induction but failed to complete the morphogenesis of the endolymphatic duct (Mansour, *et al*., 1993). The analysis of these mutants was complicated since fewer than 50% of the expected homozygous mutants were recovered at birth and the inner ear phenotype showed variation in both penetrance and expressivity. This result may be explained by a leaky expression of the mutant *Fgf3* allele which could not be entirely excluded. Therefore, in the present study it was aimed to define the function of FGF3 *in vivo* by creating an *Fgf3* null mutant deleting all exons of *Fgf3* and thus avoiding any interference caused by remnants of its coding region (section 2.1.*1*).

Mice with a complete deletion of the *Fgf3* gene showed no severe inner ear defects (Fig.2.3, 2.4 and 2.6) in contrast to the previously described *Fgf3*^{neo} mutant mice (Mansour, *et al*., 1993) . The different phenotypes observed in these two distinct mutant strains may be explained by the variations between the genetic backgrounds of both mutants. To clarify this issue the *Fgf3*$^{-/-}$ mutants have been started to be backcrossed onto the C57 Black 6 (Bl6) background. Interestingly, a few *Fgf3*$^{-/-}$ mutants showed turning behavior and therefore altered inner ear development. The affected *Fgf3*$^{-/-}$ mutants failed to form a proper cochlear and vestibular system and showed reduced cochlear ganglia. Although defects in the *Fgf3*$^{-/-}$ mutants were less severe than the ones found in the *Fgf3*^{neo} mutants analyzed by Mansour *et al.,* (1993) some similarities were observed, for example, improperly coiled cochlea and missformation of the cochlear, vestibular and tympanic ducts, reduced vestibular and cochlear epithelium as well as cochlear ganglia and unilaterally severely affected ears. In contrast to *Fgf3*$^{-/-}$ mutants, only very few *Fgf3*^{neo} mutants survived until adulthood (Mansour, *et al*., 1993).

Another possible explanation for the different phenotypes observed between the *Fgf3*^{neo} mutants and the *Fgf3*$^{-/-}$ null mutants described in this work may be the presence of the *neo*^{r} gene in the *Fgf3* locus, which might influence the expression and the function of neighboring genes. In some cases it has been determined that a cryptic splice site in *neo* interferes with normal splicing of genes (Lewandoski, 2001). To adress this issue mutants in which the whole *Fgf3* gene was replaced by the *neo*^{r} gene (*Fgf3*$^{neo/neo}$) were analyzed (section 2.1.2). Several of these *Fgf3*$^{neo/neo}$ mutants showed circling behavior and clear inner ear phenotypes affecting the morphogenesis of semicircular canals and less severely the cochlea (Table 2.1, Fig. 2.8, 2.9 and 2.10). The phenotype seen in the mutants in which *neo*^{r} replaced the *Fgf3*-coding region was more severe than the one observed in the few affected *Fgf3*$^{-/-}$ null animals without *neo*^{r} described before in this work. This suggests that the cause of the phenotype in the *Fgf3*$^{neo/neo}$ mutants could be an additive effect of the presence of the *neo*^{r} gene and the absence of the *Fgf3*-coding region.

Fgf3 is localized together with *Fgf4* and *Fgf15* on mouse chromosome 7 (Katoh, 2002). In addition, the expression pattern of these factors indicates their possible involvement during inner ear development. FGF15 is expressed in the neuroectoderm adjacent to the presumptive otic vesicle, otic placode, and pharyngeal endoderm during early otic development (Gimeno, 2002, Gimeno, 2003, Wright, 2004). FGF4 is expressed in the preplacodal and placodal otic ectoderm (Wright, *et al.*, 2003). The expression patterns of both genes suggest their participation in inner ear formation. Therefore, the possibility that neighboring genes to *Fgf3* were affected was considered. However, mouse embryos lacking *Fgf15* did not show any otic defect (Wright, 2004) and furthermore a mouse mutant in which *Fgf4* was specifically inactivated in the otic vesicle has not shown any apparent defects in inner ear formation (Alvarez, unpublished data). A possible explanation for the inner ear phenotype in the *Fgf3*$^{neo/neo}$ mutants is that either FGF4 or FGF15 could compensate the lack of FGF3 in the ko mutant, but that the expression of one or both genes is affected by the presence of *neo*^{r} and this combination results in a failure to form a normal inner ear. A mouse mutant carrying a deletion containing *Fgf3, Fgf4* and *Fgf15* on one chromosome (Lefebvre, unpublished data) and a *Fgf3* null allele (Carnicero, unpublished data) was created. The compound mutants *Fgf3*$^{-/-}$, *Fgf4*$^{+/-}$ and *Fgf15*$^{+/-}$ showed no defects during inner ear development. Thus, the reduction of expression of *Fgf4* and *Fgf15* on a *Fgf3* homozygous null background does not disturb the development of the otocyst, but the possibility exists that the remaining expression of *Fgf4* and *Fgf15* and the strong redundancy between members of the FGF family is sufficient to complete the inner ear program.

In summary, FGF3 participates in inner ear formation but its role is not essential and possibly is overtaken by other members of the FGF family, since many redundancies have been already shown for FGFs during organ development in for example limb (Bouleta A., *et al*., 2004) or teeth (Kettunen, *et al*., 2000).

3.2-FGF3 and FGF10 Play a Redundant Role for Inner Ear Formation

Despite the fact that FGF3 has been proposed as an otic inducer, its loss does not interfere with otic induction and only a later role in patterning of the otic vesicle has been reported. (Mansour, *et al*., 1993, Alvarez, *et al*., 2003). The lack of a severe phenotype in the inner ear of the *Fgf3*$^{-/-}$ mutants described in this work could be explained by redundant signals able to compensate the role of FGF3 during otic induction. The question that arises is which factor could be a good candidate to compensate the role of FGF3.

FGF10, another member of the FGF family could be this candidate, as it was reported to be implicated in inner ear formation (Pirvola, *et al*., 2000, Pauley, *et al*., 2003). FGF3 and FGF10 have been shown to be co-expressed in the developing inner ear within several structures (Pirvola, *et al*., 2000, Alvarez, *et al*., 2003) and both factors are able to bind with high affinity to the same isoforms of the FGF receptor 2 (FGFR2b) (Ornitz, *et al*., 1996, Igarashi, 1998) and alternatively the FGF receptor 1 (FGFR1b) (Ornitz, *et al*., 1996, Beer, *et al*., 2000, Pirvola, *et al*., 2002). A compensatory role for FGF3 in the absence of FGF10 during morphogenesis of the inner ear has already been suggested. This conclusion arose because a *Fgf10* null mutant showed severe malformations of posterior inner ear structures and otic ganglia (Pauley, *et al*., 2003). Since FGF3 is expressed in the otic vesicle anteriorly but not posteriorly the anterior expression of FGF3 (Pauley, *et al*., 2003; Mansour, *et al*., 1993) may have compensated the absence of FGF10 anteriorly, but not posteriorly. Likewise, in the present work it was demonstrated that FGF10 compensates the function of FGF3 during formation of the inner ear (section 2.1.*3*). It is supported by the smaller ventralized otocysts found in the *Fgf3*$^{-/-}$/*Fgf10*$^{-/-}$ double mutants which showed a variation in their sizes and expression of otic markers. In these mutants, the most affected otocysts presented a dramatic reduction or loss of otic marker expression while the less affected ones showed normal domains of expression (Table 2.1, Fig. 2.12) (Alvarez, et al., 2003). Another fact that supports this compensatory effect of FGF10 is the presence of a normal ganglion in the single *Fgf3*$^{-/-}$ mutants, whereas the *Fgf3*$^{-/-}$/*Fgf10*$^{-/-}$ double mutants showed either a high reduction or complete loss of the otic ganglion in early embryonic stages

(Fig. 2.12). It could be explained by the coexpression of FGF3 and FGF10 in the neurogenic region of the developing inner ear as already described by McKay, *et al.* (1996) and Pauley, *et al*. (2003). The remnant neuronal tissue found in some *Fgf3*$^{-/-}$/*Fgf10*$^{-/-}$ mutants lead to the conclusion that another factor might support neuronal development. FGF8 has been reported to be expressed in the delaminating neuroblasts (Pirvola, *et al.,* 2002) and therefore might partially overlap with the functions of FGF3 and/or FGF10 to give rise to the cochleovestibular ganglion.

Remnant otic structures such as cochlea, ganglion, vestibule and a canal were identified in one *Fgf3*$^{-/-}$/*Fgf10*$^{-/-}$ mutant, which survived until E12.5 (Fig. 2.13). Nevertheless, no trace of the endolymphatic duct was found. The severe defects of inner ear formation of *Fgf3*$^{-/-}$/ *Fgf10*$^{-/-}$ mutant demonstrate the important role of both FGF3 and FGF10 to give rise to the normal otocyst in a redundant fashion. On the other hand, the rudimentary otic structures found in this *Fgf3*$^{-/-}$/*Fgf10*$^{-/-}$ mutant suggest that another factor may signal during the formation of the otocyst. FGF8 was shown to be expressed in the vestibule (Fig. 2.27) which suggests that FGF8 is participating in inner formation. In other words, FGF8 may be acting in concert with FGF3 and FGF10 to carry out a normal otic morphogenesis, since the three factors are expressed throughout the development of the otocyst.
Complete lack of the endolymphatic duct in the *Fgf3*$^{-/-}$/*Fgf10*$^{-/-}$ mutant at E12.5 was found (Fig. 2.13). It has been reported that the FGF3 signal from the hindbrain is required to form the endolymphatic duct as a late inductive signal, probably in addition to a FGF3 signal acting within the otocyst itself (Mansour, *et al*., 1993, Pirvola, *et al*., 2000). FGFR2b is strongly expressed first in the dorsomedial part of the otocyst that is flanking the hindbrain and later in the developing endolymphatic duct. FGFR2b null mutants show defects in this structure (Pirvola, *et al*., 2000), but not FGF10 null mutants (Ohuchi, *et al*., 2000, Pauley, *et al*., 2003). The present data demonstrate that the lack of FGF3 and FGF10 is sufficient to disturb the formation of the endolymphatic duct.

A *Fgf3*^{neo}/*Fgf10*$^{-/-}$ double mutant reported by Wright and Mansour (2003) showed a more severe phenotype than the double mutants analyzed in this work. In the *Fgf3*^{neo}/*Fgf10*$^{-/-}$ mutant embryos the formation of the otic vesicle appeared arrested prior to invagination of the otic cup (Wright, *et al*., 2003) and they failed to express otic markers completely or in the dorsal otic ectoderm. In contrast to the *Fgf3*^{neo}/*Fgf10*$^{-/-}$ mice, the *Fgf3*$^{-/-}$/*Fgf10*$^{-/-}$ double mutants analyzed here presented a less severe phenotype since the embryos were able to form microvesicles and

at least in one case otic ganglion (Fig. 2.12 and 2.13). The presence of less severely affected inner ears exhibited by the *Fgf3*$^{-/-}$/*Fgf10*$^{-/-}$ mutants described in this study, could be explained by the phenotypic differences observed between the *Fgf3*$^{-/-}$mutants (section 2.1.*1*) described in this work and the more severe phenotype noted in *Fgf3*^{neo} animals (Mansour *et al.,* 1993).

Parallel to this study, in our lab Dr. Vendrell investigated the expression of FGF10 during early embryonic stages. The analysis showed that FGF10 is expressed in regions relevant for inner ear formation. FGF10 was expressed in the anterior and ventral mesenchyme and it was also detected dynamically expressed in the developing hindbrain next to the area where the otic placode and vesicle develop. FGF10 expression in the developing hindbrain coincided spatially and temporally with the formation of the otic placode and/or vesicle in the neighboring ectoderm, and also coincided with some of the endogenous areas of FGF3 hindbrain expression (Alvarez, *et al*., 2003). Based on the gene expression of FGF10 and FGF3 and the phenotype observed in double mutants for both genes, they do compensate for each other during the process of inner ear development. Otic induction was not inhibited in the *Fgf3*$^{-/-}$/*Fgf10*$^{-/-}$ mutants (Fig. 2.12) indicating the participation of additional factors.

In conclusion, the phenotype observed in *Fgf3*$^{-/-}$ *Fgf10*$^{-/-}$ mutants suggests that FGF3 and FGF10 signals are necessary during early and late stages of inner ear formation. A similar scenario is seen in zebrafish, where FGF3 and FGF8 have been reported to be essential for inner ear formation as a hindbrain signal in a redundant fashion and later they participate in pattering and differentiation of the otic vesicle (Leger, *et al*., 2002). A first phase of FGF3 and FGF8 signalling from the neural tube induces the expression of early otic markers and then a second phase of FGF signalling continues or maintains the induction of the early otic placode (Solomon, *et al*., 2003). Thus, both factors appear to function at multiple points during inner ear development in this species (Reifers, *et al*., 1998, Liu, *et al*., 2003).
FGF3 and FGF10 may function in a similar manner at different stages during otic induction and pattering in mice, however additional inductive signals working in concert with these factors may exist to strongly support the inner ear formation.

3.3-Differential Roles for FGF3 and FGF10 During Formation of Otic Structures

FGF3 and FGF10 homoheterozygous mutants have also been analyzed in the present study (section 2.1.4). These mutants showed different degrees of otic alterations between mice carrying different allelic combinations (*Fgf3*$^{-/-}$ *Fgf10*$^{+/-}$ or *Fgf3*$^{+/-}$ *Fgf10*$^{-/-}$) but also between mice carrying the same genotype. The *Fgf3*$^{-/-}$ *Fgf10*$^{+/-}$ mutants reached adulthood and some of them were severely affected (26%) showing circling behavior, but normal mutants were found as well (Table 2.1, Fig. 2.15 and 2.16). The affected embryos (45%) showed unilaterally ventralized otic vesicles and reduced ganglion coinciding with the phenotype described by Wright et al. (2003) for *Fgf3*^{neo} *Fgf10*$^{+/-}$ mutants (Table 2.1, Fig. 2.14).

The expression of FGF3 and FGF10 overlaps partially within the developing otocyst but FGF10 is more widely and intensively expressed when compared with FGF3, especially in the semicircular canal system (Pirvola, *et al*., 2000, Alvarez, *et al*., 2003), thus a more severe phenotype during canal formation may be expected when the expression of FGF10 is affected. It was indeed observed in the *Fgf3*$^{-/-}$ *Fgf10*$^{+/-}$ adult animals with a mutant inner ear phenotype. They presented several inner ear defects consisting of absence of the common cross with subsequent fusion of anterior and posterior canal and truncated lateral canal indicating a relative contribution of FGF10 during canal formation (Fig. 2.15). It has been reported that FGF10 is required for semicircular canal morphogenesis and indispensable for the subsequent removal of the fused cells to proceed with the hollowing of the center of each semicircular plate (Ohuchi, *et al*., 2005). In birds and mammals, the anterior and posterior canals, develop from a common vertical outpouch in the dorsal otocyst; whereas the lateral canal develops from a horizontal outpouch. In the vertical outpouch, the epithelia approach each other forming two fusion plates which fuse and reabsorb resulting in the two tube-shaped canals (anterior and posterior) connected in the middle by the common cross (Bissonnette, *et al*., 1996). Thus the defects observed in the *Fgf3*$^{-/-}$ *Fgf10*$^{+/-}$ animals suggest a failure in the hollowing process. In chicken, a similar phenotype to that found in *Fgf3*$^{-/-}$ *Fgf10*$^{+/-}$ mutants was described upon misexpression of FGFs (Chang, *et al*., 2004). The defects observed in the *Fgf3*$^{-/-}$ *Fgf10*$^{+/-}$ mutants support the role of FGFs to specify non-sensory development that appears to be conserved between birds and mammals (Chang, *et al*., 2004). In mouse and zebrafish it has been reported that loss of individual FGFs perturbed sensory but also non-sensory structures, indicating a paracrine role of FGF signaling (Mansour, *et al*., 1993, Adamska, *et al*., 2000, Phillips, et al., 2001, Leger, *et al*., 2002).

Fgf10 null mutants showed reduced anterior and lateral canals as well as an abnormal lateral crista (Pauley, *et al.,* 2003, Ohuchi, *et al.*, 2005). The *Fgf3*$^{-/-}$ *Fgf10*$^{+/-}$ mutants described in this study displayed a more severe reduction of vestibular epithelial cells and lateral crista in comparison with the reported *Fgf10* null mutants (Fig. 2.16). They showed also abnormalities in the cochlear duct and epithelium, which are normal in the *Fgf10* mutants. This finding supports further the compensatory role of FGF3, since it is expressed in the sensory regions of the inner ear (Wilkinson, *et al.*, 1988, Wilkinson, *et al.*, 1989).

The *Fgf3*$^{-/-}$ *Fgf10*$^{+/-}$ mutants formed otic ganglion although it was highly reduced (Fig. 2.16). This could be explained by the expression of FGF8 in neuroblasts (Pirvola, *et al.*, 2000). Thus, the active FGF10 allele together with the presence of FGF8 may help to partially form the otic ganglion. FGF10 and FGF8 are also expressed in delaminating neuroblasts and forming ganglion of the chicken otocyst (Alsina*, et al.*, 2004; Hidalgo-Sánchez, *et al.*, 2000) and thus may play a conserved role for ganglion formation in birds and mammals.
Fgf3$^{+/-}$ *Fgf10*$^{-/-}$ mutants were analyzed at early stages of inner ear development, since they did not reach adulthood. The complete lack of FGF10 and the partial reduction of FGF3 affects the formation of the otocyst in 20% of the embryos (Fig. 2.18), however further investigation is necessary to evaluate the inner ear development at later stages.

These results demonstrate that there is a relative contribution of FGF3 and FGF10 to promote normal otic development since the phenotypes found in mice carrying three mutant alleles (*Fgf3*$^{-/-}$ *Fgf10*$^{+/-}$) are more severe than the ones showed upon single mutation of these factors.

3.4-Role of FGF8 in Otic Formation

FGF8 has been reported to be expressed during otic vesicle morphogenesis within the developing cochlea, delaminating neuroblasts and IHC throughout life (Pirvola, *et al.*, 2002). FGFR3c which binds FGF8 with high affinity (MacArthur*, et al.*, 1995), is expressed at early embryonic stages in the mesenchyme (Ladher*, et al.*, 2005) and later in pillar cells (Mueller*, et al.*, 2002, Pirvola, *et al.*, 2002). It has been proposed that the adjacent expression of FGF8 from the IHC leads to the activation of FGFR3 and to the placement of the pillar cells in the organ of Corti (Mueller, *et al.*, 2002).

Recently, Ladher *et al*. (2005) showed that FGF8 is expressed in preplacodal ectoderm, periotic endoderm and mesenchyme prior to the formation of the otic placode in mice (Ladher, *et al*., 2005) and moreover, FGFR3c is expressed in the otic cup until it closes to form the otic vesicle (Wright, *et al.*, 2003). Based on the evidences mentioned above and the early mesoendodermal and otic expression of FGF8 in the mouse it was aimed in this study to investigate the role of this factor in early stages of otic induction in mice (section 2.1.5).

Fgf8 null mutant mice die at early gastrulation prior otic formation (Sun, *et al.*, 1999). In order to analyze the otic development in mice lacking FGF8 expression, mutants in which FGF8 has been inactivated by using the *Cre*-loxP system were used in the present study (section 2.1.5.*1*). The *Foxg1-Cre* expression specifically targets FGF8 in the tissues relevant for otic induction such as pharyngeal mesoendoderm, head ectoderm and otic placode and vesicle. The $Fgf8^{flox}/Fgf8^{\Delta 2,3}$; *Foxg1-Cre* (*Fgf8* ko) mutants displayed a failure to form many mesoderm- and neural crest-derived structures in the face, but the inner ear of these mutants showed only a delayed formation (Fig. 2.19). The lack of a phenotype upon conditional inactivation of FGF8 could indicate that other FGFs such as FGF3 or FGF10 (neural and neural or mesenchymal respectively) are compensating the lack of FGF8 from different sources. Another possible explanation for this phenomenon could be that the inactivation of FGF8 was either too late to interfere in the otic induction or not properly achieved. The lacZ reporter used to check the expression of *Foxg1-Cre* recombinase showed weaker staining in comparison with the *Fgf8* expression in mesoderm and endoderm (Alvarez, unpublished data), suggesting that probably the inactivation of FGF8 was not properly achieved in those tissues. However, the inactivation of *Fgf8* by *Foxg1-Cre* in otic placode and vesicle was already reported to occur properly by the group of Pirvola, *et al*. (2002).

In this work it has been shown that loss of FGF8 expression in the otic placode and vesicle appears not to be detrimental for the inner ear formation and suggests that other FGFs compensate for the loss of FGF8 (Fig. 2.19, 2.20, and 2.21). Similarly, in limb development FGF8 has been suggested as an endogenous inducer, (Crossley, *et al*., 1996) and in the absence of this factor, FGF4 partially rescues limb development indicating that the presence of both factors is essential for limb formation (Sun, 2002, Bouleta A., *et al*., 2004). A compensatory mechanism between other members of the FGF family may be a possible explanation for the initial otic induction upon mutation of FGF3 and FGF10 in which FGF8 might support the first steps of inner ear induction and vice versa with the contribution of other factors.

A mild phenotype in cochlear and vestibular innervation has been found in the *Fgf8* ko newborn mutants (Fig. 2.22 and 2.23). Coincidently, FGF8, FGF10 and FGF3 are also expressed in the neuroblasts delaminating from the otocyst (Pirvola, *et al.,* 2000, Pirvola, *et a*l., 2002, Pauley, *et al*., 2003) thus FGF3 and FGF10 may support the formation of the otic ganglion in *Fgf8* mutants. FGF8 expression might be important to properly form the cochleovestibular ganglion. Likewise, in zebrafish *ace* mutants with a hypomorphic mutation in the *Fgf8* gene (Reifers, *et al*., 1998), the cochleovestibular ganglion fails to express the regional marker, *Nkx5.1* (Adamska, *et al.,* 2000) indicating an aberrant ganglion differentiation. In chicken, it has been reported that FGF8 participates in the formation of the otic ganglion due to the pattern of FGF8 expression in this species and the enlarge otic ganglion found via beads application (Hidalgo-Sánchez*, et al*., 2000, Adamska*, et al*., 2001, Sanchez-Calderon, 2002, Sanchez-Calderon*, et al*., 2004). Hence, the role of FGF8 in otic ganglion formation seems to be conserved in several species.

3.5- FGF3 and FGF8 Act Redundantly During Inner ear Morphogenesis

Many evidences have lead to the conclusion that FGF3 and FGF8 are required for initial inner ear induction in zebrafish acting as redundant factors (Reifers, *et al*., 1998, Maroon, *et al*., 2002, Maves*, et al*., 2002, Liu*, et al*., 2003, Phillips, 2004). For instance, loss of both FGF3 and FGF8 resulted in a complete loss or strong reduction of otic markers and/or the otic vesicle in this species (Phillips, *et al*., 2001, Leger, *et al*., 2002, Maroon, *et al*., 2002).

Likewise, the experiments presented in this work showed that the loss of FGF3 and FGF8 in mice affects severely the development of the otocyst demonstrating the conserved capacity of these factors to support inner ear formation (section 2.1.5.2, Fig. 2.24 and 2.25). However, in zebrafish FGF3 and FGF8 are coexpressed in hindbrain (Maves, *et al*., 2002, Walshe*, et al*., 2002) which is not the case in mice.

Inner ear induction was not affected in the *Fgf3+8* mutants probably due to the late inactivation of FGF8 (see above), therefore it cannot be concluded here whether these factors are redundantly required for initial otic induction or not. The inner ear of *Fgf3+8* mutants showed normal development until E11.5, but at later stages the development of the otocyst begins to be aberrant, possible as a consequence of a failure to correctly pattern the otocyst (Fig. 2.24). The developing otocyst showed improper separation of the cavities normally found in a wild-type inner ear. At E18 the mutants possessed cavities lined by undifferentiated epithelium instead (Fig. 2.25). In this work the expression of *Fgf8* in the

vestibular system at E12.5 in the mouse was proven (Fig.2.27). Besides, *Fgf3* was reported to be expressed in sensory epithelium of the otocyst (Wilkinson, *et al*., 1988, Wilkinson, *et al.,* 1989, McKay, *et al*., 1996, Pirvola, *et al*., 2000). Thus, the expression of both *Fgf3* and *Fgf8* are relevant to form the different compartments in the otocyst. Indeed, in chicken *Fgf8* starts to be expressed in the macula of the saccule at HH 27 (it corresponds to mice E12.5-13) and slightly later is found in utricle and in the cochlear duct (Sanchez-Calderon, *et al*., 2004). Thus, FGF8 was suggested to participate in the compartmentalization of the otic vesicle together with transcription factors such as *Otx2, Gbx2* and *Pax2* (Hidalgo-Sánchez, *et al*., 2000) suggesting that FGF8 has a conserved function in birds and mammals.

Even though, the otocysts of *Fgf3+8* mutants were aberrant after a certain stage of development, the formation of rudimentary structures was observed (Fig. 2.25). This result supports again the presence of other redundant factors to ensure the development of the inner ear. Such a factor could be FGF10 since it is highly expressed in crista anlage and cochlea (Pauley, *et al*., 2003), structures developed rudimentarily in the *Fgf3+8* mutants.

The *Fgf3+8* mutants developed an altered otic epithelium. The cochlea duct was lined by an epithelium which was not comparable to the normal organ of Corti but could rather be described as an undifferentiated epithelium (Fig. 2.25). As mentioned, *Fgf8* is expressed in the outgrowing cochlea and IHCs, the pioneers of the organ of Corti, and *Fgf3* and *Fgf10* are expressed in the differentiating IHCs as well (Pirvola, *et al.,* 2002). Moreover, the *Fgfr1* (which binds FGF3) and *Fgfr3* (which binds FGF8) are expressed adjacent in the OHC and pillar cells respectively (Mueller, *et al.,* 2002, Pirvola, *et al.,* 2002). It was suggested that the IHCs stimulate differentiation of their later-emerging neighbors through FGF/FGFR signalling (Pirvola, *et al*., 2002). Thus, the lack of differentiated cells in the organ of Corti of the double *Fgf3+8* mutants observed in this work may be the result of the lack of differentiation supported by both FGF3 and FGF8. This hypothesis is supported by the absence of alterations in the organ of Corti, concerning the IHCs or their neighboring cells, upon single inactivation of FGF8 in the otic vesicle (Fig. 2.21).

The double *Fgf3+8* mutants showed an improper developed vestibular epithelium as well. As described above, expression of *Fgf8* in the vestibular sensory system was shown in this work (Fig. 2.27). This expression probably cooperates with *Fgf3*, which is also expressed in this structure, to further differentiate the vestibular sensory epithelium. The latter result is consistent with the autocrine role given to the FGF signalling (Mansour, *et al.,* 1993, Adamska, *et al*., 2000, Phillips, *et al*., 2001, Leger, *et al*., 2002).

It has been recently reported that FGF8 is required redundantly with FGF3 for inner ear induction based on the analysis of a compound *Fgf3*$^{-/-}$/*Fgf8*$^{Hyp/-}$ mouse mutant which showed no formation of otic vesicles (Ladher, *et al.*, 2005). The authors speculated that FGF8 induces or maintains mesenchymal FGF10 expression through FGFR3c, which is expressed in the mesenchyme. The *Fgf8*$^{Hyp/-}$ mutant used in the latter work had a drastic reduction of FGF8 expression due to the use of a hypomorphic allele (containing a cassette composed by the *neo*^{r} gene flanked by *frt*-sites downstream of the translation stop of *Fgf8* coding region) and a null allele for *Fgf8* (Moon, *et al.*, 2000). A question that arises concerning this result is whether the effect on otic induction is part of a secondary effect due to malformation of the hindbrain, since the mutant embryos appeared considerably smaller and although hindbrain markers were present their expression domains appeared reduced (Ladher *et al.,* 2005). For instance, compound hypomorphic *Fgf8* mutants (carrying a *Fgf8*^{neo} and a *Fgf8* null allele) were reported to have severe phenotypes during development (Meyers, *et al.*, 1998). They ranged from less affected size-reduced embryos to severely affected embryos with defects in craniofacial and central nervous system development in which the midbrain/hindbrain boundary was deleted, resulting in some cases in embryonic death and reabsortion (Meyers, *et al.,* 1998). Thus, in those *Fgf8* hypomorphic mutants the hindbrain is likely to be affected which may result indirectly in the alterations of inner ear formation. Cases in which mouse mutants such as with a defective hindbrain showed inner ear defects were described already, for example *kreisler* and *hoxa1* (Deol, 1964; Pasqualetti *et al.*, 2001; Chisaka *et al.,* 1992). Likewise, in zebrafish loss of FGF3 and FGF8 significantly alters segmental identities in the hindbrain, which leads to defects during otic development (Maves, *et al.*, 2002).

Interestingly, no trace of the otic ganglion was detected during the analysis of the *Fgf3+8* mutants (Fig 2.24 and 2.25). The neuroblasts which form the cochleovestibular ganglion delaminate from the ventral part of the otocyst, a region which shows slightly increased cell death in the *Fgf3+8* mutants (Fig. 2.26). A similar mechanism occurs during limb development in absence of FGF8 and FGF4 in which the limbs fail to form due to an excess of apoptosis (Bouleta A., *et al.*, 2004). The otocysts of *Fgf3+8* mutants show no cell death at later stages of development whereas in the wild-type inner ear a few cells undergo apoptosis. The absence of apoptotic cells at later stages in these mutants may indicate a complete shut-off of the inner ear program.

According to the results in zebrafish (Adamska, *et al.*, 2000) and chicken (Hidalgo-Sánchez, *et al.*, 2000, Sanchez-Calderon, 2002, Sanchez-Calderon, *et al.*, 2004), FGF8 seems to play an important role

for the formation of the cochleovestibular ganglion and the absence of both FGF3 and FGF8 affects severely the formation of the otic ganglion. As described before, no defects in otic formation was found in the *Fgf3*$^{-/-}$ (Fig. 2.13), complete loss or remnant otic ganglion could be found in *Fgf3*$^{-/-}$*; Fgf10*$^{-/-}$ mutants (Fig. 2.13), reduced ganglia was exhibited by *Fgf3*$^{-/-}$*; Fgf10*$^{+/-}$ (Fig. 2.16 and 2.18), and a mild defect in the cochlear and vestibular innervation was shown upon inactivation of *Fgf8*. These data together with the lack of ganglion formation in the *Fgf3+8* mutants suggest that FGF10 and FGF8 are important factors in this process. In this study, ectopic expression of FGF8 was detected upon overexpression of FGF10 in the chicken neural tube (Fig. 2.39). Such an induction was also seen upon FGF10 overexpression in mice (Alvarez and Vendrell, unpublished data) suggesting conserved mechanisms. Thus, it is suggested that FGF10 activates FGF8 expression to participate in otic ganglion development and FGF3 may participate in this process. Alternatively, they can compensate for each other to initiate and/or to maintain the otic ganglion development.

3.6-Analysis of *Fgf2*$^{-/-}$ Mutants Shows no Relevant Role for FGF2 During the Formation of the Inner Ear in Mice

FGF2 was reported to act as an otic inducer in *Xenopus* (Lombardo, *et al*., 1998, Lombardo, *et al*., 1998) and in chicken (Adamska, *et al*., 2001), although in the latter species the incidence of otic induction was lower. Later in chicken development FGF2 participates in canal formation together with *Bmp2* (Chang, *et al*., 2004). Misexpression of FGF2 in the neural tube of chicken embryos did not show any otic phenotype in our hands. By HSV-1-mediated gene transfer the capacity of FGF2 to increase the number of cells expressing hair cell markers in dissociated cochlear epithelium has been demonstrated (Carnicero, 2004). In the present work the analysis of mice lacking *Fgf2* expression showed no otic defects (Fig. 2.28 and 2.29) (Carnicero, 2004). Thus an important role in inner ear formation can not be attributed to FGF2.

3.7-Ectopic Expression of FGF3 and FGF10 Leads to the Formation of Ectopic Otic Vesicles with Otic Characteristics in Chicken Embryos

FGF3 was the first growth factor proposed as an otic inducer based on its expression pattern (Wilkinson, *et al*., 1989). For example, the implantation of beads coated with FGF3, resulted in the formation of ectopic vesicles with some otic characteristics in *Xenopus* (Lombardo, et al., 1998, Lombardo, et al., 1998). In zebrafish, injection of zygotes with antisense morpholinos (Nasevicius, 2000) designed to specifically knockdown FGF3 function led to malformation of the otic vesicles (Phillips, *et al*., 2001, Leger, *et al*., 2002, Maroon, *et al*., 2002).

In chicken, FGF3 is expressed dynamically in the hindbrain close to the prospective otic placode which is maintained in r5 and r6 during early stages of otic vesicle morphogenesis and in the surface ectoderm of the preotic territory (Mahmood, *et al*., 1995, Mahmood, *et al*., 1996, McKay, *et al*., 1996).

In the present report, the suggested role of FGF3 as an local inducer of the inner ear in the surface ectoderm next to the developing hindbrain (Represa, *et al*., 1991, Fritzsch, 1998) was confirmed in chicken embryos by misexpressing FGF3 in the neural tube (section 2.2.1, Fig. 2.31). The misexpression of FGF3 in the neural tube led to the formation of ectopic otic vesicles and moreover, to an increased size of the normotopic otocyst (Table 2.1, Fig. 2.32 and 2.35). Vendrell *et al* (2000) reported in the same species the inductive capacity of FGF3 by ectopic expression of this factor in the ectoderm via viral infection. The authors described a competent zone, which formed otic placodes in response to exogenous application of FGF3 in avian embryos. Indeed, in the present study the ectopic otic structures were found posteriorly and anteriorly to the normotopic otocyst and within the area of exogenous FGF3 expression in the neural tube. This area is contained in the competent area described by Vendrell *et al*. (2000). They suggest that FGF3 functions in two steps during inner ear development, first as an inductive signal and later participating in the process of morphogenesis (Vendrell, *et al*., 2000). The results presented in this work confirm this scenario, since the misexpresion of FGF3 did not only affect the induction but also the morphogenesis of the otocyst.

Upon FGF10 overexpression in chicken, a low percentage of ectopic otic structures in comparison with the number of ectopic otic vesicles observed upon overexpression of FGF3 was found (Table 2.2, Fig. 2.36). The stronger inductive capacity of FGF3 can be explained by its endogenous expression that may reinforce the ectopic expression of FGF3 in the hindbrain and enhances the production of ectopic otic structures. In turn, FGF10 is not

expressed in the hindbrain but only in the otic placode in chicken. The fact that several members of the FGF family can act as inducers when expressed ectopically in avian embryos has also been observed in neural tube or limb development (Cohn, *et al*., 1995, Alvarez, *et al*., 1998). The ectopic structures obtained by exogenous expression of FGF3 and FGF10 in the hindbrain were able to express otic markers (Fig. 2.33 and 2.38). The markers did not show any regionalization, but rather showed uniform staining. A similar situation has been described after transplantation of the otic placode, which develops into the otic vesicle in ectopic locations in chicken (Herbrand, *et al*., 1998). The analysis of otic markers showed that *cNkx5.1* conserved its endogenous expression pattern but this was not the case for *Pax2*, which presented variably regionalized expression. The authors proposed that *Pax2* is much more sensitive to signals from the local environment (Herbrand, *et al.,* 1998). Therefore, the little ectopic otic structures obtained in the present study may not have been in a suitable environment to express otic genes with their normal pattern.

In parallel to this work, in our laboratory the potential involvement of FGF2, FGF3, and FGF10 during otic induction was examined in mice (Alvarez and Vendrell). In order to test the capacity of these factors to act as hindbrain-derived neural signals for otic development in mammals, a misexpression approach was used in mice in which FGFs were expressed ectopically in anterior regions (r3 and r5) of the developing murine hindbrain (Alvarez, *et al*., 2003). In 85% of the FGF10 transgenic embryos analyzed the formation of small ectopic rudimentary otic vesicles which formed next to r3, r4 and r5 was observed. The capacity of FGF3 to induce ectopic otic vesicle was much lower than that of FGF10. FGF2 misexpression did no show any capacity to induce ectopic otic structures (Alvarez, *et al*., 2003).
The same approach as described above for mice was performed in chicken embryos by overexpressing FGF10 in anterior regions of the neural tube (r3 and r4) in chicken.
As already mentioned overexpression of FGF10 in the chicken neural tube induces ectopic expression of FGF8 (Fig. 2.39). During limb development it has been proposed that FGF10 may be a mesenchymal mediator inducing FGF8 expression in the overlaying ectoderm (Martin, 1998). It is difficult to ascertain the molecular interactions, but it can be speculated that both molecules form part of a cascade that is playing a role during otic formation and probably in a feedback-loop fashion as shown for limb development.
In chicken, FGF8 as well as FGF10 are not expressed in the neural tube, but they were also reported to be expressed in delaminating neuroblasts (Hidalgo-Sánchez, *et al*., 2000, Alsina, *et al*., 2004, Sanchez-Calderon, *et al*., 2004), playing probably a role in the formation of the otic ganglion.

3.8-Loss-of-function Approaches Show that FGF3 Participates in Morphogenesis of the Otic Vesicle in Chicken

In this work, controversial data presented by Represa *et al.* (Represa, *et al.*, 1991) were clarified. To explore the possibility of FGF3 as a signal required to form the otocyst from the otic placode, Represa *et al.* applied anti-sense oligonucleotides based on mouse *int-2* (FGF3) to chick explants consisting of hindbrain and otic placode. This treatment inhibited otocyst formation by blocking otic pit invagination, but several considerations seemed to argue against the conclusion that the effects on otocyst induction were due to an inhibition of *Fgf3* experiments could not be reproduced by using the same sequences. In the absence of sequence information from the chicken *Fgf3* gene, Represa *et al.* designed the oligonucleotides to the amino terminal region of the mouse gene, in which only 12 of 15 residues are conserved (Mahmood, *et al.*, 1995). Moreover, a mouse *Fgf3* probe from exon 3 hybridized at low stringency to chicken *Fgf3* DNA showed no signal (Casey, *et al.*, 1986), whereas the probe clearly detected homologous DNA in the mammalian species tested. Thus, the *Fgf3* gene from chickens has significantly diverged from mouse *Fgf3*. Thus, the results obtained by Represa *et al.* were not clear.

In this study, a re-evaluation of this issue was approached (section 2.3). Antisense morpholino oligonucleotides and siRNA expressing plasmids were used to target FGF3 in chicken embryos via electroporation *in vivo*. Both approaches led to the same results, which consisted in a failure of otocyst closure (Fig. 2.43, 2.44, 2.48). Unfortunately, a reduction of FGF3 at the protein level using morpholinos was not possible to demonstrate due to the lack of a good antibody. To confirm the result obtained with morpholinos, in which the morphogenesis of the otocyst is impaired, a second approach was applied, in which three different sequences targeting the *Fgf3* mRNA were cloned into a siRNA expressing vector (methods, section 5.1). The sequences were designed based on the *Fgf3* chicken cDNA (Mahmood, *et al.*, 1995) following a guide offered by Quiagen (siRNA design Tool) and described in Elbashir, *et al.* (2001) (methods, section 5.2.2). By *in situ* hybridization it was demonstrated that the expression of FGF3 in the neural tube of the electroporated embryos was indeed knocked down and subsequently interfered in the inner ear formation (Fig. 2.47). These data confirm the role of FGF3 as an important factor participating in inner ear formation as suggested by Represa *et al.* (1991).

These results demonstrate the importance of FGF3 as a hindbrain-derived signal that leads the otic placode to form the otic vesicle. However, an essential inductive role during otic induction cannot be assigned to FGF3 since the embryos were able to form an otic placode upon its downregulation. Even though, efficiently reduced by electroporating siRNA, the expression of FGF3 in the neural tube was not completely blocked (Fig. 2.47). Coincidently, a role for FGF8 for otic induction was recently reported in chicken embryos by applying the same technique, in which the block of the endodermal FGF8 expression was also reduced but not totally blocked and that resulted in a complete absence of the otic vesicle (Ladher, *et al.*, 2005). Mesodermal FGF19 was shown to be activated by FGF8 and to interact with the neural Wnt8c signal to trigger the expression of otic markers in chicken explants (Ladher, et al., 2000). One complication, however, is that Wnt8c also induced prospective otic ectoderm to express FGF3 (Ladher, *et al*., 2000) leaving open the question which factor(s) are directly responsible for otic induction.

This study proposes that the FGF3 signal from the hindbrain, works in concert with other factors (FGF19, FGF8 and Wnt8c) in a cascade in which FGF8 is downstream to FGF3. The activation of this cascade leads to the expression of FGF3 in the neuroectoderm and to induce the otic vesicle in the competent ectoderm. Then Wnt8c could facilitate a feedback loop that augments and maintains FGF signaling long enough to induce otic development as suggested by Phillips *et al*. (2004). FGF3 is also reported to be expressed at stage HH 8 in the lateral endoderm adjacent the prospective otic placode, which persists during otic development (Mahmood, *et al*., 1995) and may be reinforcing the hindbrain signal during otic formation.

3.9-FGF8 Act as a Restrictive Signal During Formation of the Otocyst in Chicken

Overexpression of FGF8 in chicken embryos showed different results from those obtained by FGF3 or FGF10 exogenous expression in this study (section 2.2.3). The overexpression of FGF8 into the neural tube resulted in smaller and malformed otic vesicles and reduced expression of *Pax2* (Fig. 2.41 and 2.42). Reported findings showed that FGF8-coated beads implanted within the mesoderm at late otic placodal stages (HH 11+) produced an enlargement of the cochleovestibular ganglion, associated with an increased expression of otic markers. This latter results showed the importance of the endogenous FGF8 expression in the cells migrating out of the rostro-medio-ventral quadrant of the otocyst to produce the otic

ganglion (Adamska, et al., 2001). In contrast, it was found by Dr. Vendrell (unpublished data) in our lab that implantation of FGF8-coated beads in the mesoderm at early placodal stages (HH 10) of chicken embryos resulted in smaller otic vesicles, indicating that FGF8 is playing a negative role at this stage. The different results obtained when FGF8 is overexpressed, may be valid, since the exposure to FGF8 was at different time in the two latter approaches. Likewise, in this study FGF8 was overexpressed from the neural tube before otic placode formation (HH 8-9), which leads to the expression of this factor during otocyst formation (Fig. 2.40). The latter result indicates that probably FGF8 expressed from the neural tube may act on the surface ectoderm, in which its receptor, FGFR3c is expressed (Wilke, *et al.*, 1997) to restrict the competent ectoderm to form otic vesicles, ensuring the correct placement of the otic vesicle.
Together the results obtained upon ectopic expression of FGF3 and FGF8 may be interpreted as such, that the competent otic ectoderm responds to permissive (FGF3) and restrictive signals (FGF8) by inducing an enlargement or reduced otic vesicle.

3.10-FINAL CONCLUSION

FGFs Control the Inner Ear Formation in Different Species

Many factors involved in otic formation have been studied so far, and many of them belong to the FGF family but the molecular pathways acting to execute this developmental program are not completely understood. The expression of many FGFs during this process makes it difficult to investigate the role of individual factors for inner ear formation, since they often function redundantly in a network, probably in collaboration with other factors. At the moment, it is clear that mesoderm, endoderm and neural tube are important for otic induction and development as a source of FGFs signals.

In this work, performing gain-and loss-of-function experiments in chicken, previous reports could be confirmed proposing the inductive capacity of FGF3 from the hindbrain acting on the competent otic ectoderm to induce the otic vesicle. The participation of this factor during formation of the otic vesicle from the otic placode was demonstrated as well. In the same species endodermal expression of FGF8 has been shown to play an inductive role in early phases during initiation of otic vesicle formation in concert to the mesodermal FGF19 expression most likely acting before FGF3 (Ladher, *et al.*, 2005).

The observations made in this study suggest that FGF3 may be acting coordinated with other factors, for example FGF8 and FGF19 to develop the otocyst in chicken. Activation of FGF3 seems to occur in a cascade in which the endodermal expression of FGF8 is the earliest inductive signal to form the otic placode via activation of the mesodermal FGF19 (Ladher, *et al.*, 2005). Next, the neural FGF3, which is known to be activated by FGF19, is acting as a final inducer directly on the competent otic ectoderm to give rise to the otocyst. Slightly later during otic induction, the endodermal expression of FGF3 may reinforce the otic induction. The partially overlapping expression of FGF8 and FGF3 in the endoderm adjacent to the developing otic placode, suggests either a possible compensatory effect of these factors or a direct activation of FGF3 by FGF8. Thereafter, a restrictive signal is given to the ectoderm by FGF8 after the otic placode was established to correctly place the otocyst.
Additional FGF family members may be involved in inner ear formation in this species such as FGF4 and FGF19. FGF4 is co-expressed with FGF3 in a region that will give rise to r4 -r6 of the hindbrain, (Shamim, *et al.*, 1999, Shamim, *et al.*, 1999) and thus has been suggested as and additional hindbrain-derived signal (Mahmood, *et al.*, 1995, Maroon, *et al.*, 2002).

The data presented here have demonstrated that in mice, FGF10 is essential together with FGF3 for normal otic development based on the otic phenotype found upon lack of expression of both genes. The redundancy of both factors for inner ear formation is also reinforced by the co-expression of FGF10 and FGF3 in the developing murine hindbrain (Alvarez, *et al.*, 2003). Similarly in zebrafish, FGF3 and FGF8 (expressed in the hindbrain) have been reported to play an essential and redundant role for otic induction and participate in the epithelial organization within the otic vesicle (Reifers, *et al.*, 1998, Phillips, *et al.*, 2001, Maroon, *et al.*, 2002, Liu, *et al.*, 2003). In contrast to zebrafish FGF3 and FGF8 mutants, which showed a severe failure in otic placode induction, the *Fgf3*$^{-/-}$*Fgf10*$^{-/-}$ mouse mutants presented rudimentary otic vesicles indicating that the capacity to organize the epithelium is still present. The less severe phenotype seen in mice in comparison with zebrafish could be due to loss of hindbrain markers and defective patterning in zebrafish; whereas in mice the hindbrain of *Fgf3*$^{-/-}$*Fgf10*$^{-/-}$ remains unaltered (Alvarez, Vendrell and Schimmang unpublished data).
Finally, the more severe phenotype found in otic formation in the *Fgf3*$^{neo/neo}$*Fgf10*$^{-/-}$ mutants reported by Wright and Mansour (2003) may be due to the subtle differences found between the phenotype of *Fgf3*$^{neo/neo}$ versus *Fgf3*$^{-/-}$ mutants. As explained before the *Fgf3*$^{neo/neo}$ mice described by Wright and Mansour (2003) displayed several otic defects due to incorrect otic morphogenesis, while the *Fgf3*$^{-/-}$ mutants described in this work formed normal inner ears

except for a few analyzed mutants which displayed a mild inner ear phenotypes that may be attributed to a different genetic background.

The analysis of double *Fgf3*$^{-/-}$*Fgf10*$^{+/-}$homoheterozygous mutants showed the relative contribution of FGFs during the formation of the inner ear and support the compensatory effect between FGF3 and FGF10 since the phenotype shown by the *Fgf3*$^{-/-}$*Fgf10*$^{-/-}$ mutants was stronger than the one displayed upon single mutation of FGF10 (Pauley, *et al.,* 2003).

In this study is also shown that FGF8 works redundantly with FGF3 in later stages of normal otic morphogenesis in mice. Expression of FGF8 has been detected at E12.5 in the sensory epithelium of the otocyst which coincides with the onset of otocyst malformation in compound *Fgf3+8* mutants. Thus, this expression of FGF8 redundantly with the FGF3 expression (Wilkinson, *et al*., 1988, Wilkinson, *et al*., 1989) appear relevant to continue the otic program since the individual lack of FGF3 or specific block of FGF8 in otic placode/vesicle does not affect severely inner ear development. Interestingly, in zebrafish a dynamic expression of FGF3 and FGF8 that only overlap shortly in common territories appears to be sufficient to permit them to compensate for each other in early otic development (Powles, *et al*., 2004).

In contrast to this work, a loss of the otic vesicle was found in a compound *FGF3*$^{neo/neo}$*; FGF8*$^{Hyp/-}$ double mutant (Ladher, *et al*., 2005). As already discussed, the more severe phenotype in otic development of this mutant may also arise from alterations in the hindbrain as reported in zebrafish (Maves, *et al*., 2002, Walshe, *et al*., 2002).

The analysis of the ganglion development in the different mutants (*Fgf3*$^{-/-}$, *Fgf3*$^{-/-}$*; Fgf10*$^{-/-}$, *Fgf3*$^{-/-}$*/ Fgf10*$^{+/-}$, *Fgf3+8*, *Fgf8* ko) suggests that of FGF3, FGF8 and FGF10 are participating in ganglion formation and moreover they can compensate each other during this process.

To clarify the possible inductive role of FGF8 in mice another specific *Cre*-deleter line is required. This issue is expected to be revealed by using the MORE line (Mox2*Cre*), which expresses *Cre* recombinase from the Mox2 locus, driving the expression of *Cre* throughout the epiblast following implantation with slightly mosaic Cre activity in the somatic tissue (Tallquist, *et al.*, 2000). To evaluate the possible compensatory effect of these factors during early otic initiation, double FGF3 and FGF8 mutants using FGF8-Mox2-*Cre* mice will be generated.

Electroporation in chicken explants are underway to ascertain the role of the reported expression of FGF3 in pharyngeal endoderm close to the prospective otic placode, which coincides with the expression in the hindbrain (Mahmood, *et al.*, 1995). To test this possibility siRNA against FGF3 will be electroporated at early stages (HH 7-8) into the endoderm of chick explants to knock down the expression of FGF3.
These experiments will help to further clarify the role of FGFs at different stages of otic formation in mice and chicken.

The roles of four members of the FGF family (FGF2, FGF3, FGF8 and FGF10) in inner ear formation have been characterized in this study by utilizing loss-of-function approaches in mice. Moreover, redundant interactions and relative contributions between these members have been demonstrated and their functions have been correlated with their spatial expression in the developing otocyst. Based on this study, it can be concluded that FGF3 and FGF10 play essential roles in a redundant manner to reinforce otic induction, as well as to maintain it and to pattern the otocyst. A role for FGF3 and FGF8 working redundantly to direct correct otic morphogenesis was also proposed. Complementarily in chicken embryos by applying loss- and gain-of-function experiments, the participation of FGF3 in otic induction and morphogenesis could be confirmed and as well as the important role of the hindbrain as an inducing tissue.
In summary, albeit FGFs do not show the same expression pattern in different species, similar mechanisms acting during otic formation involving FGF signalling have been shown in the two analyzed species, mice and chicken. It suggests the existence of conserved pathways during inner ear development in vertebrates.

IV-MATERIALS

4.1-Experimental Animals

4.1.*1*-Chicken Embryos (*Gallus gallus, Linnaeus 1758*)

Fertilized eggs (strain Broiler) were purchased from a local farm and stored at 17° C before incubation at 37°C with high humidity. Embryos were electroporated after incubation to obtain the desired somite stages according to the table of Hamilton and Hamburger (Hamburger, 1951).

4.1.*2*-Mice *(Mus musculus, Linnaeus 1758)*

Mice were bred on a mixed 129 xC57/Bl6 background at the UKE Hamburg. The generation of the *Fgf3* null mutant was done by Dr. Alonso and Chamero, Pablo. To generate a *Fgf3* null mutant a genomic fragment containing the *Fgf3*-coding region and a 3´ located 3.2 kb genomic fragment (Peters, 1989) were used for construction of the targeting vector. Heterozygous $Fgf3^{neo/+}$ mice were mated with deleter-cre mice (Holzenberger, 2000) to remove the *Fgf3* cDNA and the neomycin cassette. Cre-mediated excision was confirmed by Southern blot and PCR. The primer pairs used for the analysis of the wild-type; targeted and knock-out allele had the following sequences: wild-type (5´ primer; ATGGGCCTGATCTGGCTTCTGCT; 3´primer; TCCACCGCAGTAATCTCCAGGATGC); cDNAneo (5´ primer; ACGACGGGCGTTCCTTGCGCAGCTGTG; 3´ primer; CCTGGTACTATGGTGCTA); knockout (5´ primer; CATCTCCACCTCTCTCCAG; 3´primer; CCTGGTACTAT GGTGCTA) (Alvarez, *et al*., 2003). FGF10 knockout mice were genotyped by PCR according to Sekine *et al*. (Sekine, *et al*., 1999). FGF8 knockout and conditional knockout mice were kindly provided by Gail Martin (Meyers, *et a*l., 1998) and FGF2 knockout mice by Rosanna Dono (Dono, *et al*., 1998).

IV-MATERIALS

4.2-List of Solutions

4.2.*1*-Buffers

PBS:	1.3 M NaCl; 70 mM Na_2HPO_4; 30 mM NaH_2PO_4.
PBT:	0.1 % Triton X-100 in PBS
TAE (1×)	0.2 M Tris-acetate; 10 mM EDTA pH 8
Tris (1M)	121 g Tris dissolved in 800 ml ddH_2O. pH is adjusted with HCl. Adjust to 1 L with ddH_2O.
Hybridization Buffer	(whole mount) 50% Deionised Formamide; 5× SSC; 2% Boehringer Blocking powder; 10% Triton X-100; 10% CHAPS; 5 mg/ml Heparine; 10 mg/ml tRNA; 0.5 M EDTA.
Hybridization Buffer	(Slides) 1× SALT; 50% Formamide; 10% dextran sulphate; 1mg/ml tRNA; 1× Denhardt´s
Alkaline-Phosphatase	Buffer 100mM NaCl; 50mM $MgCl_2$; 100mM Tris pH 7.9; 0.1% Tween; 0.5 mg/ml Levamisol
KTBT	50 mM Tris; 150 mM NaCl; 10 mM KCl; 1% Triton X-100
Chick Ringer	7 g NaCl; 0.42 g KCl; 0.24 g Ca Cl_2 to 1 L H_2O
MABT	100mM Maleic Acid; 150mM NaCl, pH 7.5; 0.1% Tween

4.2.*2*-Solutions

PFA	4% Paraformaldehyde in PBS
SSC (20×)	3 M NaCl; 0.3 M Sodium citrate pH 7.0
LB medium:	1% Casein-Hydrolysate; 0.5% Yeast Extract; 0.5% NaCl; 0;1% Glucose; pH 7
10× SALT	114g NaCl; 14.04g pH 7.5 Tris-HCl; 1.34g Tris Base; 7.8g Na_2HPO_4; 7.1 g NaH_2PO_4; 100 ml 0.5M EDTA to 1L H_2O
Denhardt´s (50×)	1g Ficoll 400; 1g Polyvenylpyrrolodine; 1g BSA; qs to 100 ml ddH_2O
Fast Green	3,3 g/L Fast Green in PBS

4.2.*3*-Staining Solutions

(Nitroblue tretazolium)/(Br-Cl-Indol-Phosphate)	NBT/BCIP solution3.5 μl/ml NBT; 3.5 μl/ml BCIP in Alkaline-Phosphatase Buffer (AP).
Cresyl Violet	0.1% Cresyl Violet in ddH_2O. Filtered
Toluidine Blue O	0.1% Toluidine Blue O in ddH_2O. Filtered
Hematoxilin/Eosin	1 % Hematoxylin 0.4 % Eosin. Filtered

4.3-Bacterial Strains Used

XL1-Blue	SURE ® 2 supercompetent cells from Stratagene

4.4-Vectors

pLP-EGFP-C1	CMV/C-terminal fusions to EGFP (green) from Clontech
pBluescript KS+/SK-	cloning vector (Stratagene)
pGEM-Teasy	cloning vector (Promega)
pCS2+MT	cloning vector (obtained from Dr. Ingolf Bach´s Lab-ZMNH)
pSupressorNeo-IGM800	cloning vector (Biocarta)

4.5-Probes Used For *In Situ* Hybridization

Gene-Containing plasmid	Generation of the in situ antisense probe: Enzyme to linearize the plasmid and RNA polymerase	Provider of the plasmid
FGF3 (mouse)-pGEM-T	SalI, T7	M. Maconochie
FGF10 (mouse)- pGEM-T	ApaI, Sp6	Y. Alvarez
FGF8 (mouse)- pBS-KS	SmaI, T7	Y. Alvarez
FGF3 (chicken)- pBS-KS	NotI, T3	C. Pujades
FGF8 (chicken)- pBS-KS	NotI, T3	M. Ros
FGF10 (chicken)-pGEM-T	NcoI/Sp6	H. Ohuchi
Pax2 (chicken)- pBS-SK	XbaI, T3	M.Torres
Lmx1 (chicken)- pBS-KS	EcoRI, T3	F. Giraldez
Cek8 (chicken)- pBS-KS	NotI, T3	A. Nieto

4.6-Eukaryotic Expression Vectors Used

Gene-Containing plasmid	Enzyme used for cloning	Creator of the construct
FGF3 (mouse cDNA)-pCS2	EcoRI	Y. Alvarez
FGF10 (mouse cDNA)- pCS2	BamH1/NsiI	Y. Alvarez
FGF8 (mouse cDNA)- pCS2	BamHI/XhoI	Y. Alvarez
FGF10 (mouse cDNA)- pBS-KS	XhoI/ XbaI (r3,r5 enhancer-_globin promoter FGF3cDNA- IRES-LacZ)	Y. Alvarez
FGF3 (chicken-oligo)- pSuppressor	XbaI/SalI	L. Zelarayán
FGF3 (chicken-oligo)- pSuppressor	XbaI/SalI	L. Zelarayán
FGF3 (chicken-oligo)- pSuppressor	XbaI/SalI	L. Zelarayán
FGF8(chicken-oligo)- pSuppressor	XbaI/SalI	L. Zelarayán

4.7-List of Oligonucleotides and Morpholinos Used

Name	Sequence (5´-3´)	Purpose of Use
$FGF3_{(1)}$Fw	TCGAAAGCCAGTGCGGAGAGACTCTTTCAAG AGAAGAGTCTCTCCGCACTGGCTTTTTTT	Cloned into pSuppressor for loss-of-function approach in chicken
$FGF3_{(1)}$Rev	CTAGAAAAAAAGCCAGTGCGGAGAGACTCT TCTCTTGAAAGAGTCTCTCCGCACTGGCTT	Cloned into pSuppressor for loss-of-function approach in chicken
$FGF3_{(2)}$Fw	TCGAAAGGGCTTGTTCTCTGGCAGATTCAAG AGATCTGCCAGAGAACAAGCCCTTTTTTT	Cloned into pSuppressor for loss-of-function approach in chicken
$FGF3_{(2)}$ Rev	CTAGAAAAAAAGGGCTTGTTCTCTGGCAGAT CTCTTGAATCTGCCAGAGAACAAGCCCTT	Cloned into pSuppressor for loss-of-function approach in chicken
$FGF3_{(3)}$Fw	TCGAAAACACGCAGGACACAGAAATTTCAA GAGAATTTCTGTGTCCTGCGTGTTTTTTTT	Cloned into pSuppressor for loss-of-function approach in chicken
$FGF3_{(3)}$ Rev	CTAGAAAAAAAAACACGCAGGACACAGAAAT TCTCTTGAAATTTCTGTGTCCTGCGTGTTT	Cloned into pSuppressor for loss-of-function approach in chicken
$FGF8_{(3)}$ Fw	TCGAAAGCCCAGGTAACTGTTCAGTTTCAAG AGAACTGAACAGTTACCTGGGCTTTTTTT	Cloned into pSuppressor for loss-of-function approach in chicken (used as a control)
FGF8 Rev	TCGAAAGCCCAGGTAACTGTTCAGTTTCAAG AGAACTGAACAGTTACCTGGGCTTTTTTT	Cloned into pSuppressor for loss-of-function approach in chicken (used as a control)
FGF3 morpholino	GCAGCAGAAGCCAGATCAGGCCCAT	Used for loss-of-function approach in chicken
Control morpholino	CCTCTTACCTCAGTTACAATTTATAT	Used for loss-of-function approach in chicken

-Oligonucleotides were purchased from MWG-Biotech AG (Ebersberg-Germany).The oligonucleotides cloned into the pSUppressor plamisd were designed based on the following link: http://www1.qiagen.com/Products/GeneSilencing.

-Morpholinos were purchased from Gene Tools, LLC (Philomath, OR 97370).

4.8-Antibodies Used

Primary Antibodies			
Antibody (anti-)	**Source**	**Species made in**	**Used dilution**
Kcc4	Gift from T. Boettger (T. Jentsch´s Lab-ZMNH)	Guinea Pig	1:250
KCNQ4	Gift from T. Kharkovetts (T. Jentsch´s Lab-ZMNH)	Rabbit	1:50
KCNQ1	Gift from T. Kharkovetts (T. Jentsch´s Lab-ZMNH)	Rabbit	1:200
Barttin	Gift from T. Boettger (T. Jentsch´s Lab-ZMNH)	Guinea Pig	1:100
Neurofilament 160	Gift from M. Miehe (D. Riethmacher´s Lab-ZMNH)	Mouse	1:100
Secondary Antibodies			
Antibody (anti-)	**Source**	**Species made in**	**Used dilution**
Alexa 488-a mouse	Mobitech	Goat IgG(H+L)F(ab‘) 2 Fragment	1:2000
Alexa 488-a rabbit	Mobitech	Goat IgG(H+L)F(ab‘) 2 Fragment	1:2000
Cy3-a- giunea pig	Dianova	Goat IgG(H+L)	1:2000

V-METHODS

5.1-Isolation and Purification of Plasmid DNA

5.1.*1*-Analytical Scale Purification of DNA (Minipreps)

A miniculture of bacteria was started by picking a single bacterial colony from an agar plate and inoculating 3-4 ml of LB medium including an antibiotic, followed by incubation at 37°C overnight while shaking. 1.5 ml of the overnight-culture was transferred to Eppendorf reaction tubes and centrifuged 10 min. The pellet containing bacterial cells was resuspended in 250 μl of Buffer P1 (Quiagen, Cat. Nro.19051) and transfer to a microcentrifuge tube. Immediately 250 μl of Lysis Buffer P2 was added (Quiagen, Cat. Nro. 19052) and the tube were gently inverted 4–6 times to mix. 350 μl of neutralization Buffer P3 (Quiagen, Cat. Nro. 19053) was added and the tube inverted to mix gently 4–6 times. The tubes were centrifuged for 10 min at 14,000 rpm (~17,900 x g) in microcentrifuge (Eppendorf Tabletop Centrifuge, 5417) and a compact white pellet was form. The supernatants from the last centrifugation step were collected and precipitated with 70% EtOH for 30 min. at -80°C. Next, the tubes were centrifuged at 14,000 rpm for 10 min. and the EtOH was discarded. The Pellet of DNA was washed 2 times with EtOH 70 % and resuspended in 100 μl TE.

5.1.*2*-Large Scale Purification of DNA (Maxipreps)

To produce a large bacterial culture, minicultures were grown (see 5.1.1), 25-50 μl of which were used to inoculate 250 ml of LB containing 0.1 mg/ml ampicillin before incubation at 37°C O.N, shaking. Plasmids were purified using the QIAfilter Plasmid Maxiprep Kit (Qiagen) or the Concert High Purity Plasmid Maxiprep Kit (Gibco-BRL) according to the manufacturer's instructions.

5.1.*3*-Determination of DNA and RNA Concentration

The concentration of DNA and RNA in solution was spectrophotometrically determined by measuring the optical density (OD) using wavelengths of 260 nm and 280 nm (Ultrospec

3000, Pharmacia). An OD260 of 1 corresponds to approximately 50 μg/ml for double-stranded DNA, 40 μg/ml for single-stranded DNA and RNA, and 20 μg/ml for single-stranded oligonucleotides. The ratio between the readings at 260 nm and 280 nm (OD260/OD280) provides the purity of the nucleic acid, with pure preparations of DNA and RNA having OD260/OD280 values of 1.8 and 2.0, respectively. For quantifying the amount of DNA, 200 μl of a 1:50 or 1:100 dilution was assayed for absorbance.

5.1.*4*-Agarose Gel Electrophoresis

The amplified DNA was checked by appropriate enzymatic digestion and/or sequencing. Restriction enzyme-digested DNA fragments were separated in an agarose gel by electrophoresis, visualized with UV-light. DNA was separated in 0.8-2.0% agarose gels (containing 0.5 μg/ml ethidium bromide). The 10x DNA loading dye (10% glycerol, 0.25% bromophenol blue, 0.25% xylene cyanol blue) was added to the samples before loading them onto the gel together with a 1-kB DNA Ladder (Gibco-BRL) and electrophoresis at ca 100 V for 1-2 h. The separated DNA fragments were subsequently visualized and photographed using a UV-Gel Documentation System (Herolab, Wiesloch, Germany).

5.2- siRNA Cloning

Small interfering RNAs (siRNAs) have gained much attention for their powerful ability to suppress gene expression. siRNAs prevents the normal non-specific cytotoxic response provoked in most mammalian cells by dsRNA (>30 base pairs). siRNAs are 21- to 23-nucleotide RNA particles, with characteristic 2- to 3- nucleotide 3'-overhanging ends, which are generated by ribonuclease III cleavage from longer dsRNAs and they inhibit gene expression by inducing RNAi in the same fashion as dsRNA. In this study GeneSuppressor system (Biocarta) has been chosen to induce inhibition of gene expression. Sense and antisense strands constituting the siRNA duplex are transcribed by the U6 promoter, members of the type III class of Polymerase III. GeneSuppressor is a plasmid-based system to generate siRNAs for gene knockdown. Inserts cloned into GeneSuppressor plasmids express RNAs under U6 promoter in the transfected mammalian cells. The RNAs are expressed as fold-back

stem-loop structures that are processed into the siRNAs (Elbashir, *et al*., 2001, Brummelkamp, *et al*., 2002, Paddison, *et al*., 2002).

5.2.*1*-Design and Preparation of Inserts

The most critical part of the construction of the siRNA expression plasmid is the selection of the target region of the gene. For that reason, an online service provided by Quiagen was used to select the oligonucleotides. Next, a guideline described by Elabashir *et al*, (2002) that may work 80% of the time was followed to finally select the correct sequences. According to the authors for synthesis of synthetic siRNA, a target region may be selected preferably 50 to 100 nt downstream of the start codon. 5' or 3' untranslated regions and regions close to the start codon should be avoided as these may be richer in regulatory protein binding sites. siRNA was designed to produce hairpin RNAs, in which both strands of a siRNA duplex will be included within a single RNA molecule. The individual motif contained 21 nt and corresponded to the coding region of FGF3 or FGF8 (used as a control for FGF3 inhibition). The two motifs that form the inverted repeat were separated by a spacer of 9 nt (to form the hairpin loop). The transcriptional termination signal was added at the 3' end (5 Ts) of the inverted repeat as well as the restriction site for Xho I at the 5' end and Xba I at the 3' end of the primer sequences. The insert was prepared by annealing the two complementary oligonucleotides.

5.2.*2*-Cloning the Target siRNA into the pSuppressor Cassette

The inserts (designed oligonucleotides against FGF3 or FGF8 mRNA) were cloned into Sal I and Xba I sites of the pSuppressor plasmid. The pSuppressor vector DNA (from a Biocarta kit) has been digested with Sal I and Xba I to generate compatible ends for cloning. To ensure correct cloning, compatible restriction sites, Xho I at the 5' end and Xba I at the 3' end of the primer sequences were added. Xho I restriction site is compatible with Sal I site and allows cloning into the Sal I site. However, after cloning into Sal I site, both Sal I and Xho I sites are lost. Thus, the recombinant plasmids containing the inserts will not be linearized when digested with Sal I, whereas the wild type plasmid DNA will be linearized with Sal I, which was used for screening.

5.2.*3*-Hybridization/Annealing of Synthetic Oligonucleotides

10 μg of each oligonucleotide (sense and anti-sense) were combined in a total volume of 50 μl of TE, 100 mM NaCl, thereby creating a stock concentration of 200 μg/ml. The reaction was heated to 85°C for 3 min before allowing it to slowly cool down to RT.

5.2.*4*-DNA Digestion Using Restriction Enzymes

Digestion of pSuppresor using restriction enzymes were performed in the - buffer provided by the manufacturer. The reactions were set up using 1-2 U of enzyme per μg DNA and then incubated at 37°C (unless otherwise recommended by the manufacturer) for 1-2 hours. The DNA digestion was then checked on an Agarose gel (see section 5.1.*4*). Analytical digests were generally carried out with 1-2 μg DNA in a total volume of 20 μl, using the guideline: 1 U enzyme digests 1 μg DNA in 1 h.

5.2.*5*-Ligation of Oligonucleotides and Vectors

Ligation of the oligonucleotides to the digested vector DNA was catalyzed by the T4 DNA ligase. Approximately 100 ng vector DNA was combined with a 3- to 5-time molar excess of DNA insert (depending on the insert size), 1 μl of 10x T4 Ligase Buffer and 10 U of T4 DNA Ligase (Roche) in a total volume of 10 μl. The reaction was incubated O/N at 16°C before transforming competent DH5a E. coli bacteria with 5 μl of the reaction. .

5.2.*6*-Producing Competent Bacteria

To prepare competent bacteria, only autoclaved, sterile solutions and equipment were used. A glycerol culture of the DH5a E. coli strain was streaked onto an agar plate and grown O/N at 37°C. Single colonies were then picked to start small (3-5 ml) cultures. 1 ml of the overnight culture was inoculated in LB medium containing 10 mM $MgCl_2$ on a shaker until the bacteria had grown to mid-log phase (when A595 reached 0.4-0.5). The bacteria were then pelleted at 5,000 rpm for 5 min at 4°C (Beckman J2-21M/E Centrifuge, JA10 rotor). After discarding the

medium, the cell pellet was resuspended in 50 ml of ice-cooled 100 mM $CaCl_2$, transferred to a 50-ml conical tube and incubated on ice for 30 min with occasional swirling. The cells were then centrifuged in a Tabletop centrifuge (Minifuge RF, Heraeus, Hannover, Germany) for 5-10 min at 5,000 rpm, 4°C. The pellet was resuspended in 10 ml ice-cold 100 mM $CaCl_2$, 15% glycerol and incubated on ice until they were aliquoted into sterile, chilled Eppendorf 1.5 ml tubes before freezing at –80°C.

5.2.*7*-Bacterial Transformation

For each transformation, 100 μl of DH5a were removed from storage at –80°C and thawed on ice. DNA (1-25 ng) was added and the mixture incubated on ice for 30 min. Immediately following a 90-sec heatshock at 42°C, the Eppendorf reaction tubes were briefly returned to ice before adding 1 ml of LB media and incubating the tubes, shaking, at 37°C for 30-60 min. The Eppendorf reaction tubes were centrifuged at 4,000 rpm for 2 min and then approximately 1 ml of the supernatant was removed. The cells were resuspended in the remaining LB media and plated onto LB-agar plates containing ampicillin, followed by O/N incubation at 37°C.

5.2.*8*-Selecting positive clones

After performing minipreps to search for the plasmid containing the inserts, the DNA with SalI and XbaI was digested in order to check whether the SalI site was lost and XbaI present. The positive clones were confirmed by DNA sequencing.

5.2.*9*-DNA Sequencing

DNA sequencing was performed by the Service Group at the Center for Molecular Neurobiology in Hamburg, led by Dr. Kullman and Fr. Däumingen. Samples were prepared by combining ca 800 ng DNA and 15 pmol sequencing primer in a total volume of 8 μl (with H_2O).

5.3-Preparation of Morpholinos

The DNA antisense morpholino electroporated in chicken were acquired from Gene Tools. Its sequences were 3´ Carboxyfluorescein labeled in order to control the electroporation. The morpholinos were resuspend in sterile PBS at the desired concentration (250μM) and then stored at –20°C in aliquots.
After electroporation fluorescein was detected in an Axioplan-2 microscope (Zeiss)

5.4-In Ovo Electroporation

Electroporation involves the application of an electric field pulse to temporarily disrupt membrane stability, creating pores in the plasma membranes of cells through which DNA is driven as a result of its negative charge in the direction of the anode (Muramatsu, *et al*., 1997, Swartz, *et al*., 2001)

5.4.*1*-Preparation of the Embryos and DNA for Electroporation

Chicken embryos were incubated until they reached the desired stage. 4 ml of albumen was removed and then a window of about 3 cm in diameter was opened on the top of the eggshell. A Fast green solution was injected over the embryo to visualize it. The solution containing the different plasmids containing cDNAs (2 μg/μl) or morpholinos (250μM) plus a reporter GFP-expressing plasmid (0.8 μg/μl) in PBS, was injected into the lumen of the neural tube with a glass microcapillary. Before the electroporation 50μl of PBS were placed over the embryo to improve the transfection.
The plasmids used to electroporate were pCS2 and pSuppressor (se section 5.2.*1*). pCS2 is a vector of 4354 bp containing a CMV (Cytomegalovirus) promoter and including Ampicilin resistance, in which the cDNA of different FGFs were cloned in its multicloning site.

5.4.*2*-Electropration

Two parallel platinum electrodes (0.5 mm width and 4 mm length) with a distance of 5mm between them were located on both side of the embryo. Subsequently 4 pulses of 30 V, with

duration of 50 ms and a interval of 1 ms were applied using a BTX electroporator (Nakamura *et al*. 2002). The electroporated embryos were left to develop by incubation at 37°C for a required time depending on the experimental conditions. After incubation the embryos were removed from the eggs and the membranes were dissected.

A fixation step with 4% PFA was performed at 4°C for 6 h in order to enable in situ hybridization and morphological analysis (Nakamura *et al*. 2002, Swartz *et al*. 2001). The embryos were visualized with an Axiocam-2 (Zeiss) microscope and the pictures were taken with a digital camera Axiocam 2 (Zeiss).

5.5-RNA *In Situ* Hybridization Analysis with Digoxygenin (DIG)-labeled RNA Probes

5.5.*1*-Whole Mounts *In Situ* Hybridization Analysis

RNA whole-mount in situ hybridization was essentially performed as described by Conlon and Rossant (1992) using digoxigenin- and fluorescein-labelled riboprobes, which were detected by using alkaline phosphates-coupled antibodies. Plasmids containing fragments of cDNAs from the genes to be detected, were linearized by restriction enzymes, and used as templates for T3, T7 and SP6-directed RNA synthesis, using the DIG RNA Labeling Mix and accompanying protocol (Roche), thereby generating single-strand RNA antisense probes.

The embryos were removed from the membranes, fixed 10-12hs in 4% PFA and rinsed twice in PBT (PBS with Tween 0.1%) for 10 minutes. After dehydration through a graded methanol series (25%, 50%, 75% and twice with 100% methanol), they were rehydrated in the same decreasing series of methanol and washed with PBT twice for 10 minutes. Proteinase K in PBT (20 μg/ ml) was applied for 10-15 minutes at room temperature. A postfixation was carried out in 4% PFA-0.25% Glutaraldehyde in PBT for 15 minutes. The embryos were washed in PBT and incubated in hybridisation solution (deionised Formamide 50%, 5× SSC pH 7.5, tRNA 50 μg/ml, Chaps 0.1%, heparin 100μg/ml) at 62-65°C over night. The hybridization solution was changed with hybridization solution containing 1μg/ml of RNA probe and incubated at 62-65°C for 2 days. After this hybridization step embryos were washed at 65°C with solutions of different stringencies (1h in 2 × SSC-0.1% Chaps, 30 min. in 0.2 × SSC-0.1% Chaps). Then they were rinsed with KTBT (50 mM Tris-HCl, 150 mM

NaCl, 10 mM KCl, 1% Triton X-100) at room temperature and incubated in blocking solution (KTBT-20% goat serum) over night at 4°C. Subsequently, incubation with anti-DIG antibody (1:1000) in KTBT-20% goat serum was performed over night on a shaker at 4°C.Several rinses in KTBT were done for 1h during 12-24 h. 1.25 μl/ml NBT, and 0.75 μl/ml BCIP in AP buffer were used for staining. The reaction was stopped with KTBT and the embryos were postfixed in 4% PFA, to allow their posterior histological analysis.

5.5.*2*-*In situ* Hybridization on Tissue Sections

In situ hybridizations were performed essentially as described (Strahle *et al*., 1994). Briefly, mouse embryo cryosections were defrosted, and then hybridized O/N at 65°C in the presence of antisense RNA probes diluted 1:100 in hybridization buffer (0.2 M NaCl; 10 mM $NaPO_4$; 5 mM EDTA; 10 mM Tris-HCl, pH 7.5; 50% formamide; 10% dextran sulfate; 1 mg/ml tRNA (Gibco); 1x Denhardt's). They were then washed 4-5 times for 30 min at 65°C in 1x SSC, 50% formamide, 0.1% Tween-20, followed by two 30 min washes at RT in MABT (100 mM maleic acid, pH 7.5; 150 mM NaCl; 0.1% Tween-20), and then blocked 1 h at RT in MABT + 2% Blocking Reagent (Roche) + 20% heat-inactivated goat serum (Sigma). Alkaline-phosphatase-conjugated anti-DIG antibody (Roche) was diluted 1:2500 in blocking solution and incubated O/N at RT. Sections were then washed 5 x 20 min in MABT, then twice 10 min in AP Staining Buffer (100 mM NaCl; 50 mM MgCl2; 100 mM Tris-HCl, pH7.9; 0.1% Tween-20; 0.5 mg/ml levamisole). Sections were incubated with AP staining buffer containing 3.5μl/ ml of NBT and BCIP for 1-3 days until the signal developed. Sections were then washed in ddH_2O, air-dried and mounted in Histokitt mounting medium (Roth).

5.6-Tissue Preparation for Cryosections

5.6.*1*-Preparation of Embryos

Mouse embryos were dissected and fixed in 4% PFA in PBS (pH7.4) at 4°C for 2 hours to O/N, depending on the size of the tissue, equilibrated with 30% sucrose in PBS, and mounted in O.C.T. embedding medium (Tissue Tek, Sakura) at –80°C. The embryos were cryosectioned at 10 µm and the slides stored at –20°C until the assays were performed.

5.6.*2*- Preparation of Inner Ears of Adult Mice

Cardiac perfusion with 4% PFA was performed in adult mice in order to fix the inner ear structures. The inner ears were removed from the head and a fine dissection was performed. A hole was made in the oval window (vestibule). An additional hole in the cochlea was also performed by scrapping carefully with the tweezers on the top of the cochlea in order to let the PFA diffuse inside the tissue. Decalcification with Rapid Bone Decalcifier (Sigma) was performed for 15 min. and the ears were subsequently postfixed for 2-3 days at 4°C, rinsed in PBS for 10 minutes, equilibrated with 30% sucrose in PBS, and mounted in O.C.T. embedding medium at –80°C. Cryostat sections with a thickness of 12 µm were performed and the slides stored at –20°C until the assay was performed.

5.6.*3*- Preparation of Inner Ears of Mouse Embryos

Mouse embryos were dissected and the head was removed to fix it with 4% PFA in PBS (pH7.4) at 4°C for 2 hours to O/N, depending on the size of the tissue. The ears were dissected as explained in section 5.6.*2*. A posfixation for 2 hours was done at 4°C. They were equilibrated with 30% sucrose in PBS, and mounted in O.C.T. embedding medium (TissueTek, Sakura) at –80°C. The embryonic inner ears were sectioned at 10 µm and the slides stored at –20°C until the assay was performed.

5.7-Immunofluorescence Assay

The cryosections were dried 30 minutes, fixed in 4 % PFA with 0,1% Desoxycholate/NP40 for 3 min. and washed three times in PBS for 3 min. The samples were blocked for 1h with a solution containing 2%BSA, 1% Normal goat serum (NGS); 0,1% NP40 at room temperature. Primary antibody was diluted in the same solution and incubated at 4°C O/N. Primary antibody was washed with PBS 3 times for 5 min. and a second blocking step was done for 30 min. The secondary antibody was incubated for 1h at RT in darkness. Sections were subsequently washed with PBS and mounted with Vectashield mounting medium. The

fluorescence was detected in an Axioplan 2 (Zeiss) fluorescent microscope and microphotographs were made with a digital camera Axiocam 2 (Zeiss).

5.8-Dissection of Adult Inner Ears for Histology Analysis and Paint-Filling

The mice were sacrificed by cervical dislocation and the head cut under the level of the ears. The cranial cavity was opened and the parietal bone cut in the middle line to remove it. Once the ears were visualized they were carefully dissected, rinsed in PBS and fixed in 4% PFA. The following steps are explained in section 5.6.2. The ears were fixed O/N in PFA at 4 °C and subsequently stained.

5.8.*1*-Tissue Preparation for Histology

After fixation the inner ears were washed 2x PBS for 30 min, and passed through a row of ethanol solutions (25% Ethanol/PBS, 50%, 75%, 80%, 85%, 90%, 95% and 100% Ethanol/water). Embedding was performed using the Kulzer Histotechnique with Technovit 7100 (Heraeus). Sections were made on a Leica Microtome (4μm thick), stretched on top of a 42°C water bath, transferred to coated glass slides and air-dried for 12 hours at 37°C. The slides were stained with Toluidine Blue O or Hematoxylin/Eosin and mounted with Eukitt (Sigma).

5.8.*1.1*-Toluidine Blue O staining

The sections were stained in Toluidine Blue O 0,1 % in ddH_2O for 5 min. and subsequently washed with ddH_2O for 10-15 min.. They were dried at room temperature for 12 h and mounted with Eukitt (Sigma) to store them. Microphotographs of the samples were made with a digital camera as described in section 5.7.

5.8.*1.2*- Hematoxylin/Eosin staining

The slides were stained with 0,1 % hematoxylin in ddH_2O for 10 min. and washed in H_2O for 5 min. Next, they were placed in a solution containing eosin at 0,4 % in ddH_2O for 8 min. and subsequently washed in ddH_2O for 10 min. The stained slides were dried and mounted with Eukitt (Sigma). Microphotographs of the samples were made with a digital camera as described in section 5.7.

5.8.*2*-Tissue Preparation for Paint-Filling

Inner ears from embryos and adult mice were fixed with Bodian´s fixative (75% ethanol, 15% water, 5%formalin, and 5%glacial acetic acid) O/N and dehydrated in a row of ethanol solutions (25% Ethanol/PBS, 50%, 75%, 80%, 85%, 90%, 95% and 100% Ethanol/water) for 1 h in each alcohol. They were subsequently cleared in Methyl Salycilate (Sigma) for 1 to 3 days in Petri dishes. Once the specimens were cleared a Latex White-Paint diluted in acetone was injected into the lateral surface of the otocyst or through the oval window, using a micropipette or glass capillary in a dark-field illumination. The tissues can be stored in Methyl Salicylate in a glass container.

5.9-Tissue Preparation for Vibrotome sections

After whole-mount in situ hybridization embryos were fixed in 4% PFA at 4°C for 10-12h, rinsed in PBS and embedded in 15% sucrose in PBS for 1 h at room temperature. The embedding procedure was performed in gelatine (bloom 300) at 37°C for 1h. The mould of gelatine was subsequently fixed for 12 h in 4% PFA at 4°C. They were sectioned at 40-45 m on a vibrotome (TPI), and mounted with PBS-glycerol 3:1 on Histobond glass slides. The sections were visualized as described in section 5.7.

5.10- In situ Enzymatic ß-Galactosidase Staining

The enzymatic ß-galactosidase reaction with the substrate X-gal was performed on E9-E16 whole embryos. X-Gal (5-bromo-4-chloro-3-indolyl-beta-D-galactopyranoside) is a chromogenic substrate for ß-galactosidase, which hydrolyzes X-Gal forming an intense blue precipitate. This reaction was carried out on the embryos carrying the *LacZ* reporter transgene under the control of a FGF3 enhancer sequence (Powles, *et al*., 2004). After fixation the embryos were washed 2x 20 min in PBS and incubated for 12-16 hours at 30°C in the dark with the staining solution (1mg/ml X-Gal; 5mM $K_3Fe(CN)_6$; 5mM $K_4Fe(CN)_6$; 2mM $MgCl_2$; 0.02% NP-40). The staining reaction was stopped by washing the tissues with PBS. Subsequently the tissues were dehydrated and embedded in Technovit (5.8.*1*).

5.11-*In situ* Detection of Apoptosis by TUNEL

Apoptosis is a form of cell death that eliminates compromised or superfluous cells. It is controlled by multiple signaling that mediate active responses to external growth, survival, or death factors. The most common biochemical property of apoptosis is the endonucleolytic cleavage of chromatin, initially to large fragments of 50-300 kilobase pairs and subsequently to monomers and multimers of 180-200 base pairs. In this work the ApopTag® Fluorescein *In Situ* Apoptosis Detection Kit (Chemicon) was used to detect apoptotic cells in situ by indirect TUNEL. The TUNEL (Terminal deoxynucleotidyl Transferase Biotin-dUTP Nick End Labeling) method identifies apoptotic cells *in situ* by using terminal deoxynucleotidyl transferase (TdT) to transfer biotin-dUTP to the free 3'-OH of cleaved DNA. The biotin-labeled cleavage sites are then visualized by reaction with fluorescein-conjugated avidin (avidin-FITC) (Mori, *et al*., 1994).

Cryosections were fixed in 1% PFA in PBS, pH 7.4 in a coplin jar for 10 min. at room temperature. The excess liquid was drained off and sections were washed twice in PBS for 5 min., post-fixed in precooled ethanol:acetic acid 2:1 for 5 min. at -20°C and subsequently washed in PBS twice for 5 min. Immediately 75 µL/5 cm^2 of equilibration buffer (supplied with the kit) was applied directly on the specimen and incubated for at least 10 seconds at room temperature. The excess liquid was aspirated to immediately pipette onto the section 55 µL/5 cm^2 of TdT enzyme (supplied with the kit). Incubation in a humidified chamber at 37°C for 1 hour was performed. The reaction was stopped by putting the slides in a coplin jar

containing stop/wash buffer (supplied with the kit), the jar was agitated for 15 seconds, and incubated for 10 min. at room temperature. The specimen was rinsed in 3 changes of PBS for 1 min each. 65 µL/5 cm^2 of prewarmed anti-digoxigenin conjugate was applied to the slide and incubated in a humidified chamber for 30 min. at room temperature avoiding exposure to light. Two changes of PBS for 2 min. were subsequently done and 0.5-1.0 µg/ml of mounting medium containing DAPI was placed on each slide which was covered with a coverslip. The fluorescence was detected as described in section 5.7.

5.12-Hearing Test

The auditory tests were performed by Hannes Maier in the faculty of medicine (University of Hamburg). Auditory evoked brain-stem responses (ABR) to clicks were recorded in mice anaesthetized with Rompun/Ketanest before the hearing measurement. Acoustic stimulation and recording of evoked potentials used an Evoselect system (Pilot Blankenfelde). Bioelectric potentials were recorded by subcutaneous silver electrodes at the vertex (reference), forehead (ground), and ventrolateral to the stimulated ear (active). Acoustic click stimuli were delivered mono-aurallyusing a Beyer DT-48 earphone, and were monitored with a probe microphone (MK301, Microtech Gefell) integrated into the earpiece. Calibration was done in a 19 ml volume using a second probe microphone (Brüel & Kjær 4135) with a sound-level meter (Brüel & Kjær 2215). Click stimuli had a main component of approximately 200ms duration and a flat spectrum (±5 dB) with an upper corner frequency of 5.5 kHz. Alternating clicks were applied at a rate of 21 per s and averaged 400–2,000 times (described in (Boettger, 2002))

6-GENERAL ABBREVIATIONS

AP	Alkaline-Phosphatase
bp	Base pairs
cDNA	Complementary DNA
cm, mm	Centimeter, millimeter
ddH_2O	Double distilled water
dNTPs	Deoxyribonucleoside triphosphates
DMSO	Dimethyl sulfoxide
DNA	Deoxyribonucleic acid
DTT	Dithiothreitol
EDTA	Ethylenediaminetetra-acetate
EtOH	Ethanol
FA	Formaldehyde
g, mg, μg	Gram, milligram, microgram
h, min, sec	Hour, minute, second
kb	Kilobases
kDA	Kilodaltons
L, ml, μl	Liter, milliliter, microliter
M, mM, μM	Molar, miilimolar, micromolar
MeOH	Methanol
mRNA	Messenger RNA
NP-40	Nonidet P-40
OD	Optical density
O/N	Overnight
PBS	Phosphate-buffered saline
PBT	Phosphate-buffered saline- triton
PCR	Polymerase chain reaction
PFA	Paraformaldehyde
qs	Bring to a total volume of
RNA	Ribonucleic acid
rpm	Rotations per minute
RT	Room temperature
SDS	Sodium dodecyl sulfate

Tris	Tris (hydroxymethyl) aminomethane
UTR	Untranslated region
V	Volts
X-gal	5-bromo-4-chloro-3-indolyl-ß-D-galactoside
Specialized Abbreviation	
CRE	Cre recombianse
FGF	Fibroblast growth factor
FGF8 ko	$Fgf8^{flox}/Fgf8^{\Delta 2,3}$.; *Foxg1-Cre*
FGF3+8 ko	$Fgf3^{-/-}$; *Foxg1-Cre*; $Fgf8^{flox}/Fgf8^{\Delta 2,3}$.
flox	**F**lank with l**ox**P sites
Foxg1	Fork head box
E8-E18.5	Embryonic stages (day of gestation)
EGFP	Enhance green fluorescence protein
HH	Hamilton Hamburger
Kcc4	K-Cl cotransporter
KCNQ1/4	potassium voltage-gated channel/4
Ko	Knockout
r	Rhombomeres
siRNA	Small interference RNA
VES	Vestibule
wt	wild-type

VII-BIBLIOGRAPHY

Acampora, D., Merlo, G. R., Paleari, L., Zerega, B., Postiglione, M. P., Mantero, S., Bober, E., Barbieri, O., Simeone, A. and Levi, G. (1999). Craniofacial, vestibular and bone defects in mice lacking the Distal-less-related gene Dlx5. *Development* **126**, 3795-809.

Adamska, M., Herbrand, H., Adamski, M., Krüger, M., Braun, T. and Bober, E. (2001). FGFs control the pattering of the inner ear but are not able to induce the full program. *Mech Dev* **109**, 303-313.

Adamska, M., Leger, S., Brand, M., Hadrys, T., Braun, T. and Bober, E. (2000). Inner ear and lateral line expression of a zebrafish Nkx5-1 gene and its downregulation in the ears of FGF8 mutant, ace. *Mech Dev* **97**, 161-5.

Alsina, B., Abello, G., Ulloa, E., Henrique, D., Pujades, C. and Giraldez, F. (2004). FGF signaling is required for determination of otic neuroblasts in the chick embryo. *Dev Biol* **267**, 119-134.

Alvarez, I. S., Araujo, M. and Nieto, M. A. (1998). Neural induction in whole chick embryo cultures by FGF. *Dev Biol* **199**, 42-54.

Alvarez, Y., Alonso, M. T., Vendrell, V., Zelarayan, L. C., Chamero, P., Theil, T., Bosl, , M.R., K., S., , Maconochie, M., Riethmacher, D. and Schimmang, T. (2003). Requirements for FGF3 and FGF10 during inner ear formation. *Development* **130**, 6329-6338.

Anniko, M. and Wikstrom, S. O. (1984). Pattern formation of the otic placode and morphogenesis of the otocyst. *Am J Otolaryngol* **5**, 373-81.

Baglioni, C. and Nilsen, T. W. (1983). Mechanisms of antiviral action of interferon. *Interferon* **5**, 23-42.

Baird, R. A., Burton, M. D., Fashena, D. S. and Naeger, R. A. (2000). Hair cell recovery in mitotically blocked cultures of the bullfrog saccule. *Proc Natl Acad Sci U S A* **97**, 11722-9.

Baker, C. V. a. B.-F., M. (2001). Vertebrate cranial placodes I. Embryonic induction. *Dev Biol* **232**, 1-61.

Beer, H. D., Vindevoghel, L., Gait, M. J., Revest, J. M., Duan, D. R., Mason, I., Dickson, C. and Werner, S. (2000). Fibroblast growth factor (FGF) receptor 1-IIIb is a naturally occurring functional receptor for FGFs that is preferentially expressed in the skin and the brain. *J Biol Chem* **275**, 16091-7.

Bissonnette, J. P. and Fekete, D. M. (1996). Standard atlas of the gross anatomy of the developing inner ear of the chicken. *J Comp Neurol* **368**, 620-630.

Boettger, T., Hubner, CA., Maier, H., Rust, MB., Beck, FX., Jentsch, TJ. (2002). Deafness and renal tubular acidosis in mice lacking the K-Cl co-transporter Kcc4. *Nature* **416**, 878-878.

Bouleta A., Moonb, A., B., A. and Capecchi, a. M. R. (2004). The roles of Fgf4 and Fgf8 in limb bud initiation and outgrowth. *Dev Biol* **273**, 361-372.

Bourikas, D. and Stoeckli, E. T. (2003). New tools for gene manipulation in chicken embryos. *Oligonucleotides* **13**, 411-9.

Brown, S. T., Martin, K. and Groves, A. K. (2003). Molecular basis of inner ear induction. *Curr Top Dev Biol* **57**, 115-49.

Brummelkamp, T. R., Bernards, R. and Agami, R. (2002). A system for stable expression of short interfering RNAs in mammalian cells. *Science* **296**, 550-3.

Carnicero, E., Zelarayan, L.C., Ruttiger, L., Knipper, M., Alvarez, Y., Alonso, M.T., Schimmang, T. (2004). Differential roles of fibroblast growth factor-2 during development and maintenance of auditory sensory epithelia. *J Neurosci Res* **77**, 787-797.

Casey, G., Smith, R., McGillivray, D., Peters, G. and and Dickson, C. (1986). Characterization and chromosome assignment of the human homolog of int-2, a potential proto-oncogene. *Mol. Cell. Biol.* **6**, 502-510.

Chang, W., Brigande, J. V., Fekete, D. M. and Wu, D. K. (2004). The development of semicircular canals in the inner ear: role of FGFs in sensory cristae. *Development* **131**, 4201-11.

Chisaka, O., Musci, T. S. and Capecchi, M. R. (1992). Developmental defects of the ear, cranial nerves and hindbrain resulting from targeted disruption of the mouse homeobox gene Hox-1.6. *Nature* **355**, 516-20.

Cohn, M. J., Izpisua-Belmonte, J. C., Abud, H., Heath, J. K. and Tickle, C. (1995). Fibroblast growth factors induce additional limb development from the flank of chick embryos. *Cell* **80**, 739-46.

Couly, G., Coltey, P. and Le Douarin, N. M. (1993). The triple origin of skull in higher vertebrate: a study in quail-chick quimeras. *Development* **117**, 409-429.

Crossley, P. H. and Martin, G. R. (1995). The mouse Fgf8 gene encodes a family of polypeptides and is expressed in regions that direct outgrowth and patterning in the developing embryo. *Development* **121**, 439-51.

Crossley, P. H., Minowada, G., MacArthur, C.A., and Martin, G. R. (1996). Roles for FGF8 in the induction, initiation, and maintenance of chick limb development. *Cell* **84**, 127-136.

De Burlet, H. (1934). Vergleichende Anatomie des Statoakustosche Organs. a) Die innere Ohrsphäre; b) Die Mittlere Ohrsphäre. In Handbuch der Vergleichenede Anatomie del Wilbeltiere (ed. L. Bolk, E. Göppert, E. Kallius and W. Lubosh), pp. 1293-1432. Berlin: Urban and Schwarzenberg.

De Moerlooze, L., Spencer-Dene, B., Revest, J., Hajihosseini, M., Rosewell, I. and Dickson, C. (2000). An important role for the IIIb isoform of fibroblast growth factor receptor 2 (FGFR2) in mesenchymal-epithelial signalling during mouse organogenesis. *Development* **127**, 483-92.

Deol, M. S. (1964). The Abnormalities of the Inner Ear in Kreisler Mice. *J Embryol Exp Morphol* **12**, 475-90.

Deol, M. S. (1966). Influence of the neural tube on the differentiation of the inner ear in the mammalian embryo. *Nature* **209**, 219-20.

Depew, M. J., Liu, J. K., Long, J. E., Presley, R., Meneses, J. J., Pedersen, R. A. and Rubenstein, J. L. (1999). Dlx5 regulates regional development of the branchial arches and sensory capsules. *Development* **126**, 3831-46.

Dono, R., Texido, G., Dussel, R., Ehmke, H. and Zeller, R. (1998). Impaired cerebral cortex development and blood pressure regulation in FGF2 deficient mice. *Embo J* **17**, 4213-4225.

Elbashir, S. M., Martinez, J., Patkaniowska, A., Lendeckel, W. and Tuschl, T. (2001). Functional anatomy of siRNAs for mediating efficient RNAi in Drosophila melanogaster embryo lysate. *Embo J* **20**, 6877-88.

Estevez, R., Boettger, T., Stein, V., Birkenhager, R., Otto, E., Hildebrandt, F., Jentsch, TJ. (2001). Barttin is a Cl- channel beta-subunit crucial for renal Cl- reabsorption and inner ear K+ secretion. *Nature* **414**, 558-561.

Fekete, D. M., Muthukumar, S. and Karagogeos, D. (1998). Hair cells and supporting cells share a common progenitor in the avian inner ear. *J Neurosci* **18**, 7811-21.

Fekete, D. M. and Wu, D. K. (2002). Revisiting cell fate specification in the inner ear. *Curr Opin Neurobiol* **12**, 35-42.

Feledy, J. A., Morasso, M. I., Jang, S. I. and Sargent, T. D. (1999). Transcriptional activation by the homeodomain protein distal-less 3. *Nucleic Acids Res* **27**, 764-70.

Frenz, D. A., Liu, W., Williams, J. D., Hatcher, V., Galinovic-Schwartz, V., Flanders, K. C. and Van de Water, T. R. (1994). Induction of chondrogenesis: requirement for synergistic interaction of basic fibroblast growth factor and transforming growth factor-beta. *Development* **120**, 415-24.

Fritzsch, B. (1992). The water-to-land transition: evolution of the tetrapod basilar papilla, middle ear and auditory nuclei. In The Evolutionary Biology of hearing (ed. D. P. Webster, AN. Fay, RR.), pp. 351-175. New York: Springer-Verlag.

Fritzsch, B. (2001b). The morphology and function of fish ears. In The laboratory fish (ed. G. Ostrander), pp. 250-259. Academic Press.

Fritzsch, B., Barald, F:, and LOmax, M. (1998). Development of the auditory system. In Early embriology of vertebrate ear (ed. E. W. Rubel, P. AN. and R. Fay), pp. 80-145. New york: Springer-Verlag.

Gimeno, L., Brulet, P., Martinez S. (2003). Study of Fgf15 gene expression in developing mouse brain. *Gene Expr Patterns* **3**, 473-481.

Gimeno, L., Hashemi, R., Brulet, P., Martinez, S. (2002). Analysis of Fgf15 expression pattern in the mouse neural tube. *Brain Res Bull.* **57**, 297-299.

Giraldez, F. (1998). Regionalized organizing activity of the neural tube revealed by the regulation of lmx1 in the otic vesicle. *Dev Biol* **203**, 189-200.

Graham, A. and Begbie, J. (2000). Neurogenic placodes: a common front. *Trends Neurosci* **23**, 313-6.

Granata, A., Quaderi, N.A. (2003). The Opitz syndrome gene MID1 is essential for establishing asymmetric gene expression in Hensen's node. *Dev Biol* **258**, 397-405.

Gray, H. (2000). Anatomy of the Human Body. In The Internal Ear or Labyrinth (ed. W. H. Lewis), pp. 1047-1059. New York: Philadelphia: Lea & Febiger.

Griffiths, A. J., Gelbart, W. M., Miller, J. H. and Lewontin, R. C. (1999). Modern Genetic Analysis. In Genes Mutations (ed. F. Tenney S., N., Rossignol, R., O'Neill, J.), pp. 221-228. New York: WH Freeman and Company.

Haddon, C. and Lewis, J. (1996). Early ear development in the embryo of the zebrafish, Danio rerio. *J Comp Neurol* **365**, 113-28.

Haddon, C., Mowbray, C., Whitfield, T., Jones, D., Gschmeissner, S. and Lewis, J. (1999). Hair cells without supporting cells: further studies in the ear of the zebrafish mind bomb mutant. *J Neurocytol* **28**, 837-50.

Hamburger, V. a. H., H. L. (1951). A series of normal stages in the development of the chick embryo. *J. Morphol.* **88**, 49-92.

Hatini, V., Ye, X., Balas, G. and Lai, E. (1999). Dynamics of placodal lineage development revealed by targeted transgene expression. *Dev Dyn* **215**, 332-43.

Heasman, J. (2002). Morpholino oligos: making sense of antisense? *Dev Biol* **243**, 209-14.
Hebert, J. M. and McConnell, S. K. (2000). Targeting of cre to the Foxg1 (BF-1) locus mediates loxP recombination in the telencephalon and other developing head structures. *Dev Biol* **222**, 296-306.

Heller, N. and Brandli, A. W. (1999). Xenopus Pax-2/5/8 orthologues: novel insights into Pax gene evolution and identification of Pax-8 as the earliest marker for otic and pronephric cell lineages. *Dev Genet* **24**, 208-19.

Herbrand, H., Guthrie, S., Hadrys, T., Hoffmann, S., Arnold, H. H., Rinkwitz-Brandt, S. and Bober, E. (1998). Two regulatory genes, cNkx5-1 and cPax2, show different responses to local signals during otic placode and vesicle formation in the chick embryo. *Development* **125**, 645-54.

Hidalgo-Sánchez, M., Alvarado-Mallart, R. M. and Alvarez, I. S. (2000). Pax2, Otx2, Gbx2 and FGF8 expression in early otic vesicle development. *Mech Dev* **95**, 225-229.

Hilfer, S. R., Esteves, R. A. and Sanzo, J. F. (1989). Invagination of the otic placode: normal development and experimental manipulation. *J Exp Zool* **251**, 253-64.

Hogan, B. L. (1999). Morphogenesis. *Cell* **96**, 225-33.

Holzenberger, M., Lenzner, C., Leneuve, P., Zaoui, R., Hamard, G., Vaulont, S., Bouc, YL. (2000). Cre-mediated germline mosaicism: a method allowing rapid generation of several alleles of a target gene. *Nucleic Acids Res* **28**, E92.

Hossain, W. A. and Morest, D. K. (2000). Fibroblast growth factors (FGF-1, FGF-2) promote migration and neurite growth of mouse cochlear ganglion cells in vitro: immunohistochemistry and antibody perturbation. *J Neurosci Res* **62**, 40-55.

Hutson, M. R., Lewis, J. E., Nguyen-Luu, D., Lindberg, K. H. and Barald, K. F. (1999). Expression of Pax2 and patterning of the chick inner ear. *J Neurocytol* **28**, 795-807.

Igarashi, M., Finch, P.W., Aaronson, S.A. (1998). Characterization of recombinant human fibroblast growth factor (FGF)-10 reveals functional similarities with keratinocyte growth factor (FGF-7). *J Biol Chem* **273**, 13230-13235.

Kaestner, K. H., Knochel, W. and Martinez, D. E. (2000). Unified nomenclature for the winged helix/forkhead transcription factors. *Genes Dev* **14**, 142-6.

Kandel, E. R., Schwartz, J. H. and Jesell, T. M. (2000). Principles of Neural Science. In The Induction and Patterning of the Nervous System (ed. T. Jessell, and Sanes, Joshua.), pp. 1020-1040. USA: McGraw-Hill Companies.

Karabagli, H., Karabagli, P., Ladher, R. K. and Schoenwolf, G. C. (2002). Comparison of the expression patterns of several fibroblast growth factors during chick gastrulation and neurulation. *Anat Embryol (Berl)* **205**, 365-70.

Katahira, T. and Nakamura, H. (2003). Gene silencing in chick embryos with a vector-based small interfering RNA system. *Dev Growth Differ* **45**, 361-7.

Katoh, M. (2002). WNT anf FGF gene clusters. *Int J Oncology* **21**, 1269-1273.

Kawakami, Y., Capdevila, J., Buscher, D., Itoh, T., Rodriguez Esteban, C. and Izpisua Belmonte, J. C. (2001). WNT signals control FGF-dependent limb initiation and AER induction in the chick embryo. *Cell* **104**, 891-900.

Kettunen, P., Laurikkala, J., Itaranta, P., Vainio, S., Itoh, N. and Thesleff, I. (2000). Associations of FGF-3 and FGF-10 with signaling networks regulating tooth morphogenesis. *Dev Dyn* **219**, 322-32.

Kharkovets, T., Hardelin, J.P., Safieddine, S., Schweizer, M., El-Amraoui, A., Petit, C., Jentsch, T.J. (2000). KCNQ4, a K+ channel mutated in a form of dominant deafness, is expressed in the inner ear and the central auditory pathway. *Proc Natl Acad Sci U S A* **97**, 4333-4338.

Khvorova, A., Reynolds, A. and Jayasena, S. D. (2003). Functional siRNAs and miRNAs exhibit strand bias. *Cell* **115**, 209-16.

Kimura, J., Katahira, T., Araki, I. and Nakamura, H. (2004). Possible role of Hes5 for the rostrocaudal polarity formation of the tectum. *Dev Growth Differ* **46**, 219-27.

Knouff, R. (1935). the developmental pattern of ectodermal placodes in rana pipiens. *J.of Comp. Neuro.* **62**, 17-71.

Kobayashi, D., Kobayashi, M., Matsumoto, K., Ogura, T., Nakafuku, M. and Shimamura, K. (2002). Early subdivisions in the neural plate define distinct competence for inductive signals. *Development* **129**, 83-93.

Kos, R., Reedy, M. V., Johnson, R. L. and Erickson, C. A. (2001). The winged-helix transcription factor FoxD3 is important for establishing the neural crest lineage and repressing melanogenesis in avian embryos. *Development* **128**, 1467-79.

Kos, R., Tucker, R. P., Hall, R., Duong, T. D. and Erickson, C. A. (2003). Methods for introducing morpholinos into the chicken embryo. *Dev Dyn* **226**, 470-7.

Kos, R., Tucker, R., Hall, R., Duong,T., Erickson, C. (2003). Methods for Introducing Morpholinos into theChicken Embryo. *Dev Dyn* **226**, 470 - 477.

Ladher, R. K., Anakwe, K. U., Gurney, A. L., Schoenwolf, G. C. and Francis-West, P. H. (2000). Identification of synergistic signals initiating inner ear development. *Science* **290**, 1965-7.

Ladher, R. K., Wright, T. J., Moon, A. M., Mansour, S. L. and Schoenwolf, G. C. (2005). FGF8 initiates inner ear induction in chick and mouse. *Genes Dev* **19**, 603-13.

Lanford, P. J., Presson, J. C. and Popper, A. N. (1996). Cell proliferation and hair cell addition in the ear of the goldfish, Carassius auratus. *Hear Res* **100**, 1-9.

Lawoko-Kerali, G., Rivolta, M. N. and Holley, M. (2002). Expression of the transcription factors GATA3 and Pax2 during development of the mammalian inner ear. *J Comp Neurol* **442**, 378-91.

Lee, K. H. and Cotanche, D. A. (1996). Potential role of bFGF and retinoic acid in the regeneration of chicken cochlear hair cells. *Hear Res* **94**, 1-13.

Leger, S. and Brand, M. (2002). Fgf8 and Fgf3 are required for zebrafish ear placode induction, maintenance and inner ear patterning. *Mech Dev* **119**, 91-108.

Lewandoski, M. (2001). Conditional Control of Gene Expression in the Mouse. *Nature Reviews Genetics* **2**, 743-755.

Lewis, E., Leverenz, EL. and Bialek, W. (1985). The vertebrate inner ear. Boca raton,FL: CRC Press, pp 256..

Li, C. W., Van De Water, T., Ruben, R. and Shea, C. (1978). The fate mapping of the eleventh and twelfth day mouse otocyst: an in vitro study of the sites of origin of the embryonic inner ear sensory structures. *J Morphol* **157**, 240-268.

Liu, D., Chu, H., Maves, L., Yan, Y. L., Morcos, P. A., Postlethwait, J. H. and Westerfield, M. (2003). Fgf3 and Fgf8 dependent and independent transcription factors are required for otic placode specification. *Development* **130**, 2213-24.

Liu, P., Jenkins, N. A. and Copeland, N. G. (2003). A highly efficient recombineering-based method for generating conditional knockout mutations. *Genome Res* **13**, 476-84.

Lombardo, A., Isaacs, H. V. and Slack, J. M. (1998). Expression and functions of FGF-3 in Xenopus development. *Int J Dev Biol* **42**, 1101-7.

Lombardo, A. and Slack, J. M. (1998). Postgastrulation effects of fibroblast growth factor on Xenopus development. *Dev Dyn* **212**, 75-85.

Löwenstein, O. a. and Thornhill, R. (1970). The labyrinth Of Myxine: anatomy, ultrastructure and electrophysiology. *Proc R Soc Lond B Biol Sci* **176**, 21-42.

Luo, T., Matsuo-Takasaki, M. and Sargent, T. D. (2001). Distinct roles for Distal-less genes Dlx3 and Dlx5 in regulating ectodermal development in Xenopus. *Mol Reprod Dev* **60**, 331-7.

MacArthur, C. A., Lawshe, A. X. J., Santos-Ocampo, S., Heikinheimo, M., Chellaiah, A. T. and DM., O. (1995). FGF-8 isoforms activate receptor splice forms that are expressed in mesenchymal regions of mouse development. *Development* **121**, 3603-3613.

Mahmood, R., Kiefer, P., Guthrie, S., Dickson, C. and Mason, I. (1995). Multiple roles for FGF-3 during cranial neural development in the chicken. *Development* **121**, 1399-410.

Mahmood, R., Mason, I. J. and Morriss-Kay, G. M. (1996). Expression of Fgf-3 in relation to hindbrain segmentation, otic pit position and pharyngeal arch morphology in normal and retinoic acid-exposed mouse embryos. *Anat Embryol (Berl)* **194**, 13-22.

Manley, G. (2000). Cochlear mechanism from phylogenetic viewpoint. *PNAS* **97**, 11736-11743.

Manley, G., and Köppl Christine. (1998). Phylogenetic development of the cochlea and its innervation. *Curr Opin in Neuro.* **8**, 468-474.

Mansour, S. L., Goddard, J. M. and Cappechi, M. R. (1993). Mice homozygous for a targeted disruption of the proto-oncogene *int-2* have developmental defects in the tail and the inner ear. *Development* **117**, 13-28.

Mansouri, A., Chowdhury, K. and Gruss, P. (1998). Follicular cells of the thyroid gland require Pax8 gene function. *Nat Genet* **19**, 87-90.

Marin, F. and Charnay, P. (2000). Hindbrain patterning: FGFs regulate Krox20 and mafB/kr expression in the otic/preotic region. *Development* **127**, 4925-35.

Maroon, H., Walshe, J., Mahmood, R., Kiefer, P., Dickson, C. and Mason, I. (2002). Fgf3 and Fgf8 are required together for formation of the otic placode and vesicle. *Development* **129**, 2099-108.

Martin, G. R. (1998). The roles of FGFs in the early development of vertebrate limbs. *Genes Dev* **12**, 1571-86.

Maves, L., Jackman, W. and Kimmel, C. B. (2002). FGF3 and FGF8 mediate a rhombomere 4 signaling activity in the zebrafish hindbrain. *Development* **129**, 3825-37.

McKay, I. J., Lewis, J. and Lumsden, A. (1996). The role of FGF-3 in early inner ear development: an analysis in normal and kreisler mutant mice. *Dev Biol* **174**, 370-8.

McKay, I. J., Muchamore, I., Krumlauf, R., Maden, M., Lumsden, A. and Lewis, J. (1994). The kreisler mouse: a hindbrain segmentation mutant that lacks two rhombomeres. *Development* **120**, 2199-211.

McManus, M. and Sharp, P. (2002). Gene Silencing in Mammals by Small Interfering RNAs. *Nature Reviews Genetics* **3**, 737-747.

Mendonsa, E. S. and Riley, B. B. (1999). Genetic analysis of tissue interactions required for otic placode induction in the zebrafish. *Dev Biol* **206**, 100-12.

Meyers, E. N., Lewandoski, M. and Martin, G. R. (1998). An Fgf8 mutant allelic series generated by Cre- and Flp-mediated recombination. *Nat Genet* **18**, 136-41.

Model, P. G., Jarret, L. S. and Bonazzoli, R. (1981). Cellular contacts between hindbrain and prospective ear during inductive interaction in the axolotl embryo. *J Embryol Exp Morphol* **66**, 27-41.

Moon, A. M. and Capecchi, M. R. (2000). Fgf8 is required for outgrowth and patterning of the limbs. *Nat. Genet.* **26**, 455-459.

Mori, C., Nakamura, N., Okamoto, Y., Osawa, M. and Shiota, K. (1994). Cytochemical identification of programmed cell death in the fusing fetal mouse palate by specific labelling of DNA fragmentation. *Anat Embryol (Berl)* **190**, 21-28.

Morsli, H., Choo, D., Ryan, A., Johnson, R. and Wu, D. K. (1998). Development of the mouse inner ear and origin of its sensory organs. *J Neurosci* **18**, 3327-35.

Mueller, K. L., Jacques, B. E. and Kelley, M. W. (2002). Fibroblast Growth Factor Signaling Regulates Pillar CellDevelopment in the Organ of Corti. *The Journal of Neuroscience* **22**, 9368-9377.

Muramatsu, T., Mizutani, Y., Ohmori, Y. and Okumura, J. (1997). Comparison of three nonviral transfection methods for foreign gene expression in early chicken embryos in ovo. *Biochem Biophys Res Commun* **230**, 376-80.

Nakamura, H., Watanabe, Y. and Funahashi, J. (2000). Misexpression of genes in brain vesicles by in ovo electroporation. *Dev Growth Differ* **42**, 199-201.

Nasevicius, A., Ekker, S.C. (2000). Effective targeted gene 'knockdown' in zebrafish. *Nat Genet* **26**, 216-220.

Nieto, M. A., Gilardi-Hebenstreit, P., Charnay, P. and Wilkinson, D. G. (1992). A receptor protein tyrosine kinase implicated in the segmental patterning of the hindbrain and mesoderm. *Development* **116**, 1137-50.

Noden, D. and Van De Water, T. (1986). The developing ear: Tissue origins and interactions. In The biology of of change in otolaryngology (ed. R. Ruben, T. Van De Water and E. Rubel), Amsterdam: Elsevier.

Noramly, S. and Grainger, R. M. (2002). Determination of the emrbyonic inner ear. *J. Neurobiology* **53**, 100-128.

Oesterle, E. C., Bhave, S. A. and Coltrera, M. D. (2000). Basic fibroblast growth factor inhibits cell proliferation in cultured avian inner ear sensory epithelia. *J Comp Neurol* **424**, 307-26.

Ohuchi, H., Hori, Y., Yamasaki, M., Harada, H., Sekine, K., Kato, S. and Itoh, N. (2000). FGF10 acts as a major ligand for FGF receptor 2 IIIb in mouse multi-organ development. *Biochem Biophys Res Commun* **277**, 643-9.

Ohuchi, H., Nakagawa, T., Yamamoto, A., Araga, A., Ohata, T., Ishimaru, Y., Yoshioka, H., Kuwana, T., Nohno, T., Yamasaki, M., *et al.* (1997). The mesenchymal factor, FGF10, initiates and maintains the outgrowth of the chick limb bud through interaction with FGF8, an apical ectodermal factor. *Development* **124**, 2235-44.

Ohuchi, H., Yasue, A., Ono, K., Sasaoka, S., Tomonari, S., Takagi, A., Itakura, M., Moriyama, K., Noji, S. and Nohno, T. (2005). Identification of cis-element regulating expression of the mouse Fgf10 gene during inner ear development. *Dev Dyn* **233**, 177-187.

Ornitz, D. M. and Itoh, N. (2001). Fibroblast growth factors. *Genome Biol* **2**, REVIEWS3005.

Ornitz, D. M., Xu, J., Colvin, J. S., McEwen, D. G., MacArthur, C. A., Coulier, F., Gao, G. and Goldfarb, M. (1996). Receptor specificity of the fibroblast growth factor family. *J Biol Chem* **271**, 15292-7.

Ortega, S., Ittmann, M., Tsang, SH., Ehrlich, M., Basilico, C. (1998). Neuronal defects and delayed wound healing in mice lacking fibroblast growth factor 2. *Proc Natl Acad Sci U S A* **95**, 5672-5677.

Paddison, P. J., Caudy, A. A., Bernstein, E., Hannon, G. J. and Conklin, D. S. (2002). Short hairpin RNAs (shRNAs) induce sequence-specific silencing in mammalian cells. *Genes Dev* **16**, 948-58.

Pasqualetti, M., Neun, R., Davenne, M. and Rijli, F. M. (2001). Retinoic acid rescues inner ear defects in Hoxa1 deficient mice. *Nat Genet* **29**, 34-9.

Pauley, S., Wright, T. J., Pirvola, U., Ornitz, D., Beisel, K. and Fritzsch, B. (2003). Expression and function of FGF10 in mammalian inner ear development. *Dev Dyn* **227**, 203-15.

Pera, E. and Kessel, M. (1999). Expression of DLX3 in chick embryos. *Mech Dev* **89**, 189-93.

Peters, G., Brookes, S., Smith, R., Placzek, M., Dickson, C. (1989). The mouse homolog of the hst/k-FGF gene is adjacent to int-2 and is activated by proviral insertion in some virally induced mammary tumors. *Proc Natl Acad Sci U S A* **85**, 5678-5682.

Pfeffer, P. L., Gerster, T., Lun, K., Brand, M. and Busslinger, M. (1998). Characterization of three novel members of the zebrafish Pax2/5/8 family: dependency of Pax5 and Pax8 expression on the Pax2.1 (noi) function. *Development* **125**, 3063-74.

Phillips, B. T., Bolding, K. and Riley, B. B. (2001). Zebrafish fgf3 and fgf8 encode redundant functions required for otic placode induction. *Dev Biol* **235**, 351-65.

Phillips, B. T., Storch, E.M., Lekven, A.C., Riley, B.B. (2004). A direct role for Fgf but not Wnt in otic placode induction. *Development* **131**, 923-931.

Pickles, J. and Chir, B. (2002). Roles of Fibroblast Growth Factors. *Audiol Neurootol* **7**, 36-39.

Pickles, J. O. (2001). The expression of fibroblast growth factors and their receptors in the embryonic and neonatal mouse inner ear. *Hear Res* **155**, 54-62.

Pickles, J. O. and van Heumen, W. R. (1997). The expression of messenger RNAs coding for growth factors, their receptors, and eph-class receptor tyrosine kinases in normal and ototoxically damaged chick cochleae. *Dev Neurosci* **19**, 476-87.

Pirvola, U., Spencer-Dene, B., Xing-Qun, L., Kettunen, P., Thesleff, I., Fritzsch, B., Dickson, C. and Ylikoski, J. (2000). FGF/FGFR-2(IIIb) signaling is essential for inner ear morphogenesis. *J Neurosci* **20**, 6125-34.

Pirvola, U., Xing-Qun, L., Virkkala, J., Saarma, M., Murakata, C., Camoratto, A. M., Walton, K. M. and Ylikoski, J. (2000). Rescue of hearing, auditory hair cells, and neurons by CEP-1347/KT7515, an inhibitor of c-Jun N-terminal kinase activation. *J Neurosci* **20**, 43-50.

Pirvola, U., Ylikoski, J., Trocovik, R., Hérbert, J. M., McConnell, S. and Partanen, J. (2002). FGFR1 is required for the development of the auditory sensory ephitelium. *Neuron* **35**, 671-680.

Powles, N., Marshall, H., Economou, A., Chiang, C., Murakami, A., Dickson, C., Krumlau, f. R. and Maconochie, M. (2004). Regulatory analysis of the mouse Fgf3 gene: control of embryonic expression patterns and dependence upon sonic hedgehog (Shh) signalling. *Dev Dyn* **230**, 44-56.

Prass, R. L., Gutnick, H. N. and Williams, D. E. (2004). Ear anatomy. In http://www.earaces.com/ (ed. P. C. Atlantic Coast Ear Specialist), USA.

Presson, J. C., Lanford, P. J. and Popper, A. N. (1996). Hair cell precursors are ultrastructurally indistinguishable from mature support cells in the ear of a postembryonic fish. *Hear Res* **100**, 10-20.

Reifers, F., Bohli, H., Walsh, E. C., Crossley, P. H., Stainier, D. Y. and Brand, M. (1998). Fgf8 is mutated in zebrafish acerebellar (ace) mutants and is required for maintenance of midbrain-hindbrain boundary development and somitogenesis. *Development* **125**, 2381-95.

Represa, J., Leon, Y., Miner, C. and Giraldez, F. (1991). The int-2 proto-oncogene is responsible for induction of the inner ear. *Nature* **353**, 561-3.

Riley, B. B., Phillips, B.T. (2003). Ringing in the new ear: resolution of cell interactions in otic development. *Dev Biol* **261**, 289-312.

Rinkwitz, S., Bober, E. and Baker, R. (2001). Development of the vertebrate inner ear. *Ann N Y Acad Sci* **942**, 1-14.

Rinkwitz-Brandt, S., Arnold, H. H. and Bober, E. (1996). Regionalized expression of Nkx5-1, Nkx5-2, Pax2 and sek genes during mouse inner ear development. *Hear Res* **99**, 129-38.

Rosenquist, G. C. (1966). A radiographic study of labeled grafts in the chick balstoderm: development from primitive streak stages to stage 12. *Contrib. Embryol.* **38**, 71-110.

Sakagami, M., Fukazawa, K., Matsunaga, T., Fujita, H., Mori, N., Takumi, T., Ohkubo, H., Nakanishi, S. (1991). Cellular localization of rat Isk protein in the stria vascularis by immunohistochemical observation. *Hear Res* **56**, 168-172.

Sanchez-Calderon, H., Martin-Partido, G. and Hidalgo-Sanchez, M. (2004). Otx2, Gbx2, and Fgf8 expression patterns in the chick developing inner ear and their possible roles in otic specification and early innervation. *Gene Expr Patterns* **4**, 659-669.

Sanchez-Calderon, H., Martin-Partido, G., Hidalgo-Sanchez, M. (2002). Differential expression of Otx2, Gbx2, Pax2, and Fgf8 in the developing vestibular and auditory sensory organs. *Brain Res Bull.* **57**, 321-323.

Sauer, B. (1998). Inducible gene targeting in mice using the Cre/lox system. *Methods* **14**, 381-92.

Schellart, N. and Popper, A. (1992). Functional aspects of the evolution of the auditory system of actinopterigian fish. In The Evolutionary Biology of Hearing (ed. D. P. Webster, AN. Fay, RR.), pp. 295-321. New York: Springer-Verlag.

Sekine, K., Ohuchi, H., Fujiwara, M., Yamasaki, M., Yoshizawa, T., Sato, T., Yagishita, N., Matsui, D., Koga, Y., Itoh, N., *et al.* (1999). Fgf10 is essential for limb and lung formation. *Nat Genet* **21**, 138-141.

Semizarov, D., Frost, L., Sarthy, A., Kroeger, P., Halbert, D. N. and Fesik, S. W. (2003). Specificity of short interfering RNA determined through gene expression signatures. *Proc Natl Acad Sci U S A* **100**, 6347-52.

Shamim, H., Mahmood, R., Logan, C., Doherty, P., Lumsden, A. and Mason, I. (1999). Sequential roles for Fgf4, En1 and Fgf8 in specification and regionalisation of the midbrain. *Development* **126**, 945-59.

Shamim, H. and Mason, I. (1999). Expression of Fgf4 during early development of the chick embryo. *Mech Dev* **85**, 189-92.

Sheng, G., dos Reis, M. and Stern, C. D. (2003). Churchill, a zinc finger transcriptional activator, regulates the transition between gastrulation and neurulation. *Cell* **115**, 603-13.

Solomon, K. S., Kudoh, T., Dawid, I. B. and Fritz, A. (2003). Zebrafish foxi1 mediates otic placode formation and jaw development. *Development* **130**, 929-40.

Soriano, P. (1999). Generalized lacZ expression with the ROSA26 Cre reporter strain. *Nat Genet* **21**, 70-71.

Spivak-Kroizman, T., Lemmon, M., Dikic, I., Ladbury, J., Pinchasi, D., Huang, J., Jaye, M., Crumley, G., Schlessinger, J. and Lax, I. (1994). Heparin-induced oligomerization of FGF molecules is responsible for FGF receptor dimerization, activation, and cell proliferation. *Cell* **79**, 1015-24.

Steel, K. P. (1999). Perspectives: biomedicine. The benefits of recycling. *Science* **285**, 1363-1364.

Stolte, D., Huang, R. and Christ, B. (2002). Spatial and temporal pattern of Fgf-8 expression during chicken development. *Anat Embryol (Berl)* **205**, 1-6.

Streit, A. (2001). Origin of the vertebrate inner ear: evolution and induction of the otic placode. *J. Anat.* **199**, 99-103.

Streit, A. (2002). Extensive cell movements accompany formation of the otic placode. *Dev Biol* **249**, 237-54.

Streit, A. (2004). Early development of the cranial sensory nervous system: from a common field to individual placodes. *Dev Biol* **276**, 1-15.

Sugiyama, S. and Nakamura, H. (2003). The role of Grg4 in tectal laminar formation. *Development* **130**, 451-62.

Sui, G., Soohoo, C., Affar el, B., Gay, F., Shi, Y. and Forrester, W. C. (2002). A DNA vector-based RNAi technology to suppress gene expression in mammalian cells. *Proc Natl Acad Sci U S A* **99**, 5515-20.

Sun, X., Mariani, F.V., Martin, G.R.,. (2002). Functions of FGF signalling from the apical ectodermal ridge in limb development. *Nature* **418**, 501– 508.

Sun, X., Meyers, E. N., Lewandoski, M. and Martin, G. R. (1999). Targeted dsiruption of FGF8 causes failure of cell migration in the gastrulating mouse embryos. *Genes Dev* **13**, 1834-1846.

Svoboda, P., Stein, P. and Schultz, R. M. (2001). RNAi in mouse oocytes and preimplantation embryos: effectiveness of hairpin dsRNA. *Biochem Biophys Res Commun* **287**, 1099-104.

Swartz, M., Eberhart, J., Mastick, G. S. and Krull, C. E. (2001). Sparking new frontiers: using in vivo electroporation for genetic manipulations. *Dev Biol* **233**, 13-21.

Takeuchi, J. K., Koshiba-Takeuchi, K., Matsumoto, K., Vogel-Hopker, A., Naitoh-Matsuo, M., Ogura, K., Takahashi, N., Yasuda, K. and Ogura, T. (1999). Tbx5 and Tbx4 genes determine the wing/leg identity of limb buds. *Nature* **398**, 810-4.

Tallquist, M. D. and Soriano, P. (2000). Epiblast-restricted Cre expression in MORE mice: a tool to distinguish embryonic vs. extra-embryonic gene function. *Genesis* **26**, 113-115.
Torres & Giraldez. (1998). The development of the vertebrate inner ear. *Mechanism of development* **71**, 5-21.

Torres, M., Gomez-Pardo, E. and Gruss, P. (1996). Pax2 contributes to inner ear patterning and optic nerve trajectory. *Development* **122**, 3381-91.

Van De Water, T. (1983). Embryonesis of the inner ear: "in vitro studies". In Development of Auditory and Vestibular System (ed. R. Romand), pp. 337-374. New York: Academic Press.

Vendrell, V., Carnicero, E., Giraldez, F., Alonso, M. T. and Schimmang, T. (2000). Induction of inner ear fate by FGF3. *Development* **127**, 2011-9.

Walshe, J., Maroon, H., McGonnell, I. M., Dickson, C. and Mason, I. (2002). Establishment of hindbrain segmental identity requires signaling by FGF3 and FGF8. *Curr Biol* **12**, 1117-23.

Werner, G. (1960). Das Labyrinth der Wirbeltiere. Jena (Germany)Fischer-Verlag, pp309.

Wilke, T. A., Gubbels, S., Schwartz, J. and Richman, J. M. (1997). Expression of fibroblast growth factor receptors (FGFR1, FGFR2, FGFR3) in the developing head and face. *Dev Dyn* **210**, 41-52.

Wilkinson, D. G., Bhatt, S. and McMahon, A. P. (1989). Expression pattern of the FGF-related proto-oncogene int-2 suggests multiple roles in fetal development. *Development* **105**, 131-6.

Wilkinson, D. G., Peters, G., Dickson, C. and McMahon, A. P. (1988). Expression of the FGF-related proto-oncogene int-2 during gastrulation and neurulation in the mouse. *Embo J* **7**, 691-5.

Williams, B. R. (1999). PKR; a sentinel kinase for cellular stress. *Oncogene* **18**, 6112-20.

Wright, T. J., Hatch, E. P., Karabagli, H., Karabagli, P., Schoenwolf, G. C. and Mansour, S. L. (2003). Expression of mouse fibroblast growth factor and fibroblast growth factor receptor genes during early inner ear development. *Dev Dyn* **228**, 267-72.

Wright, T. J., Ladher, R., McWhirter, J., Murre, C., Schoenwolf ,G.C,, Mansour, S.L. (2004). Mouse FGF15 is the ortholog of human and chick FGF19, but is not uniquely required for otic induction. *Dev Biol* **269**, 264-275.

Wright, T. J. and Mansour, S. L. (2003). Fgf3 and Fgf10 are required for mouse otic placode induction. *Development* **130**, 3379-3390.

Wu, D. K., Nunes, F. D. and Choo, D. (1998). Axial specification for sensory organs versus non-sensory structures of the chicken inner ear. *Development* **125**, 11-20.

Xu, X., Weinstein, M., Li, C., Naski, M., Cohen, R. I., Ornitz, D. M., Leder, P. and Deng, C. (1998). Fibroblast growth factor receptor 2 (FGFR2)-mediated reciprocal regulation loop between FGF8 and FGF10 is essential for limb induction. *Development* **125**, 753-65.

Yasuda, K., Momose, T. and Takahashi, Y. (2000). Applications of microelectroporation for studies of chick embryogenesis. *Dev Growth Differ* **42**, 203-6.

Yntema, C. (1950). An analysis of the induction of the ear from foreign ectoderm in the salamander embryo. *Journal of Experi. Zoology* **113**, 211-214.

Yu, J. Y., DeRuiter, S. L. and Turner, D. L. (2002). RNA interference by expression of short-interfering RNAs and hairpin RNAs in mammalian cells. *Proc Natl Acad Sci U S A* **99**, 6047-52.

Zou, D., Silvius, D., Fritzsch, B. and Xu, P. X. (2004). Eya1 and Six1 are essential for early steps of sensory neurogenesis in mammalian cranial placodes. *Development* **131**, 5561-72.

Zuo, J. (2002). Transgenic and gene targeting studies of hair cell function in mouse inner ear. *J Neurobiol* **53**, 286-305.